Identification of Targetable Vulnerabilities During Latent KSHV Infection

Daniel Holmes

A dissertation
submitted in partial fulfillment of the
requirements for the degree of

Doctor of Philosophy

University of Washington

2020

Reading Committee:

Michael Lagunoff, Chair

Adam Philip Geballe

Jason G Smith

Program Authorized to Offer Degree:
Department of Microbiology

University of Washington

Abstract

Identification of Targetable Vulnerabilities During Latent KSHV Infection

Daniel Holmes

Chair of the Supervisory Committee:
Professor Michael Lagunoff
Department of Microbiology

Viruses are defined as obligate intracellular parasites that require host processes to replicate. Latent virus life cycles are no exception to this definition, as viruses are still reliant on host machinery for continued proliferation and maintenance of viral genomes, even in the absence of lytic replication. In this thesis, I used essentiality screening to identify host factors on which Kaposi's Sarcoma Associated Herpesvirus (KSHV) relies for the proliferation and survival of latently infected cells. KSHV is the etiological agent of Kaposi's Sarcoma (KS), an endothelial cell-based tumor where more than 90% of the endothelial cells in the tumor are latently infected with KSHV. While traditional therapies for herpesviruses target lytic replication, the prevalence of latency in KS necessitates exploration of options for intervening in this stage of the viral life cycle. I performed CRISPR/Cas9 screening using lentiviral vectors encoding a library of single guide RNAs (sgRNAs) targeting every protein coding gene in the human genome. I compared mock infected and KSHV infected endothelial cells eight days post infection to identify genes essential to latent KSHV infection. Additional sub-pool screening was carried out targeting genes from the initial whole genome screen to validate the results. Among the list of hits, were a number of genes involved in mitochondrial translation. This is a reasonable pathway for chemical inhibition, as mitochondrial ribosomes are sensitive to antibiotics targeting bacterial ribosomes due to their shared ancestry. I found

that treatment of latently infected endothelial cells results in suppression of cellular proliferation relative to mock infected controls. Additionally, antibiotic treatment of KSHV latently infected primary effusion lymphomas (PELs) induces cell death. I also found that inhibition of respiration, either chemically or by eliminating mitochondrial genomes from cells, results in suppressed proliferation and cell death. The dependence on mitochondrial function led me to characterize the status of mitochondria during KSHV infection. I found that latent KSHV infection leads to more interconnected mitochondrial networks, higher mitochondrial transcript levels, and increased mitochondrial genome copies. In attempting to determine how KSHV facilitates mitochondrial changes, I found that three latent proteins localize to the mitochondria. In experiments following up on a metabolomic screen carried out by our lab, I found that the latent locus of KSHV is essential for accumulation of lipid droplets during infection. I also found that lipid droplet formation is essential for cell survival during latent infection, but that this requirement is lost during infection with a mutant virus lacking the latent miRNA cluster. This work improves our understanding of the role of mitochondrial function in the persistence of latently infected cells and provides possible specific therapeutic targets for the main proliferating cells in KS tumors.

TABLE OF CONTENTS

LIST OF FIGURES

LIST OF TABLES

ACKNOWLEDGMENTS

I have a number of people to thank for supporting me in my career and life. First, I would like to thank Michael Lagunoff for his support over my time as a graduate student and for helping me grow into an independent scientist. I would also like to thank my previous mentors in science Randal Halfmann, Chris Brown, Kay Bidle. I will always be grateful for my time in the Halfmann lab and the guidance and encouragement from Randal has been invaluable to me. I really appreciate Kay giving me a place in his lab as an undergraduate, and Chris for spending the time to carefully train me. I would also like to thank my lab mates past and present. In particular I would like to thank Mike Maniscalco, for being a good friend in our time as undergraduates. I would also like to thank Sorna Kamara and Xin Cai, for making the Halfmann Lab such a great place to work. From the Lagunoff Lab I would like to thank Terri Dimaio for always being open to talking science, and for giving valuable guidance, sometimes without even having to say a word. I would also like to thank Zoi Sychev, Krystal Fontaine, Hanna Hong, Erica Sanchez, and Danny Vogt for being supportive lab mates. I would like to thank my two mentees, Maddie Hart and Jie Yin. Maddie, you came into the lab with a tremendous enthusiasm. You match that enthusiasm with an excellent mind for science, and I have enjoyed watching you continue to succeed since leaving our lab. Jie, you are one of the brightest people I have met, and you grew into a strong, resilient scientist during your time in the Lagunoff Lab. It was a real privilege to work with you in the lab, and I am so proud of how well you are doing now. I would also like to thank the other graduate students of the Microbiolgy Department. In particular, I would like to thank Kaitlyn LaCourse, Phil Burke, Alan Bohn, Katie and Sam Carpentier,

and Hannah Tabakh for being great friends. And Hannah, thank you so much for helping with all of my questions about library cloning.

I would also like to thank my family, both by blood and by law. I'd like to thank my parents, Anne and Steve for the love and support you gave me over the years. Thank you for encouraging me to use my curiosity to find new interests, then supporting me in developing those interests, whether or not you knew much about them. I would also like to thank my sister Laurie for being an amazing sister, even when I could be a pain of a brother. I'm so proud of who you have become. I'd also like to thank Subi, for being a welcome reminder of the importance of work/life balance. Finally, I want to thank Leighann. I appreciate everything you have done for us, and that includes bringing me into your loving family. You have been an unbelievably supportive partner while also being well accomplished in your own career, and I feel immensely privileged that I get to spend my life with you.

DEDICATION

I dedicate this work to my parents Anne and Steve. I also dedicate this work to my wife Leighann. Thank you for everything you have done to get me to where I am today.

Chapter 1

INTRODUCTION

1.1 Herpes Viruses

The Herpesviridae are large DNA viruses infecting animals from bivalves to humans. Separation of herpesvirus into the alpha, beta, and gamma sub families predated the mammalian radiation and have co-evolved with their hosts [90]. Due at least in part to this history of co-evolution, herpesviruses possess a high level of host specificity. Herpesvirus viral particles, or virions, range from roughly 120-260 nm in diameter and encode between 70 and 750 open reading frames [71]. There are four major morphological characteristics of herpesvirus virions: an inner core containing the viral genomic DNA, the protein capsid icosahedron, a relatively unstructured tegument (or matrix) between the capsid and the outermost lipid bi-layer envelope, which displays the virally encoded glycoproteins.

All members of the herpesvirus family have both lytic and latent programs as part of their cellular life cycles. When a virus enters a cell it either proceeds directly to lytic replication or establishes latency in a process that is often cell type dependent. Latently infected cells have the potential to reactivate and enter lytic replication to produce infectious virions. The triggers of lytic replication *in vivo* are poorly understood. Herpesviruses lytic replication takes the form of a virologically classic regulatory cascade, where genes are transcribed in a temporal pattern. The initial set of immediate-early lytic replication genes encode proteins which are essential for the activation of early gene transcription. Additionally, immediate-early genes are often responsible for regulation of the cell cycle, RNA processing,

and inhibition of host immune responses. Immediate-early genes are followed by expression of early genes which occurs independent of viral DNA synthesis. These genes require the synthesis of immediate early genes for expression. The primary function of the early genes revolves around viral DNA synthesis. Lastly, late gene expression depends on the prior synthesis of viral DNA. Late genes encode the structural components of the virion and the glycoproteins for insertion into the membrane. Late genes facilitate production of viral particles which bud off the cell and infect new cells. Importantly, lytic replication often leads to the death of the infected cell.

Latency is one of the defining characteristics of herpesviruses. While the process of producing new virus particles during lytic replication is similar across the family, there is a striking variety of different latent programs among the herpesviruses. Commonly, latency is characterized by the expression of few, if any, viral genes. There is also no production of virions during the latent phase of the virus life cycle and the replication of the viral genome only occurs during cell division. The ability of herpesviruses to manipulate host cells in order to establish long-term, non-productive infections is the primary focus of this thesis. The ability of many herpesviruses to cause certain diseases is linked to latent infection, either by allowing a burst of lytic replication well after primary infection, or by inducing inflammation and cellular proliferation, potentially leading to the formation of neoplastic cells.

There are currently nine known herpesvirus that infect primarily humans. The three major families are the alphaherpesviruses, betaherpesviruses, and gammaherpesvirus. The alphaherpesvirus family includes Herpes Simplex Virus (HSV-1 or HHV-1), Herpes Simplex Virus 2 (HSV-2 or HHV-2), and Varicella-Zoster Virus (VZV or HHV-3). HSV-1 and HSV-2 typically cause oral cold sores and genital cold sores, respectively. VZV is the etiological agent of chicken pox, however, later in life the virus can reactivate from latency and lead to severe complications due to either shingles or postherpetic neuralgia. The be-

taherpesviruses include Human Cytomegalovirus (HCMV or HHV-5), HHV-6A, HHV-6B, and HHV-7. HCMV is the leading infectious cause of deafness in infants and can cause a number of other childhood birth defects. HCMV can also cause significant problems following immune suppression, including pneumonia, colitis, and hepatitis. HHV-6A and HHV-6B share approximately 88% identity with one another and are considered distinct viruses with a closely related ancestor. HHV-6A, HHV-6B, as well as HHV-7 can cause the childhood disease roseola. The gammaherpesviruses include Epstein-Barr Virus (EBV or HHV-4) and Kaposi's Sarcoma-Associated Herpesvirus (KSHV or HHV-8). EBV infection can commonly cause mononucleosis and rarely cause Burkitt's lymphoma, nasopharyngeal carcinoma, and gastric cancer. The EBV associated cancers occur at high rates in specific geographic regions, Burkitt's lymphoma in sub-Saharan Africa and nasopharyngeal carcinoma in southeast Asia. It has recently been shown that a variant of the EBV BALF2 is highly associated with nasopharyngeal carcinoma in China, suggesting a direct role for a viral protein in the progression of disease [138]. KSHV is the etiological agent of Kaposi's Sarcoma (KS), which is an endothelium-based tumor. KSHV also causes two lymphoproliferative disorders, Primary Effusion Lymphoma (PEL) and multicentric Castleman's Disease (MCD). This thesis focuses on KSHV infection in the context of endothelial cell infection as a model of KS.

1.2 KS and PEL

KS was first reported in 1872 by the Hungarian dermatologist Moritz Kaposi [68]. He described a multifocal, red pigmented sarcoma on the skin of elderly European men. This form is now known as classic KS, which is one of at least four currently recognized epidemiological forms [18]. Classic KS primarily occurs in elderly men of Mediterranean or Jewish ancestry and tumors typically occur on the extremities. This form of the disease usually causes little pain or discomfort for patients aside from being disfiguring. The second form of KS, first documented in around 1947, is referred to as endemic KS, which occurs in Africa and incudes

a severe lymphadenopathic form of Kaposi's Sarcoma in children [30]. This form of KS occurs in the absence of immune suppression and the precise reason for its occurrence in some populations but not others remains unclear. In 1981 a new, highly aggressive form of KS was reported in men who have sex with men (MSM) [42]. Shortly after this was reported it was found that these men were suffering from severe immune deficiency, later determined to be caused by infection with the human immunodeficiency virus (HIV) [4]. This form of KS is referred to as epidemic KS or AIDS-related KS. The fourth type of KS occurs in people who receive immunosuppressants during the course of medical treatment. This is referred to as iatrogenic KS and is of concern following solid organ transplant. There have been reports of a fifth form of KS in MSM who do not have HIV [76]. Importantly, all epidemiological forms of KS display the same histopathology, with the spindle cells being the main proliferating component.

In addition to KS, KSHV also causes PEL, which is a B cell lymphoma that involves cancer expansion in peritoneal, pleural, and pericardial cavities [17]. PEL tumor cells are often co-infected with EBV, but EBV is not necessarily essential for PEL formation. PEL is considerably difficult to manage clinically, with one-year survival rates only around 40% [40]. Importantly, optimal treatment options for PEL remain to be found.

1.3 KSHV

The epidemiology of KS during the first decade of the AIDS epidemic suggested that the cause of the disease was a second infectious agent (other than HIV). Specifically, the incidence of KS among gay and bisexual AIDS patients was approximately twenty times higher than the incidence in hemophiliac AIDS patients [6]. This discrepancy prompted the search for the pathogen causing KS which led to sequences homologous to, but distinct from, EBV and the primate gammaherpesvirus *herpesvirus saimiri* to be identified by representational difference analysis [19]. Later work cloning and sequencing the entire KSHV genome allowed

the novel virus to be classified as a lymphotropic herpesvirus. Within the lymphotropic herpesviruses, there are two groups, the *lymphocryptoviruses* and the *rhadinoviruses*. KSHV falls in to the *rhadinovirus* family along with *herpesvirus saimiri*. The KSHV genome is approximately 165 kbp with a unique region of roughly 145 kbp. The non-unique region is a series of GC rich terminal repeats which contains a variable number of 801 bp repeats. While KSHV was initially annotated with 81 open reading frames (ORFs), more recent analysis indicates a much higher number of protein coding genes and non-coding RNAs [2].

All herpesviruses share a set of six conserved gene blocks which encode the components and enzymes for replicating the viral genome and producing new infectious particles [71]. However, like the other herpesviruses, KSHV has some genes which are unique. Many of these genes are homologs of mammalian genes which were acquired and then slowly diverged over long periods of time. For example, KSHV encodes a homolog of the human interleukin 6 gene which can act through the cellular receptor gp130 in the absence of normally required co-receptors to induce the Jak-Stat pathway [93]. KSHV also includes a homolog of the cellular bcl2 family of apoptosis inhibitors, which has been shown to suppress autophagy during lytic replication [37].

Latency is the primary state of KSHV in the majority of infected cells with the KS tumor. Latency is also the default state of most cells when cultured. Confirmation of infection can be done by immunofluorescence (IFA) using antibodies specific to the latency associate nuclear antigen (LANA), the major latent protein, and determination of the fraction of cells expressing lytic genes with antibodies targeting the lytic protein ORF59 [36]. During latency the viral episome is maintained in the nucleus of the cell where it is replicated and segregates into daughter cells during mitosis. In cultured endothelial cell systems KSHV establishes latency in greater than 90% of infected cells while just a small percentage of cells actively express lytic genes [74]. Treatment of cultured latently infected cells with histone deacetylase inhibitors induces lytic gene expression and can reactivate cells to produce virus,

especially in patient-derived B-cell lymphomas. Both latent and lytic stages of the KSHV life cycle are important contributors to the pathogenesis of KSHV associated cancers.

During the latent phase of KSHV's life cycle, there are only a few viral genes expressed. This set of genes includes LANA, viral cyclin (vCyc), viral FLICE (FADD-Homologous ICE/CED-3-Like Protease, or Caspase-8) inhibitory protein (vFLIP), the three Kaposin family members A, B, and C, as well as a cluster of miRNAs with 12 loci encoding ~18 mature miRNAs [18, 28, 69, 16, 120]. LANA, vCyc, and vFLIP are all expressed from the same viral promoter. Alternative splicing leads to mature mRNAs which contain either the LANA coding region, or the vCyc and vFLIP coding regions. The Kaposins are expressed from a separate promoter and the different proteins produced are the result of a complex translation process. The miRNAs are expressed by processing of the other latent transcripts, with miR-k10 and miR-K12 actually encoded within the kaposin coding region. LANA, the most well studied of the latent proteins, is primarily responsible for tethering the viral episome to the host genome in order to ensure that daughter cells inherit the viral genome after cell division. LANA does this by binding to both the terminal repeats on the viral genome and to host histones in complex with the human genome. Also relevant to pathogenesis, LANA binds to and inhibits the function of the major tumor suppressors p53 and pRB [35, 107].

vCyc's known function involves activation of host cyclin-dependent kinase 6. Overexpression of vCyc leads to initiation of significant DNA damage in the host genome, triggering the activation of the p53 tumor suppressor and induction of apoptosis [101]. Another group has shown a different phenotype, where vCyc overexpression actually causes oncogene induced senescence [77]. vFLIP's primary known function involves activation of the NF-KB pathway. vFLIP forms a physical interaction with the inhibitor of KB kinase gamma protein (IKKγ), which then leads to activation of the pathway and expression of NF-KB responsive genes [33]. The NF-KB modulatory function of vFLIP has been linked to a number of potentially oncogenic functions during KSHV infection, including inhibition of apoptosis. vFLIP

is also responsible for the spindle cell morphology observed during latent KSHV infection of endothelial cells [47].

The Kaposin locus encodes three separate gene products. Kaposin A (KapA) is a 60 amino acid, hydrophobic protein found in intracellular as well as plasma membranes [97]. Of note, KapA is sufficient to transform Rat-1 fibroblasts, but the precise mechanism of transformation is not known [96]. KapB and KapC share two sets of repeating sequences, which are bordered by unique sequences on either side. KapC's unique region includes KapA, which implies that KapC is essentially a membrane-bound isoform of KapB. KapB's known function is the binding and activation of the MAP kinase-associated protein kinase 2 (MK2) [89]. MK2 regulates the AU-rich elements (AREs) which are found in the 3'UTRs of many cytokines, growth factors, and oncogenes. While AREs are normally rapidly degraded in the cytoplasm, activation of MK2 stabilizes the mRNAs, allowing translation of the encoded gene. Thus, overexpression of KapB leads to stabilization and increased expression of transcripts possessing AREs.

The above functions are not exhaustive, there are likely other, undiscovered functions for KSHV latent proteins. A KSHV-host protein interaction network was generated by the Glaunsinger lab [23]. This work yielded a large number of both low and high confidence interactions. While many of the known interactions were identified, confirming the validity of the screen, a large number of previously unidentified interactions were found. Among these, many viral proteins were found to interact with mitochondrial proteins. This includes the latent gene set, where several viral proteins have many interaction partners in the mitochondria (Figure 1.1). These interactions are of interest because the mitochondria are the central nexus of cellular metabolism and is an important signaling hub for apoptosis and innate immunity.

Mammalians miRNAs are 21 to 23 nucleotide small RNAs that are capable of regulating gene expression. miRNAs are produced by the cleavage of larger RNAs by Drosha, a nuclear

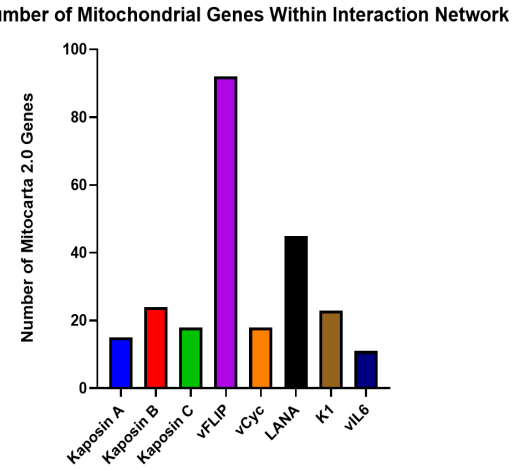

Figure 1.1: Reanalysis of Davis et al., 2015: KSHV latent proteins have many interaction partners which localize to the mitochondria of the cell, where they currently have no described function. Mitochondrial localization of bait proteins is determined by presence on the human mitocarta 2.0 gene set.

ribonuclease. The Drosha generated product is cleaved in the cytoplasm by Dicer, another endonuclease. The end result of this cleavage is a partial duplex RNA, one strand of which is transferred to the RNA-induced silencing complex (RISC) in the cytoplasm. RISC then binds to mRNA which is complementary to the miRNA and if the sequences have a high level of similarity, cleavage of the mRNA occurs. A secondary mode of silencing occurs when pairing is not perfect, where RISC sits on the mRNA and suppresses translation.

The KSHV latent miRNA cluster has a number of possible functions that have been described. miRNA-K11 has a similar seed sequence to cellular miR-155, meaning the targeted transcripts have a high level of overlap [117, 44]. miR-155's targets include the transcriptional repressor BACH1, and the proapoptotic factor XAF1. miR-K5 was found to target the Bcl2-associated proapoptotic protein BCLAF1 [147]. The miRNA cluster has also been implicated in many other processes associated with KSHV, including expression of cytokines, immune evasion, inhibition of tumor suppressors, and angiogenesis [43]. Of particular relevance for

this thesis, the miRNA cluster was found to be sufficient for the induction of Warburg metabolism in primary lymphatic endothelial cells [142]. An important aspect of the miRNA cluster is that no single miRNA was sufficient, and the expression of the entire cluster was necessary to observe the phenotype.

1.4 KSHV Culture Systems

Choice of culture system is important for studying KSHV mediated oncogenesis, as many of the pathways that KSHV alters will already be dysregulated in many transformed cell lines. For this reason, it is preferable to conduct studies in primary cells or so-called "soft" immortalized cells with exogenous expression of human telomerase (hTert) [129]. Our lab has established a system in human endothelial cells. Human dermal microvascular endothelial cells (hDMEVCs) immortalized with hTert are able to reproduce the infection rates which are observed in KS patient tumors [74]. These tert-immortalized microvascular endothelial (TIME) cells are desirable for the ability to grow indefinitely without displaying all the characteristics of fully transformed cells. TIME cells can be infected with KSHV so that over 90% of the cells are infected and less than 5% of the cells express lytic proteins, similar to what is observed in KS tumors. Additionally, as infected TIME cells divide, they gradually lose the KSHV episome, which is also what occurs in cultured KS spindle cells. TIME cells are also useful because they can be grown to large numbers, enabling large scale interrogations of the changes which occur during KSHV infection. This includes, but is not limited to gene expression analysis, proteomics, metabolomics, and essentiality screening.

A number of other cell culture systems have been developed for studying KS. These include the tert-immortalized-vascular endothelium TIVE cells as well as a primary rat mesenchymal (MM) cell model [1, 65]. TIVE cells are derived from major vasculature, which is different from the microvasculature which is believed to be closer to the origin of the KS spindle cell based on the typical presentation of KS tumors in the skin and on RNA-seq data

suggested infected TIME cells have similiar gene expression patters to KS tumors [127]. The main advantage of the MM system over other culture systems, is that KSHV infection enables MM cells to produce tumors when injected into an mouse model. While the MM system allows for examination of *in vivo* pathogenesis in an animal model, the use of animal models in human viral oncogenesis has been historically problematic as murine cells are considerably easier to transform and findings often don't reproduce in human cells. As an example, MM cells display decreased glucose consumption when infected with KSHV, however TIME cells and primary HMVECs display increased glucose consumption [25]. Within KS tumors, increased glucose consumption has actually been observed with positron emission tomography (PET) scanning with fluorodeoxyglucose labeled with radioactive fluorine-18 [102]. Additionally, comparison of gene expression by RNA-seq of a number of different infection system showed that KSHV infected TIME cells are the closest to the expression profile of KS tumors [127].

Another culture system of note is the SLK cell line originally reported to be isolated from KS tumor samples [55]. However, tandem repeat analysis showed that these cells were actually indistinguishable from the human renal cell carcinoma cell line Caki-1 [119]. Even though the use of the SLK cell line as a model for KS has ceased with this revelation, the cell line is a valuable tool for the production of recombinant viruses and for studying lytic replication of KSHV [98].

Patient derived PELs are used to study this lymphoma in culture. A number of isolates have been obtained over the years and cells harboring just KSHV or KSHV with EBV have been isolated. In contrast to endothelial cell models, these cells retain the virus after passaging. The KSHV latent gene vFLIP has been shown to be essential for continued proliferation of cells in culture [49]. There is no perfect uninfected control for these model systems, but PELs can be compared to cultured EBV-associated Burkitt's lymphoma B cells with (e.g. RAJI cells) or without EBV (e.g. BJAB cells). Importantly, primary B cells

cannot be transformed by KSHV alone, while EBV is capable of transforming B cells *in vitro* [32].

1.5 CRISPR/Cas9 Screening

An unusual stretch of DNA sequence was discovered in 1987 and was later named clustered regularly interspaced short palindromic repeat (CRISPR) DNA based on the repetitive elements within the sequence [59]. The function of these sequences was not understood until years later when genome sequencing across many different bacterial and archaeal species revealed that these sequences were present within many different species. It was also found that a number of genes around the CRISPR sequences were also well-conserved, leading to their naming CRISPR-associated (Cas) genes [61]. Lastly, the sequences in-between the repeat elements were noted to be matches to bacteriophage sequences, which led investigators to hypothesize that these systems were sequence-directed immune systems [92, 106, 13, 86]. Another group showed that the DNA within the repeat element is taken into the bacteria genomes following phage challenge, and then confers resistance to subsequent phage infections [3]. A large body of work followed which determined that two small RNAs, CRISPR RNA (crRNA) and a trans-activating crRNA (tracrRNA) are required to target the restriction endonuclease Cas9 to DNA which matches the non-repeat sequences crRNA [14, 27]. Work developing CRISPR systems as tools led to the realization that a single fused RNA formed from crRNA and tracrRNA called a single guide RNA (sgRNA) is sufficient for Cas9 targeting [62]. Finally, in 2012, researchers showed that the sgRNA can be customized to target specific sequences in eukaryotic cells, allowing precise, targeting editing in human genomes [63, 21, 87]. The mechanisms of editing either rely on host non-homologous end-joining (NHEJ) to generate frameshift mutations and produce a truncated, presumably non-functioning protein, or host homology directly repair (HDR) to repair the break caused by Cas9 with a provided template.

Chapter 3 of this thesis is based on an application of CRISPR/Cas9 technology to simultaneously screen for the effects of thousands of gene knockouts in the same experiment. This whole genome screening (WGS) approach was developed by several groups independently and published around the same time [114, 132, 72]. An important aspect of this approach is that it is more effective at overcoming limitations to screening in diploid cell lines relative to previous methods. To demonstrate this, a group compared essentially screening results from the near-haploid KBM7 leukemia cell line to results from the pseudo-diploid HL60 leukemia cell line [132]. They found similar results between the cell lines, supporting the idea that CRISPR screening systems function well enough to support loss-of-function screens in diploid cell lines despite the difficulty in generating knockouts in the presence of two alleles. High-throughput DNA synthesis approaches allow for large libraries of sgRNA sequences targeting potentially every gene in the human genome. These libraries can be cloned into lentiviral vectors and coupled with Cas9 expression to create a lentiviral library which is capable of generating a pool of knock-out cells. These libraries can be used to determine the list of essential genes for a specific cell line by using next-generation sequencing (NGS) to sequence the lentiviral sgRNAs and quantify changes in sgRNA counts between initial (immediately post transduction) and final cell populations. Another way to design CRISPR/Cas9 Screens is to compare sgRNA abundance in control cells versus cells treated with a stressor. A number of different CRISPR/Cas9 screens have been performed to identify essential genes during infection with different viruses [80, 85, 73, 34, 145, 78]. CRISPR/Cas9 screening has even been put use in other KSHV systems, but chapter 3 of this thesis will go into detail about the first of these screens performed in KSHV infected human endothelial cells.

1.6 Cancer Biology

1.6.1 Oncogenesis

The process of oncogenesis is generally understood as a multistep process by which cells acquire the ability to persist outside of the normal pattern of growth in the affected organism [50]. The complexity and extended length of time involved makes studying oncogenic transformation directly a challenge. In humans, many cell types accumulate significant numbers of mutations over a person's lifetime, but few of these cells will actually progress into cancer. As an example, adult stem cells in the colon, liver, and small intestine accumulate around 36 mutations per year [11]. In comparing neoplastic cells in a patient to untransformed cells of the same developmental lineage, identifying which mutations are involved in the progression of disease and which are bystanders is nearly impossible given the number of candidate driver mutations. Comparison of mutations common across cancers in different cell types has enabled identification of pathways which are disturbed in large fractions of cancers. However, this approach has not identified the drivers for all cancers, presumably because some are cell lineage or cancer type specific. Studying viral oncogenic systems theoretically makes it possible to ask questions about oncogenesis more generally. Beginning with either primary cells or cells that are not fully transformed, such as TIME cells, allows the direct effects of viral infection on a variety of oncogenic phenotypes to be assayed.

1.6.2 Cancer Metabolism

The altered metabolic phenotype of cancer tissues was first reported by Otto Warburg nearly a century ago [134]. He observed decreased oxygen consumption and increased acidification of the media through lactate production, a phenomenon now referred to as the Warburg effect. Warburg induction is thought to benefit cancer cells by rapidly generating the anabolic substrates needed for rapid cellular proliferation [53]. In addition to the gly-

colytic phenotype observed by Warburg, a number of other cellular metabolic pathways have been found to be altered in cancer cells relative to noncancerous cells of the same lineage. These include fatty acid synthesis (FAS), fatty acid storage in lipid droplets, and glutamine metabolism [24, 22]. Fatty acid synthesis is essential for the production of new cellular lipid membranes. The main pathway for fatty acid synthesis involves generation of acetyl-CoA and malonyl-CoA from citrate to generate palmitate, a 16-carbon long chain fatty acid. This reaction requires 14 NADPH for each palmitate generated and requires the enzyme fatty acid synthase (FASN). Once palmitate has been synthesized it can become the substrate for elongation reactions which add additional two-carbon units with each sequential reaction. As fatty acids accumulate in the cytoplasm after synthesis, cells require a way to store them before they lead to a form of cell death termed lipotoxicity [105]. To avoid death, cells sequester fatty acids in the form of triglycerides and sterol esters into lipid droplets. Lipid droplets serve to store lipids for future use in the generation of cellular membranes for proliferation or for energy via B-oxidation. Accumulation of lipid droplets can signal either increased synthesis or decreased oxidation. Glutamine is considered to be a conditionally essential amino acid for certain cancer cells. It can be used to ameliorate reactive oxygen species accumulation through production of glutathione or to anapluerotically support the TCA cycle when pyruvate is being used to produce lactate instead of entering the TCA cycle. All of the above pathways have been established as hallmarks of cellular metabolism in cancer.

1.6.3 Mitochondrial Biology

Mitochondria originated as endosymbiotic bacteria within ancestors of modern eukaryotes [46]. Most mitochondrial genes are located in the nucleus where they are transcribed and translated by the machinery of the host cell. However, a subset of 13 mitochondrial genes, tRNAs, and rRNAs are retained on a ~16 kbp genome within the mitochondrial matrix.

These genes must be transcribed and translated within the mitochondria machinery mostly supplied from the host genome. As mitochondria are the central metabolic hub of the cell, it is reasonable to expect that changes in mitochondria could be involved in metabolic alterations in cancer. Otto Warburg initially proposed this hypothesis in the 1950s [135], however, he spent the remainder of his career unable to demonstrate a causal relationship between mitochondrial function an oncogenesis. Recent advances in mitochondrial biology and cellular metabolism have reinvigorated interest in mitochondria for cancer biology. The relevance of mitochondria carries over into virology as well, since mitochondria are also signaling hubs for programmed cell death and innate immunity. Indeed, a wide variety of pathogens encode proteins which localize to and alter the function of mitochondria [123].

There are few different points at which mitochondrial function can be inhibited. One is the regulation of mitochondrial network morphology. Mitochondrial form interwoven networks of organelles within cells and the form of those networks has been found to have an effect on the metabolism of the cell [7, 82, 131]. Competing processes of fusion and fission govern the level of interconnectedness of the network with more fragmented networks associated with decreased oxygen consumption [45]. Mitochondrial transcription is another possible point of interference in mitochondrial function. Suppression of transcription is best observed in the context of NF-KB activation, which coincidentally occurs during KSHV latency and is facilitated by the viral protein vFLIP. In addition to relocating to the nucleus to turn on expression of NF-KB responsive genes, a portion of liberated RelA localizes to the mitochondria and binds to the mitochondrial genome, inhibiting transcription of mitochondrial genes [64]. A third source of interference is mitochondrial translation. This is observed in disease associated mutants in the human population for a variety of mitochondrial translation machinery components, including tRNA synthetases and mitochondrial ribosomal subunits [12]. In addition, toxicity from antibiotic treatments is often thought to be related to mitochondrial toxicity, which has been shown in the case of the suppression of bone marrow and

deafness [58, 116].

While many cancer cells display decreased mitochondrial respiration, mitochondrial function often remains essential [31]. Mitochondrial ribosomes share a more recent common ancestor with bacterial ribosomes than the eukaryotic ribosomes in mammalian cells. Structural similarity due to that shared ancestry allows for the selective treatment of cells with antibiotics targeting bacterial translation. Cancer cells have been shown to be sensitive to antibiotic treatment in a number of different *in vitro* systems [75].

1.7 Viruses And Cellular Metabolism

Viruses have no inherent metabolism of their own and require host cells to generate the substrates and energy necessary for replication. While it is not obvious that different viruses would have different requirements of cellular metabolism, metabolic characterization of a wide variety of viruses has demonstrated a surprising breadth of metabolic characteristics [110]. This includes not just the requirements of viral genome replication and virus particle assembly, but also the persistence of latent infection.

Recent advances in mass-spectrometry have enabled metabolomic evaluation of viral infection [94]. These advances enabled quantitation of a large number of metabolites simultaneously. Additionally, heavy isotope labeled metabolic substrates can track metabolites through pathways using a technique termed metabolic flux analysis [94, 95, 128, 9, 56]. With these approaches, a number of viruses have been evaluated from a metabolic standpoint, leading to identification of specific pathways which are altered during infection with each virus. These studies did more than just emphasize the presence of metabolic alterations, they also identified druggable metabolic dependencies. Chemical inhibition of steps in glycolysis, glutamine metabolism, and fatty acid synthesis have been shown to reduce viral titers or reduce proliferation or induce cell death in infected cells.

1.8 KSHV and Host Metabolism

Our lab has previously demonstrated that endothelial cells latently infected with KSHV induce the Warburg effect [25]. The observed characteristics includes decreased oxygen consumption, even in the presence of atmospheric oxygen levels. It also includes the extracellular acidification of the media, caused by production of lactate, suggesting that glucose carbon is being shunted into lactate production to regenerate NAD+, presumably to support additional glycolysis. Chemical inhibition of either glycolysis or lactate production selectively induces apoptosis in infected cells. This paper was the first instance of a latent viral infection inducing and requiring Warburg metabolism for the persistence of infected cells. A few years later another group demonstrated that the latent miRNA cluster is sufficient to induce Warburg metabolism during latent KSHV infection of primary lymphatic endothelial cells [142]. The mechanism proposed is that the miRNAs suppress mitochondrial biogenesis through two separate mechanisms. One is the suppression of the mitochondrial heat shock protein HSP9A. HSP9A is essential for the import and export of proteins in the mitochondria and is also predicted to be a target of multiple viral miRNAs. The second gene is EGLN2, which is a prolyl-hydroxylase that negatively regulates HIF stability in the presence of oxygen. When the miRNA knocks EGLN2 down, the predicted effect is HIF stabilization leading to a decrease in mitochondrial biogenesis. The authors show that miRNA over-expression recapitulates the phenotypes of strong suppression of these two genes in both target protein expression, and in the induction of Warburg metabolism. However, there is no demonstration of necessity in the context of viral infection, nor were they able to identify single miRNAs which reproduce the effect in the absence of the entire cluster.

To globally examine the metabolic changes which occur during latent KSHV infection, our lab performed a global metabolomic screen [26]. Nearly 200 different metabolites were analyzed for changes between mock (control infection) and latent KSHV infection in TIME cells. Metabolites from many major metabolic pathways were significantly upregulated at

48- and 96-hours post infection. Over half of the long-chain fatty acids measured were significantly elevated. Following the screen, the lab confirmed that fatty acids accumulate in cells in the form of storage organelles called lipid droplets. These organelles can be stained using lipid specific fluorescent dyes and analyzed by flow cytometry. Importantly, just as with Warburg induction, chemical inhibition of separate steps in the FAS pathway can induce apoptosis in latently infected endothelial cells but not in uninfected controls. The rate limiting step of the FAS pathway involves the enzyme acetyl-CoA carboxylase (ACC1) which can be inhibited with the drug TOFA. Supplementation of TOFA treated cells with the downstream metabolite palmitate was able to partially rescue cell death, indicating that the products of FAS are at least partially required for survival. Work done in parallel by another group also found that FAS is increased and essential for the survival of latently infected PELs [8]. In an additional follow-up paper on our screen, our lab also found that glutamine metabolism is essential for the survival of latently infected endothelial cells [109]. The glutaminase inhibitor BPTES or glutamine removal from the media were both able to induce cell death in latently infected endothelial cells.

1.9 Hypotheses

Latent KSHV infection of endothelial cells induces changes in a number of cellular systems, including metabolism. Metabolomic screening, global gene expression analysis, and proteomic analysis have yielded targets for therapeutic intervention based on upregulated pathways during infection. However, it is possible that KSHV infection induces vulnerabilities in the absence of obvious changes in previous large-scale screens. I hypothesize that whole genome CRISPR/Cas9 screening can identify these vulnerabilities by directly testing for the essentiality of specific genes during latent KSHV infection, and this will form the basis for work in chapter 3. Chapter 4 follows up on CRISP/Cas9 Screening by pursuing mitochondrial translation as a potential therapeutic target during latent KSHV infection. I

hypothesize that inhibition of mitochondrial translation is essential for the proliferation and survival of latently infected cells. The project described chapter 5 follows up on our lab's previous work on fatty acid synthesis. I have two related hypotheses which are at the center of this project. The first is that the latent locus of KSHV is sufficient for the accumulation of lipid droplets during KSHV infection and lipid droplet formation is essential during KSHV infection. The second is that sensitivity to FAS and lipid droplet inhibition are genetically separable based on the presence or absence of the latent miRNA cluster.

Chapter 2

MATERIALS AND METHODS

Cell Lines

TIME cells were maintained in EBM-2 media (Lonza) which was supplemented with an EGM™-2 MV SingeQuot™ Microvascular Endothelial Cell Growth Medium BulletKit™ (Lonza) containing 5% FBS, hydrocortisone, hFGF-B, VEGF, R3-IGF-1, Ascorbic acid, hEGF, as well as gentamycin and amphotericin-B. After the screen was performed, we discovered the presence of *Mycoplasma arginini* in TIME cells. The Plasmotest™ mycoplasma detection kit (Invivogen) was used to find that TIME cells test positive for mycoplasma after a minimum of 72 hours of growth in the absence of antibiotic. This was confirmed by performing a genomic DNA extraction using the PureLink™ Genomic DNA Mini Kit (Invitrogen) followed by the LookOut® Mycoplasma Detection Kit (Sigma-Aldrich). 293 and 293T cells were grown in DMEM (+L-glut, +Pen/Strep, +4.5g/L glucose, +sodium pyruvate) (Fisher). B-cell lymphomas were grown in RPMI 1640 (+L-glut, +Pen/Strep, + 2-mercaptoethanol) (Fisher). iSLK cells for BAC16 virus production were grown in DMEM (+L-glut, +Pen/Strep, +4.5g/L glucose, +sodium pyruvate). All 293T cells, B-cell lymphomas, iSLK cells, and the mitochondrial lacking TIME cells in Figures 4B and 4C were negative for mycoplasma by both the Invivogen and Invitrogen kits listed above.

KSHV Virus

Virus was obtained from two seperate producer cell lines. Patient derived BCBL-1 cells were treated with 12-O-tetradecanoyl-phorbol-13-acetate (TPA to induce reactivation. Cell

supernatants collected after 48 hours, were filtered through 0.45 µm filters and then spun at 25000g for three hours. The virus pellets were then resuspended in serum-free EBM-2 media and stored at -80°C. iSLK cells were treated with sodium butyrate and doxycycline to induce production of BAC16 derived virus. This was used to generate both wild type and ΔmiRNA viruses. Both BAC16 construct containing iSLK lines were gifted to the lab from Rolf Renne. Virus aliquots were prepared from supernatants in the same manner as with BCBL-1 derived virus.

Transfection

293T cells were seeded at ~10k cells per cm2 the night before transfection. Transit 293T (Mirus Bio) was used to transfect plasmids as indicated by the manufacturer. After 24 hours the media on the cells is replaced with fresh serum containing media. In the case of lentivirus production, the masses of each plasmid used were 8 µg of psPAX2, 4 µg of pMD2.G, and 8 µg of the lentiviral vector. Culture supernatants were collected at 48 and 72 hours post transfection and filtered through 0.45 µm filters before aliquoting and freezing.

Proliferation Assay

Time cells were seeded at $1x10^4$ cells per cm2 then treated once settled. After the specified length of time, when assessing cell death, the time cells were treated with trypsin and counted after trypan blue staining for cell viability. When assessing cell proliferation, TIME cells are washed twice with PBS and fixed with 100% methanol. After fixing, the cells were stained with crystal violet for 10 minutes then rinsed with diH2O until dye no longer washes off. The plates are allowed to dry overnight before scanning with a Typhoon imager (GE) using a 532 nm laser and a 670BP30 filter. The resulting images were analyzed in ImageJ to measure cell confluence in each well. The MRPS34 data in figure 2 was obtained by resuspending the crystal violet with 500 µl 10% glacial acetic acid after staining and measuring 200 µl of the

resulting solution in a 96 well plate reader at 570nm. All transformed B-cell proliferation assays began with viable cell concentrations of $2x10^5$. 48 hours after treatment cells were stained with trypan blue and counted using a TC-20 Cell Counter (BioRad).

RT-qPCR

Cell lysates were harvested using Nucleospin RNA II Kits (Macherey Nagel). RNA was quantified by Nanodrop and the quality of each sample was assessed on a 1% agarose gel in tris-acetate-EDTA buffer to ensure that no degradation of samples had occurred. 500 ng of RNA was used for each 20 µL reverse transcription reaction with the iScript Select cDNA Synthesis Kit (BioRad) using poly-dt primers for viral and nuclear genes and random primers when targeting genes encoded in the mitochondrial genome. qPCR was subsequently carried out using SsoAdvanced(TM) Universal SYBR® Green Supermix (BioRad). Primers targeting HPRT were used as a reference and primers targeting mitochondrial genome sequences were used to assess transcript levels. Primer sequences are available in the supplemental primer table.

qPCR for Mitochondrial Genome Quantitation

Cell lysates were harvested using PureLink™ Genomic DNA Mini Kits (Invitrogen). The resulting genomic DNA is used as template for qPCR with SsoAdvancedTM Universal SYBR® Green Supermix (BioRad). Primers targeting Prox1 were used as a reference for cellular genomic DNA and primers targeting the mitochondrial genome were used to quantify mitochondrial genome copy number. Primer sequences are available in the primer table.

CRISPR/Cas9 Whole Genome Library

The one half of the Human Activity-Optimized CRISPR Knockout Library was transformed into Endura electro-competent cells (Lucigen). Sufficient colony forming units to

achieve ~1000x coverage of the library was harvested using the Plasmid Plus Maxi Kit (Qiagen). The resulting plasmid prep was transfected into 293T cells as mentioned above for production of lentivirus. The resulting lysate was titered onto TIME cells using cell viability after selection as a proxy for infection. 36 T225s containing $4.5x10^6$ TIME cells per flask seeding the evening before transduction were treated with the lentiviral library. This amounts to roughly 150 million cells transduced at an MOI of ~0.6 to achieve at least 500x coverage of the library. Transduced time cells were selected for three days and grown for an additional four days until two sets of 34 T225s could be seeded. The day after seeding, one set of the TIME cells was infected with KSHV purified from BCBL-1 cells as previously described (Punjabi et al., 2007). Two days after infection, the TIME cells were split and infected again. The infection rates for the cells were counted by immunofluorescence for LANA and ORF59. For the next 8 days the cells were split every two days and reseeded to 4.5 million TIME cells per flask, maintaining 34 flasks for each sample. At each passage the culture supernatants were collected and dead cell pellets were frozen after centrifugation. At the end of the experiment all live cells were collected and dead cell samples were pooled for uninfected and infected cells. Genomic DNA was harvested from all samples using the Blood and cell culture DNA maxi kit (Qiagen). The genomic DNA was used as template for Illumina sequencing amplicons as described in Wang et al., 2014.

CRISPR/Cas9 Sub-pool Screening

A list of genes for sub-pool screening was generated by taking the top 350 genes by MAGeCK score from the whole genome live cell screen, the top 350 genes by log fold change from the whole genome dead cell screen, and 100 genes which showed no significant change in either direction for both the live and dead cell screens as controls. The sgRNAs targeting those 800 genes were pulled from three published CRISPR/Cas9 screens (add citations). Duplicate sgRNAs were removed and additional 500 non-targeting controls were added. This

pool of sgRNAs was synthesized by Custom Array, Inc. Preparation of library closely followed the Nature Protocols paper from the Zhang lab [66]. The library was amplified using NEBNext High Fidelity PCR Master Mix (New England Biolabs). The PCR product gel purified and cleaned by phenol-chloroform extraction and ethanol precipitation. The amplified library was cloned into linearized lentiCRISPR v2 (Addgene plasmid #52961) by Gibson assembly using NEBuilder® HiFi DNA Assembly Master Mix (New England Biolabs). The resulting product was precipitated with isopropanol and cleaned by phenol-chloroform extraction and ethanol precipitation. The product was resuspended in TE and 100 ng/µl (or 2500 ng for 25 µl competent cells) was transformed into Endura ElectroCompetent cells according to the manufacturer's instructions. Transformation efficiency was determined by spot dilution series and additional transformations were performed to achieve at least 1000x coverage of the library (or ~10 million unique transformants for our ~10,000 sgRNA library). Transformation reactions were incubated in 100 ml LB overnight at 30 °C and then purified using the Maxi EF kit (Machery-Nagel) according to the manufacturer's instructions. The resulting plasmid prep was transfected into 293T cells for lentivirus prep and titering as in the whole genome screen mentioned above. The experiment itself was carried out identically to the whole genome screen, except that the library was roughly 1/9th the size, so the required number of cells was proportionately lower (we used 4 T225s per replicate), and the experiment was done twice. The sequencing was carried out similarly to the whole genome sequencing, except that the library was designed to use the standard Illumina indexing primers, rather than the custom indexing primers used for the Human Activity Optimized CRISPR Knock-out Library.

Analysis of CRISPR/Cas9 Library Screening

Illumina sequencing results were analyzed using MAGeCK version 5.6 [79]. sgRNAs were counted after deconvolution of samples allowing for up to one uncalled base per guide. The

live cell screen was analyzed using uninfected as the control and KSHV infected TIME cells as the treatment group. The sgRNA counts were normalized based on median read counts and the distribution of non-targeting sgRNAs was used to generate the null-distribution. The dead cell sequencing results were analyzed in an identical manner, except the sgRNA counts were normalized based on total read counts. All other parameters used the default settings for MAGeCK.

Western Blot Analysis

Cells were harvested using trypsin to remove adherent cells and then pelleting cells and washing once with PBS. Cell Pellets were lysed with RIPA buffer [50 mM Tris-HCl, pH 7.6, 150 mM NaCl, 1 mM EDTA, 1% Nonidet P-40, 0.5% deoxycholate, 0.1% SDS, 1 mM sodium orthovanadate, 1 mM sodium fluoride, 40 mM β-glycerophosphate, and Complete Mini protease inhibitor tablet (Roche)]. Cell lysate was quantified using the Peirce BCA assay (ThermoFisher Scientific), and equal masses of protein were loaded to a 4-20% polyacrylamide gel (BioRad). The protein was transferred to a PVDF membrane and blotted using the appropriate primary antibody at the dilutions mentioned in the table above. Blots were treated with LI-COR IRdye secondary antibodies prior to imaging on either a LI-COR Odyssey® CLx or Odyssey® Fc system.

Mitochondrial Immunofluorescence

TIME cells were fixed to glass chamber well slides with 4% paraformaldyhyde. After blocking and probing with an anti-COXIV primary antibody and fluorescent secondary antibodies, the cells were mounted with Vectasheild mounting medium w/ DAPI (Vector laboratories). Images were captured using a Retiga R6 camera (Teledyne Photometrics). Images were analyzed in FIJI [112] using macros adapted from [91]. Resulting outputs for mitochondrial number, average length, and total volume were quantified per cell and plotted

in PRISM8 (Graphpad Software).

Mitochondrial Fractionation

Cell pellets were resuspended in PBS and processed using the Mitochondria Isolation Kit for Cultured Cells (ThermoFisher Scientific). The manufacturer's recommendations were followed to achieve a high purity mitochondrial fraction through differential centrifugation which after purification was lysed with RIPA buffer. Protein concentrations of the resulting lysate, paired cytoplasmic fraction, and whole cell lysate were quantified and equal masses of each fraction were processed as previously mentioned. To check the validity of the purification blots were probed with primary antibodies targeting 5 mitochondrial proteins to confirm enrichment and GAPDH to check for cytoplasmic contamination of the mitochondrial fraction.

Lipid Droplet Assay

48 hours post infection, mock, KSHV infected, and KLAR-hdAd5 infected TIME cells were resuspended and fixed with 4% paraformaldehyde for 10 minutes at room temperature. The lipid droplet fluorescence assay kit (Cayman Chemical) was used for the preparation and staining of samples. The cell suspensions were washed and stained with the lipid specific dye Nile Red, which fluoresces green-yellow when associated with neutral lipids within lipid droplets upon excitation with a 488nm laser, for 15 minutes. Individual samples were analyzed on a FACS Canto Cell analyzer (BD Biosciences). Analysis was performed with FloJo flow cytometry software (Becton, Dickinson and Company).

Table 2.1: Oligonucleotides

Oligo Name	Sequence (5'-3')	Application
NTC_F	AAAGGACGAAACACCGACAT TGTTAGTAACGACTCGTTTT AGAGCTAGAAATAGCAAG	Cloning NTC sgRNA into pRRL LentiCRISPR
NTC_R	CTTGCTATTTCTAGCTCTAA AACGAGTCGTTACTAACAAT GTCGGTGTTTCGTCCTTT	Cloning NTC sgRNA into pRRL LentiCRISPR
MRPS34_sgRNA_AF	AAAGGACGAAACACCGAAAT GGAGACACAAGCACCGGTTT TAGAGCTAGAAATAGCAAG	Cloning MRPS34 targeting sgRNA into pRRL LentiCRISPR
MRPS34_sgRNA_AR	CTTGCTATTTCTAGCTCTAA AACCGGTGCTTGTGTCTCCA TTTCGGTGTTTCGTCCTTT	Cloning MRPS34 targeting sgRNA into pRRL LentiCRISPR
MRPS34_sgRNA_BF	AAAGGACGAAACACCGGAAG ACTGAGAGCGAGGCGGTTTT AGAGCTAGAAATAGCAAG	Cloning MRPS34 targeting sgRNA into pRRL LentiCRISPR
MRPS34_sgRNA_BR	CTTGCTATTTCTAGCTCTAA AACCGCCTCGCTCTCAGTCT TCCGGTGTTTCGTCCTTT	Cloning MRPS34 targeting sgRNA into pRRL LentiCRISPR
BCL2L1_sgRNA_AF	AAAGGACGAAACACCGAGTA AAGCAAGCGCTGAGGGGTTT TAGAGCTAGAAATAGCAAG	Cloning BCL2L1 targeting sgRNA into pRRL LentiCRISPR

Continued on the next page

Table 2.1 – continued from previous page

Oligo Name	Sequence (5'-3')	Application
BCL2L1_sgRNA_AR	CTTGCTATTTCTAGCTCTAA AACCCCTCAGCGCTTGCTTT ACTCGGTGTTTCGTCCTTT	Cloning BCL2L1 targeting sgRNA into pRRL LentiCRISPR
BCL2L1_sgRNA_BF	AAAGGACGAAACACCGCAGC AGTAAAGCAAGCGCTGGTTT TAGAGCTAGAAATAGCAAG	Cloning BCL2L1 targeting sgRNA into pRRL LentiCRISPR
BCL2L1_sgRNA_BR	CTTGCTATTTCTAGCTCTAA AACCAGCGCTTGCTTTACTG CTGCGGTGTTTCGTCCTTT	Cloning BCL2L1 targeting sgRNA into pRRL LentiCRISPR
HPRT_F	GAACGTCTTGCTCGAGATGT G	RT-qPCR Reference for Gene Expression
HPRT_R	CCAGCAGGTCAGCAAAGAAT T	RT-qPCR Reference for Gene Expression
PROX1_F	CCAAGGTTCTGAGCAGGATG T	qPCR Reference for Genomic DNA
PROX1_R	CATACGAGTTCGCCCTCTTC A	qPCR Reference for Genomic DNA

Continued on the next page

Table 2.1 – continued from previous page

Oligo Name	Sequence (5'-3')	Application
MT-CO2_F	ACGCATCCTTTACATAACAGAC	RT-qPCR for mitochondrial transcripts using random hexamer primers and for mitochondrial genome quantification
MT-CO2_R	GCCAATTGATTTGATGGTAAGG	RT-qPCR for mitochondrial transcripts using random hexamer primers and for mitochondrial genome quantification
MT-ND6_F	GCTTTGTATGATTATGGGCGT	RT-qPCR for mitochondrial transcripts using random hexamer primers

Continued on the next page

Table 2.1 – continued from previous page

Oligo Name	Sequence (5'-3')	Application
MT-ND6_R	CACCAACAAACAATGTTCAACC	RT-qPCR for mitochondrial transcripts using random hexamer primers
MT-ND4_F	CCCTTCCTTGTACTATCCCT	RT-qPCR for mitochondrial transcripts using random hexamer primers
MT-ND4_R	TTTGTCGTAGGCAGATGGAG	RT-qPCR for mitochondrial transcripts using random hexamer primers
RT_vFLIP_F	AGCTGTGTGCGAGGGATATT	RT-qPCR for viral transcripts
RT_vFLIP_R	GGCGATAGTGTTGGGAGTGT	RT-qPCR for viral transcripts
RT_vCyc_F	ACGAGGTCAACACCCTGATT	RT-qPCR for viral transcripts
RT_vCyc_R	CGCCTGTAGAACGGAAACAT	RT-qPCR for viral transcripts

Continued on the next page

Table 2.1 – continued from previous page

Oligo Name	Sequence (5'-3')	Application
RT_LANA_F	TTGCCACCCACGCAGTCT	RT-qPCR for viral transcripts
RT_LANA_R	GGACGCATAGGTGTTGAAGA GTCT	RT-qPCR for viral transcripts
RT_K12_F	AGGCTTAACGGTGTTTGTGG	RT-qPCR for viral transcripts
RT_K12_R	CTCGTGTCCTGAATGCTACG	RT-qPCR for viral transcripts
RT_miRNACluster_F	CCCGCACCGCCGATGGATTA	RT-qPCR for viral transcripts
RT_miRNACluster_R	TCCACGCTCGCGTATGCCTC	RT-qPCR for viral transcripts
sgRNA_barcode_F	ATGATACGGCGACCACCGAG ATCTACACCGACTCGGTGCC ACTTTT	Generation of template for Illumina sequencing
sgRNA_barcode_R_1	CAAGCAGAAGACGGCATACG AGATCGCTGGATTTTTCTTG GGTAGTTTGCAGTTTT	Generation of template for Illumina sequencing
sgRNA_barcode_R_2	CAAGCAGAAGACGGCATACG AGATCTAACTCGGTTTCTTG GGTAGTTTGCAGTTTT	Generation of template for Illumina sequencing

Continued on the next page

Table 2.1 – continued from previous page

Oligo Name	Sequence (5'-3')	Application
sgRNA_barcode_R_3	CAAGCAGAAGACGGCATACG AGATCTAACAGTTTTTCTTG GGTAGTTTGCAGTTTT	Generation of template for Illumina sequencing
sgRNA_barcode_R_4	CAAGCAGAAGACGGCATACG AGATCATACTCAATTTCTTGG GTAGTTTGCAGTTTT	Generation of template for Illumina sequencing
Illumina_HiSeq_Read1	CGGTGCCACTTTTTCAAGTT GATAACGGACTAGCCTTATT TTAACTTGCTATTTCTAGCT CTAAAAC	Read 1 HiSeq Primer
Illumina_HiSeq_Index	TTTCAAGTTACGGTAAGCAT ATGATAGTCCATTTTAAAAC ATAATTTTAAAACTGCAAAC TACCCAAGAAA	Indexing HiSeq Primer
NGS-Lib-Fwd-1	AATGATACGGCGACCACCGA GATCTACACTCTTTCCCTACA CGACGCTCTTCCGATCTTAA GTAGAGGCTTTATATATCTT GTGGAAAGGACGAAACACC	Generation of staggered template for Illumina sequencing of sub-pool

Continued on the next page

Table 2.1 – continued from previous page

Oligo Name	Sequence (5'-3')	Application
NGS-Lib-Fwd-2	AATGATACGGCGACCACCGA GATCTACACTCTTTCCCTACA CGACGCTCTTCCGATCTATC ATGCTTAGCTTTATATATCT TGTGGAAAGGACGAAACACC	Generation of staggered template for Illumina sequencing of sub-pool
NGS-Lib-Fwd-3	AATGATACGGCGACCACCGA GATCTACACTCTTTCCCTACA CGACGCTCTTCCGATCTGAT GCACATCTGCTTTATATATC TTGTGGAAAGGACGAAACAC C	Generation of staggered template for Illumina sequencing of sub-pool
NGS-Lib-Fwd-4	AATGATACGGCGACCACCGA GATCTACACTCTTTCCCTACA CGACGCTCTTCCGATCTCGA TTGCTCGACGCTTTATATAT CTTGTGGAAAGGACGAAACA CC	Generation of staggered template for Illumina sequencing of sub-pool
NGS-Lib-Fwd-5	AATGATACGGCGACCACCGA GATCTACACTCTTTCCCTACA CGACGCTCTTCCGATCTTCG ATAGCAATTCGCTTTATATA TCTTGTGGAAAGGACGAAAC ACC	Generation of staggered template for Illumina sequencing of sub-pool

Continued on the next page

Table 2.1 – continued from previous page

Oligo Name	Sequence (5'-3')	Application
NGS-Lib-Fwd-6	AATGATACGGCGACCACCGA GATCTACACTCTTTCCCTACA CGACGCTCTTCCGATCTATC GATAGTTGCTTGCTTTATAT ATCTTGTGGAAAGGACGAAA CACC	Generation of staggered template for Illumina sequencing of sub-pool
NGS-Lib-Fwd-7	AATGATACGGCGACCACCGA GATCTACACTCTTTCCCTACA CGACGCTCTTCCGATCTGAT CGATCCAGTTAGGCTTTATA TATCTTGTGGAAAGGACGAA ACACC	Generation of staggered template for Illumina sequencing of sub-pool
NGS-Lib-Fwd-8	AATGATACGGCGACCACCGA GATCTACACTCTTTCCCTACA CGACGCTCTTCCGATCTCGA TCGATTTGAGCCTGCTTTAT ATATCTTGTGGAAAGGACGA AACACC	Generation of staggered template for Illumina sequencing of sub-pool

Continued on the next page

Table 2.1 – continued from previous page

Oligo Name	Sequence (5'-3')	Application
NGS-Lib-Fwd-9	AATGATACGGCGACCACCGA GATCTACACTCTTTCCCTACA CGACGCTCTTCCGATCTACG ATCGATACACGATCGCTTTA TATATCTTGTGGAAAGGACG AAACACC	Generation of staggered template for Illumina sequencing of sub-pool
NGS-Lib-Fwd-10	AATGATACGGCGACCACCGA GATCTACACTCTTTCCCTACA CGACGCTCTTCCGATCTTAC GATCGATGGTCCAGAGCTTT ATATATCTTGTGGAAAGGAC GAAACACC	Generation of staggered template for Illumina sequencing of sub-pool
NGS-Lib-KO-Rev- 1	CAAGCAGAAGACGGCATACG AGATTGTTGCCAGTGACTGG AGTTCAGACGTGTGCTCTTC CGATCTCCGACTCGGTGCCA CTTTTTCAA	Generation of template for Illumina sequencing with unique sample bar code
NGS-Lib-KO-Rev- 2	CAAGCAGAAGACGGCATACG AGATGTCAGTGTGTGACTGG AGTTCAGACGTGTGCTCTTC CGATCTCCGACTCGGTGCCA CTTTTTCAA	Generation of template for Illumina sequencing with unique sample bar code

Continued on the next page

Table 2.1 – continued from previous page

Oligo Name	Sequence (5'-3')	Application
NGS-Lib-KO-Rev- 3	CAAGCAGAAGACGGCATACG AGATACGTTGGAGTGACTGG AGTTCAGACGTGTGCTCTTC CGATCTCCGACTCGGTGCCA CTTTTTCAA	Generation of template for Illumina sequencing with unique sample bar code
NGS-Lib-KO-Rev- 4	CAAGCAGAAGACGGCATACG AGATCGCAAGAAGTGACTGG AGTTCAGACGTGTGCTCTTC CGATCTCCGACTCGGTGCCA CTTTTTCAA	Generation of template for Illumina sequencing with unique sample bar code
NGS-Lib-KO-Rev- 5	CAAGCAGAAGACGGCATACG AGATGAAGCCAAGTGACTGG AGTTCAGACGTGTGCTCTTC CGATCTCCGACTCGGTGCCA CTTTTTCAA	Generation of template for Illumina sequencing with unique sample bar code
NGS-Lib-KO-Rev- 6	CAAGCAGAAGACGGCATACG AGATCTTCCAGAGTGACTGG AGTTCAGACGTGTGCTCTTC CGATCTCCGACTCGGTGCCA CTTTTTCAA	Generation of template for Illumina sequencing with unique sample bar code

Continued on the next page

Table 2.1 – continued from previous page

Oligo Name	Sequence (5'-3')	Application
NGS-Lib-KO-Rev- 7	CAAGCAGAAGACGGCATACG AGATTCGAGAAGGTGACTGG AGTTCAGACGTGTGCTCTTC CGATCTCCGACTCGGTGCCA CTTTTTCAA	Generation of template for Illumina sequencing with unique sample bar code
NGS-Lib-KO-Rev- 8	CAAGCAGAAGACGGCATACG AGATATCCTCAGGTGACTGG AGTTCAGACGTGTGCTCTTC CGATCTCCGACTCGGTGCCA CTTTTTCAA	Generation of template for Illumina sequencing with unique sample bar code
NGS-Lib-KO-Rev- 9	CAAGCAGAAGACGGCATACG AGATAGAGAAGGGTGACTGG AGTTCAGACGTGTGCTCTTC CGATCTCCGACTCGGTGCCA CTTTTTCAA	Generation of template for Illumina sequencing with unique sample bar code
NGS-Lib-KO-Rev- 10	CAAGCAGAAGACGGCATACG AGATAATACGCGGTGACTGG AGTTCAGACGTGTGCTCTTC CGATCTCCGACTCGGTGCCA CTTTTTCAA	Generation of template for Illumina sequencing with unique sample bar code

Table 2.2: Plasmids

Name	Type	Product #	Source	Depositor	Application	Ref
pRRL LentiCRISPR	Plasmid		Kind gift of Daniel Stetson (University of Washington)		CRISPR/Cas9 Gene Knock-out	
LentiCRISPR v2	Plasmid	52961	Addgene	Feng Zhang	CRISPR/Cas9 Gene Knock-out	[111]
Human Activity-Optimized CRISPR Knockout Library	Pooled Library	1000000067	Addgene	David Sabatini, Eric Lander	Whole Genome CRISPR/Cas9 Screening	[132]
pMA3287	Plasmid	46883	Addgene	Mikhail Alexeyev	Mitochondria genome curing	[115]
pMA3288	Plasmid	46885	Addgene	Mikhail Alexeyev	Mitochondria genome curing	[115]

Continued on the next page

Table 2.2 – continued from previous page

Name	Type	Product #	Source	Depositor	Application	Ref
pLenti CMV rtTA3 Hygro (w785-1)	Plasmid	26730	Addgene	Eric Campeau	Tet-on effector expression	
pLX302	Plasmid	25896	Addgene	David Root	Gateway™ Destination Vector	[139]
pDONR221	Plasmid	12536017	ThermoFisher		For making Gateway™ Entry Plasmids	
pPUR-KLAR	Plasmid		Kind gift of Rolf Renne (University of Florida)		Expression	
p3xFLAGCMV 10	Plasmid		Lagunoff Lab		Expression	
3XFLAG10-vCyc	Plasmid		Lagunoff Lab		Expression	
3XFLAG10-KapC	Plasmid		Lagunoff Lab		Expression	
3XFLAG10-KapB	Plasmid		Lagunoff Lab		Expression	

Continued on the next page

Table 2.2 – continued from previous page

Name	Type	Product #	Source	Depositor	Application	Ref
pcDNA3.1	Plasmid				Expression	
pcDNA3 3XFLAG LANA	Plasmid		Kind gift of Tim Rose (University of Washington)		Expression	
pLX302_3xFLAG-vFLIP-HS	Plasmid		This thesis		Expression	
pLX302-vFLIP-HS_V5	Plasmid		This thesis		Expression	
psPAX2	Plasmid	12260	Addgene	Didier Trono	Lentiviral packaging plasmid	
pMD2.G	Plasmid	12259	Addgene	Didier Trono	VSV-G Env Expressing Plasmid	
pC4HSU_KLAR	BAC		Lagunoff Lab		Expression of KSHV Latent Locus	

Table 2.3: Primary Antibodies

Target Protein	Company	Product #	Species	Western Blot Dilution	IFA Dilution
ATP5A	Abcam	ab110411	Mouse	1:1000	N/A
UQCRC2					
SDHB					
MT-CO2					
NDUFB8					
MT-CO2	Abcam	ab110258	Mouse	1:1000	1:500
GAPDH	Proteintech	60004-1-1g	Mouse	1:5000	N/A
COXIV	Cell Signaling	4850	Rabbit	N/A	1:200
COXIV	Cell Signaling	11967	Mouse	N/A	1:200
LANA	Gift from A. Polson and D. Ganem		Rabbit	1:2000	1:1000
ORF59	Advanced Biotechnologies	13-211-100	Mouse	N/A	1:3000
FLAG Tag	Sigma-Aldrich	F3165	Mouse	1:1000	1:500
V5 Tag	Proteintech	14440-1-ap	Rabbit	1:1000	1:200
MRPS34	Novus	NBP2-45432	Mouse	1:1000	N/A

Table 2.4: Secondary Antibodies

Antibody Name	Target Species	Company	Product #	Species	Western Blot Dilution	IFA Dilution
IRDye 680RD	Mouse	LI-COR	926-68070	Goat	1:10,000	N/A
IRDye 680RD	Rabbit	LI-COR	926-68071	Goat	1:10,000	N/A
IRDye 800CW	Mouse	LI-COR	926-32210	Goat	1:10,000	N/A
IRDye 800CW	Rabbit	LI-COR	926-32211	Goat	1:10,000	N/A
Alexa Fluor 488 F(ab')2 fragment	Mouse	Invitrogen	A-11017	Goat	N/A	1:1000
Alexa Fluor 488 F(ab')2 fragment	Rabbit	Invitrogen	A-11070	Goat	N/A	1:1000
Alexa Fluor 594 F(ab')2 fragment	Mouse	Invitrogen	A-11020	Goat	N/A	1:1000
Alexa Fluor 594 F(ab')2 fragment	Rabbit	Invitrogen	A-11072	Goat	N/A	1:1000

Chapter 3

CRISPR/CAS9 SCREENING FOR ESSENTIAL GENES DURING LATENT KSHV INFECTION OF HUMAN ENDOTHELIAL CELLS

3.2 is adapted from an accepted manuscript [57], 3.3 is currently unpublished data

3.1 Abstract

Kaposi's Sarcoma associated-Herpesvirus (KSHV) is the etiologic agent of Kaposi's Sarcoma (KS) and Primary Effusion Lymphoma (PEL). The main proliferating component of KS tumors is a cell of endothelial origin termed the spindle cell. Spindle cells are predominantly latently infected with only a small percentage of cells undergoing viral replication. As there is no direct treatment for latent KSHV, identification of host vulnerabilities in latently infected endothelial cells could be exploited to inhibit KSHV associated tumor cells. Using a pooled CRISPR/Cas9 lentivirus library, we identified host factors which are essential for the survival or proliferation of latently infected endothelial cells in culture, but not their uninfected counterparts. To distinguish between knock-outs inhibiting cellular proliferation and those inducing cell death, we collected the dead cells floating in the culture supernatant and sequenced this population to positively screen for the induction of cell death in addition to sequencing the live cells to negatively screen for the inhibition of proliferation. To validate our initial screen, we synthesized a custom CRISPR/Cas9 lentiviral library targeting the top 350 genes by MAGeCK score from our live cell screen, as well as the top 350 genes by median log fold change in our dead cell screen. This sub-pool screen gave us the power

to identify strongly selective hits from our initial screen, including the negative apoptosis regulator BCL2L1.

3.2 Introduction

Kaposi's Sarcoma (KS) predominately arises in the context of immune suppression in the developed world but not in sub-Saharan Africa, where KS is common in both HIV positive and negative patients [18]. While antiretroviral therapy eliminates KS in many patients with AIDS, not all cases are resolved. KS tumors are complex, highly vascularized lesions whose primary proliferating component is the spindle cell, a cell that expresses markers of endothelium. The majority of spindle cells are latently infected with KSHV with just a small percentage of cells expressing lytic transcripts [146]. Herpesvirus infections are classically treated with nucleoside analogs but this has not been effective for KS treatment, presumably because cellular latency is the predominant state of the virus in the tumor cells. Traditional chemotherapeutics are effective in some patients, but their toxicity and inaccessibility mean they are not realistic options in settings with limited resources where KSHV is more prevalent [18]. Therefore, a comprehensive examination of the cellular processes which are essential for latently infected cells has utility in identifying gene products that can be targeted with existing, accessible therapies.

Cultured human endothelial cells infected with KSHV recapitulates the proportion of latent and lytic cells seen within KS tumors providing a culture model for KSHV latency in tumors [74]. Using cell culture systems, our lab has identified several cellular pathways which can be used to selectively target latently infected cells *in vitro* [25, 26, 109, 121]. Recently developed lentivirus encoded CRISPR/Cas9 based screening platforms have enabled large scale interrogation of so called Achilles genes within a population of human cells [132]. These screens can be used to identify factors that are essential to the survival of cancer cells. Similar approaches have been used to identify genes which are critical for the survival of

B-cell lymphomas infected with EBV [85]. Another important study identified genes critical for survival of primary effusion lymphoma cells (PELs) [88]. PELs are a non-Hodgkin's B-cell lymphoma which all maintain latent KSHV infection, though a majority of cases also contain EBV. While many interesting genes were identified and the study was able to compare EBV positive to EBV negative PELs, it lacked a true uninfected control for KSHV. Another study utilized KSHV infected rat mesenchymal embryonic stem cells [48] to identify genes important for KSHV transformation in this rat cell system. However, to date no CRISPR/Cas9 essentiality screens have been performed in a human cell type relevant to KS spindle cells with mock infected controls. To identify host factors which are required for survival and proliferation of latently infected endothelial cells, we performed a genome-wide CRISPR/Cas9 screen followed by smaller sub-pool screening to validate candidate essential genes in human tert-immortalized microvascular endothelial cells (TIME cells).

3.3 Results

3.3.1 Whole Genome Screen Results

To determine the host factors required for cells latently infected with KSHV to proliferate and survive, we used half of the Human Activity-Optimized CRISPR/Cas9 lentivirus library [132] to generate a mutant pool of cells containing gRNA and Cas9 expressing lentiviruses targeting 18,166 human genes with 5 gRNAs each (Figure 3.1A). Approximately 150 million cells were transduced at an MOI of ~0.6 and two days later were placed under selection with puromycin for three days, the time by which non-transduced TIME cells in a control flask were completely killed. The cells were grown out for an additional two days and then split into two sets of flasks, each representing approximately 1000x coverage of the lentiviral library in 90 million cells. Once the cells were settled half were infected with KSHV obtained from induction of BCBL-1 cells. Two days later these cells were reinfected with KSHV to ensure that infection rates remained sufficiently high for the remainder of the

experiment. After the second infection 91% of cells stained positive for LANA, a marker of KSHV latency. For eight days the cells were passaged, splitting to maintain representation of the library. At each passage the dead cells in the supernatant of both the control and KSHV infected samples were pelleted. At the end of the 8 days, the live cells were harvested. Genomic DNA was harvested from the live cell samples as well as the dead cell samples and next-generation sequencing libraries were prepared and sequenced. gRNA abundances were calculated and the changes in representation of guides targeting different genes between infected and uninfected samples using MAGeCK [79]. sgRNAs depleted in the live cells infected with KSHV relative to the uninfected population were identified (Figure 3.1B and Supplementary Table 1). 146 genes were significantly depleted from the live cell population of latently infected TIME cells as compared to the uninfected TIME cells using a false discovery rate cut-off of 0.25 (Table3.1). Importantly, this list is enriched for genes whose products localize to mitochondria, which will be addressed in chapter 4 of this thesis. In addition to essential factors, two genes, KCTD10 and HSPA4, were significantly enriched in our live cell screen during KSHV infection relative to mock infection. Their enrichment in our live cell screen implies that these two genes restrict the growth of KSHV infected cells but not mock infected controls. ~1600 genes were enriched in the dead cell population by greater than 2.75 fold median log fold change across sgRNAs for each gene when comparing the infected cells to the uninfected cells (Figure 3.2 and Supplemental Table 2). From the whole genome screen, groups of possible essential genes can be identified and pursued with targeted screening.

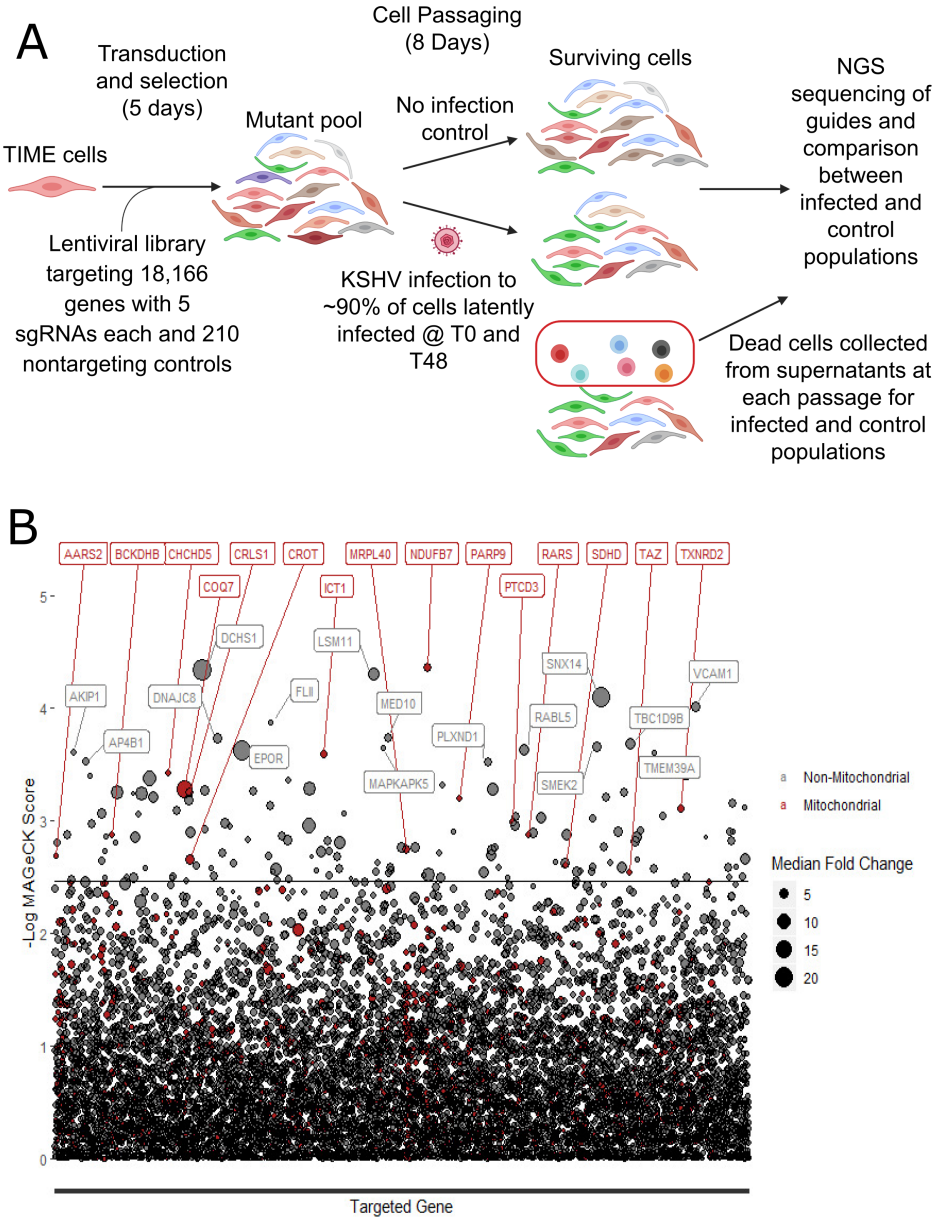

Figure 3.1: CRISPR/Cas9 Whole Genome Screen to Identify Essential Host Factors During KSHV Infection of Endothelial Cells: (A) Schematic of TIME cell whole genome screen of KSHV infected cells. (B) Plot of the results of the live cell screen. The back line represents the false discovery rate cut-off of 0.25. The size of the circles represents the magnitude of the median log fold change for all sgRNAs for that particular gene. All red circles accompanied by red text are genes whose gene products localize to mitochondria.

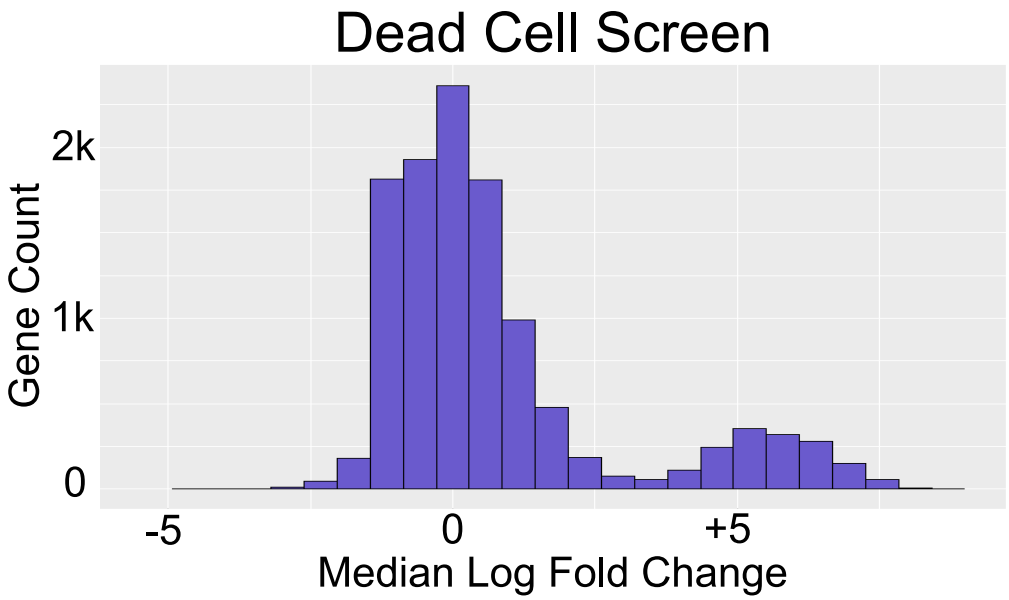

Figure 3.2: Dead Cell Screen Histogram: Genes plotted using the median log-fold change data from the dead cell screen. There is a bi-modal distribution where a subset of genes in the library fall into a second peak where the median for those genes represents a 2.75 or greater log2 fold change in KSHV infected cells when compared to uninfected controls.

Table 3.1: List of Genes Significantly Depleted

Gene Symbol	Gene Name	sg RNAs	Rank	sgRNAs Depleted	Median Log FC
NDUFB7	NADH:ubiquinone oxidoreductase subunit B7	5	1	4	-2.1
DCHS1	dachsous cadherin-related 1	5	2	4	-4.4
LSM11	LSM11, U7 small nuclear RNA associated	5	3	5	-3.0
SNX14	sorting nexin 14	5	4	3	-4.2
VCAM1	vascular cell adhesion molecule 1	5	5	4	-2.4
FLII	FLII actin remodeling protein	5	6	2	-0.2
DNAJC8	DnaJ heat shock protein family (Hsp40) member C8	5	7	4	-2.4
MED10	mediator complex subunit 10	5	8	5	-1.7
TBC1D9B	TBC1 domain family member 9B	5	9	4	-2.5
SMEK2	protein phosphatase 4 regulatory subunit 3B	5	10	5	-2.1
MAPKAPK5	MAPK activated protein kinase 5	5	11	3	-0.5
RABL5	RAB5C, member RAS oncogene family	5	12	3	-2.5
EPOR	erythropoietin receptor	4	13	4	-4.3
TMEM39A	transmembrane protein 39A	5	14	2	-0.2
AKIP1	A-kinase interacting protein 1	4	15	2	-0.8

Continued on the next page

Table 3.1 – continued from previous page

Gene Symbol	Gene Name	sg RNAs	Rank	sgRNAs Depleted	Median Log FC
ICT1	mitochondrial ribosomal protein L58	5	16	3	-1.5
AP4B1	adaptor related protein complex 4 subunit beta 1	5	17	5	-1.7
PLXND1	plexin D1	4	18	4	-2.0
UBQLN1	ubiquilin 1	5	19	5	-3.3
CHCHD5	coiled-coil-helix-coiled-coil-helix domain containing 5	4	20	2	-0.9
ARHGAP22	Rho GTPase activating protein 22	5	21	2	-0.3
CCDC71L	coiled-coil domain containing 71 like	5	22	4	-3.5
GLG1	golgi glycoprotein 1	4	23	3	-1.1
NSF	N-ethylmaleimide sensitive factor, vesicle fusing ATPase	5	24	3	-0.9
COQ7	coenzyme Q7, hydroxylase	5	25	4	-3.9
POLR1C	RNA polymerase I and III subunit C	5	26	5	-2.9
HEXB	hexosaminidase subunit beta	5	27	5	-3.1
DCUN1D5	defective in cullin neddylation 1 domain containing 5	4	28	3	-2.2
FAM171B	family with sequence similarity 171 member B	5	29	5	-1.8
CRLS1	cardiolipin synthase 1	5	30	5	-2.1

Continued on the next page

Table 3.1 – continued from previous page

Gene Symbol	Gene Name	sg RNAs	Rank	sgRNAs Depleted	Median Log FC
BRD2	bromodomain containing 2	5	31	4	-3.1
SYDE2	synapse defective Rho GTPase homolog 2	5	32	5	-1.8
CAPS	calcyphosine	5	33	4	-3.2
C4orf29	abhydrolase domain containing 18	5	34	1	0.2
CCNL2	cyclin L2	5	35	5	-2.7
SPC24	SPC24 component of NDC80 kinetochore complex	5	36	4	-1.8
PARP9	poly(ADP-ribose) polymerase family member 9	5	37	3	-1.2
CREBRF	CREB3 regulatory factor	5	38	5	-2.2
ZNF462	zinc finger protein 462	5	39	4	-2.1
FKTN	fukutin	5	40	4	-2.0
ZNF813	zinc finger protein 813	5	41	2	-0.2
TXNRD2	thioredoxin reductase 2	5	42	5	-1.6
CMKLR1	chemerin chemokine-like receptor 1	4	43	3	-2.0
KCNJ12	potassium inwardly rectifying channel subfamily J member 12	5	44	1	-0.1
ATL1	atlastin GTPase 1	5	45	5	-2.2
CACNB1	calcium voltage-gated channel auxiliary subunit beta 1	5	46	4	-1.1
TOR1AIP1	torsin 1A interacting protein 1	5	47	4	-1.4

Continued on the next page

Table 3.1 – continued from previous page

Gene Symbol	Gene Name	sg RNAs	Rank	sgRNAs Depleted	Median Log FC
PTRHD1	peptidyl-tRNA hydrolase domain containing 1	5	48	4	-1.8
SLC6A15	solute carrier family 6 member 15	5	49	4	-1.5
RMI1	RecQ mediated genome instability 1	5	50	4	-2.5
PTCD3	pentatricopeptide repeat domain 3	5	51	5	-1.7
DYNC1I2	dynein cytoplasmic 1 intermediate chain 2	5	52	4	-2.2
ARHGEF18	Rho/Rac guanine nucleotide exchange factor 18	5	53	4	-2.0
PTPN14	protein tyrosine phosphatase non-receptor type 14	5	54	4	-2.4
HECTD1	HECT domain E3 ubiquitin protein ligase 1	5	55	4	-3.5
EFCAB13	EF-hand calcium binding domain 13	5	56	4	-0.9
DCUN1D2	defective in cullin neddylation 1 domain containing 2	5	57	3	-1.3
THEMIS2	thymocyte selection associated family member 2	5	58	5	-1.5
ZNF382	zinc finger protein 382	5	59	4	-1.3
STK17A	serine/threonine kinase 17a	5	60	3	-2.4

Continued on the next page

Table 3.1 – continued from previous page

Gene Symbol	Gene Name	sg RNAs	Rank	sgRNAs Depleted	Median Log FC
ZNF483	zinc finger protein 483	5	61	2	-0.2
OSTF1	osteoclast stimulating factor 1	5	62	2	-0.2
CRTC3	CREB regulated transcription coactivator 3	5	63	3	-2.8
RBPMS	RNA binding protein, mRNA processing factor	5	64	4	-2.1
BCKDHB	branched chain keto acid dehydrogenase E1 subunit beta	4	65	3	-0.9
SEC24B	SEC24 homolog B, COPII coat complex component	5	66	4	-2.6
RARS	arginyl-tRNA synthetase 1	5	67	3	-0.9
ADD3	adducin 3	5	68	4	-2.1
GBP4	guanylate binding protein 4	5	69	5	-2.1
ATXN7L3	ataxin 7 like 3	5	70	2	-0.1
WNT9A	Wnt family member 9A	4	71	1	1.0
C7orf43	microtubule associated protein 11	5	72	4	-2.5
TFEB	transcription factor EB	4	73	3	-2.5
GLCCI1	glucocorticoid induced 1	5	74	4	-2.2
EXOSC5	exosome component 5	5	75	3	-0.7
ZNF438	zinc finger protein 438	5	76	4	-1.8
IL15	interleukin 15	5	77	5	-1.7
TDRD3	tudor domain containing 3	4	78	4	-2.2

Continued on the next page

Table 3.1 – continued from previous page

Gene Symbol	Gene Name	sg RNAs	Rank	sgRNAs Depleted	Median Log FC
ITSN2	intersectin 2	5	79	3	-3.0
BLMH	bleomycin hydrolase	5	80	2	-0.3
ABCB1	ATP binding cassette subfamily B member 1	5	81	5	-1.3
POU4F1	POU class 4 homeobox 1	5	82	4	-1.6
MMS22L	MMS22 like, DNA repair protein	5	83	4	-2.3
MXD3	MAX dimerization protein 3	5	84	4	-2.2
SP110	SP110 nuclear body protein	5	85	4	-1.8
MRPL40	mitochondrial ribosomal protein L40	5	86	4	-2.0
POLE4	DNA polymerase epsilon 4, accessory subunit	4	87	3	-2.4
ATP6V1F	ATPase H+ transporting V1 subunit F	5	88	2	-0.6
IL17RA	interleukin 17 receptor A	5	89	4	-1.6
HSPBP1	HSPA (Hsp70) binding protein 1	5	90	3	-2.7
NPFF	neuropeptide FF-amide peptide precursor	5	91	4	-1.1
DTWD2	DTW domain containing 2	5	92	5	-1.7
AARS2	alanyl-tRNA synthetase 2, mitochondrial	5	93	2	-0.1

Continued on the next page

Table 3.1 – continued from previous page

Gene Symbol	Gene Name	sg RNAs	Rank	sgRNAs Depleted	Median Log FC
POLE	DNA polymerase epsilon, catalytic subunit	5	94	4	-2.7
FIGNL1	fidgetin like 1	4	95	4	-1.2
ITFG2	integrin alpha FG-GAP repeat containing 2	5	96	4	-1.8
HIP1R	huntingtin interacting protein 1 related	5	97	1	0.2
ZNF837	zinc finger protein 837	5	98	4	-2.5
TEX2	testis expressed 2	5	99	2	0.0
CROT	carnitine O-octanoyltransferase	4	100	4	-2.3
ATP11C	ATPase phospholipid transporting 11C	4	101	4	-1.5
RRNAD1	ribosomal RNA adenine dimethylase domain containing 1	5	102	2	-0.3
SRFBP1	serum response factor binding protein 1	5	103	2	-0.6
EIF3L	eukaryotic translation initiation factor 3 subunit L	5	104	5	-1.3
MAGI1	membrane associated guanylate kinase, WW and PDZ domain containing 1	5	105	3	-0.6

Continued on the next page

Table 3.1 – continued from previous page

Gene Symbol	Gene Name	sg RNAs	Rank	sgRNAs Depleted	Median Log FC
SDCCAG8	serologically defined colon cancer antigen 8	4	106	3	-2.1
CUL7	cullin 7	5	107	3	-1.2
SDHD	succinate dehydrogenase complex subunit D	5	108	3	-1.2
SLC7A1	solute carrier family 7 member 1	4	109	4	-1.6
ZNF566	zinc finger protein 566	5	110	1	0.0
ZNF343	zinc finger protein 343	5	111	3	-2.0
SULT1E1	sulfotransferase family 1E member 1	5	112	4	-2.7
DHRS13	dehydrogenase/reductase 13	5	113	2	-0.2
PPP1R37	protein phosphatase 1 regulatory subunit 37	5	114	3	-0.8
MEIS1	Meis homeobox 1	5	115	5	-2.0
CBX8	chromobox 8	5	116	2	-0.4
TMEM45A	transmembrane protein 45A	5	117	4	-1.8
FUK	fucose kinase	5	118	4	-2.8
JAK2	Janus kinase 2	5	119	5	-2.0
HOOK2	hook microtubule tethering protein 2	5	120	2	-0.5
MED9	mediator complex subunit 9	4	121	3	-1.3
SLC48A1	solute carrier family 48 member 1	4	122	4	-1.7

Continued on the next page

Table 3.1 – continued from previous page

Gene Symbol	Gene Name	sg RNAs	Rank	sgRNAs Depleted	Median Log FC
LYAR	Ly1 antibody reactive	5	123	5	-1.6
SKIL	SKI like proto-oncogene	5	124	3	-0.8
FOXJ3	forkhead box J3	5	125	2	-0.1
SH3RF2	SH3 domain containing ring finger 2	5	126	3	-2.3
PLCB1	phospholipase C beta 1	5	127	4	-2.8
MEAF6	MYST/Esa1 associated factor 6	5	128	5	-1.5
TAZ	tafazzin	5	129	3	-0.9
NCAPH	non-SMC condensin I complex subunit H	5	130	2	-0.4
IL1RL1	interleukin 1 receptor like 1	5	131	5	-1.2
NECAP2	NECAP endocytosis associated 2	5	132	3	-3.2
CKAP4	cytoskeleton associated protein 4	5	133	4	-1.4
ZNF736	zinc finger protein 736	5	135	5	-1.6
C5orf22	chromosome 5 open reading frame 22	5	136	3	-2.2
NPRL2	NPR2 like, GATOR1 complex subunit	5	137	5	-2.3
CIAO1	cytosolic iron-sulfur assembly component 1	5	138	2	-0.2
ZNF358	zinc finger protein 358	5	139	3	-0.8
PRRC2B	proline rich coiled-coil 2B	5	141	2	-0.2

Continued on the next page

Table 3.1 – continued from previous page

Gene Symbol	Gene Name	sg RNAs	Rank	sgRNAs Depleted	Median Log FC
ATP6V1C2	ATPase H+ transporting V1 subunit C2	5	140	1	0.0
UCHL1	ubiquitin C-terminal hydrolase L1	5	143	4	-2.0
KIF11	kinesin family member 11	5	145	2	0.5
GLI2	GLI family zinc finger 2	5	144	4	-1.6
AHR	aryl hydrocarbon receptor	5	146	4	-2.0
FUT1	fucosyltransferase 1 (H blood group)	5	147	5	-1.7
CPE	carboxypeptidase E	5	148	3	-1.0

3.3.2 Sub-pool Validation Screen Results

To validate the whole genome screen detailed above, the top 350 genes by MAGeCK rank in the live cell screen, the top 350 genes by median log fold change from the dead cells screen, and 100 genes whose median log fold change values were near zero in both the live cell and dead cell screens were complied into a list of targets for the sub pool. We used gRNAs from the half of the Human Activity-Optimized CRISPR/Cas9 lentivirus library that was not used from the initial screen as well as gRNAs from two other commonly used CRISPR/Cas9 libraries, the Toronto Knockout Library [52], and the Brunello Library [29]. After duplicates were eliminated, this left us with approximately 13 gRNAs per gene and 500 gRNAs which were non-targeting to use as controls. The library was synthesized, cloned, and virus particles made as described by the Zhang lab [66]. Cells were transduced and selected as was done in the whole genome screen above. Two replicate experiments were run and their results were compared to confirm gene essentiality. Both the mock infected

and KSHV infected cells showed a decrease in abundance of sgRNAs targeting genes which are considered generally essential in the Cancer Dependency map [126] when compared to the initial population of transduced cells (Figure 3.3A for mock, 3.3B for KSHV). sgRNAs targeting nonessential genes remained at relatively similar levels between initial and final transduced cells populations. The selective depletion of gRNAs targeting essential genes indicates that our screen was functioning as expected over the course of the experiment. The weaker relative MAGeCK scores in the KSHV infected population is likely due to the reduced proliferation rate in KSHV infected cells causing slower depletion of essential alleles relative to controls and non essential genes. Comparison of mock infected and KSHV infected live cell populations at the end of the experiment showed little correlation between replicates (Figure 3.4A, Table 3.2). Similarly, the sequenced dead cell populations did not show a strong correlation between replicates. However, there are a number of genes whose scores correlated between samples (Figure 3.4B). A number of mitochondrial localizing genes have well correlated scores in the live cell screen, including MRPS34 which will be examined in chapter 4 of this thesis. The anti-apoptotic, mitochondrial dysfunction responsive BCL2L1 had the highest combined score in the two replicates and viability assays confirmed that two sgRNAs selectively induced cell death following KSHV infection when compared to a non-targeting control sgRNA (Figure 3.5). 8 of the 12 sgRNAs tested were significantly depleted across both replicates, while the other four sgRNAs unchanged. While far from saturation, sgRNA target sequences were spread out across the coding sequence. The two sgRNAs showing the largest change in both replicates target the BH3 domain of BCL2L1, with one of the guides being completely absent in the KSHV sample of both replicates while remaining present in the initial and mock infection samples. The high intolerance for loss suggests an essential function for this domain, such that in-frame mutations still result in loss of the cell from the infected population. This is of interest as the BH3 domain is essential for sequestering pro-apoptotic factors, and a paralog of BCL2L1, MCL1 was one of the top

scoring genes in a screen of PELs [88]. These two factors have been describes as being the primary BCL2-family proteins which sequester the pro-apoptotic protein BAK [137], indicating there may be a shared pathway through which both KHSV infected endothelial cells and KSHV infected PELs may be dependent. Sub-pool screening informed by whole genome screening enabled more precise identification of genes on which KSHV infected endothelial cells are dependent for survival.

3.4 Discussion

While traditional chemotherapies and newer personalized medical approaches have improved clinical outcomes for KS in the developed world, cost and availability limit their utility in developing countries (Cesarman et al., 2019). As KS is the third most common cancer in Sub-Saharan Africa, there is a need for readily available therapies. Whole genome essentiality screens have already been applied to a number of different cancers [51, 5] as well as human viral infections [103, 80, 145]. These screens are an effective source of potential therapeutic targets in preclinical work. We used CRISPR/Cas9 lentiviral library screening to identify cellular genes whose function is essential for the survival of human endothelial cells latently infected with KSHV, the cell type most relevant for KS spindle cells. We found 146 potential targets in our initial whole genome screen, a number of which can be targeted with approved drugs or drugs which are in clinical trials. Our initial screen was limited by physical and practical constraints. TIME cells are large relative to many other cultured cell types, for example 293T cells reach approximately $3x10^5$ per cm^2 at confluence while TIME cells only reach roughly $5x10^4$ per cm^2, meaning around seven times the culture surface area would be needed to achieve the same representation in a transduced population. For this reason we chose to transduce just half of the CRISPR/Cas9 library, and do so at an MOI of ~0.6. Even with these compromises, nearly the entire cell culture capacity of the laboratory was taken for several weeks. For these reasons, we decided against an additional replicate

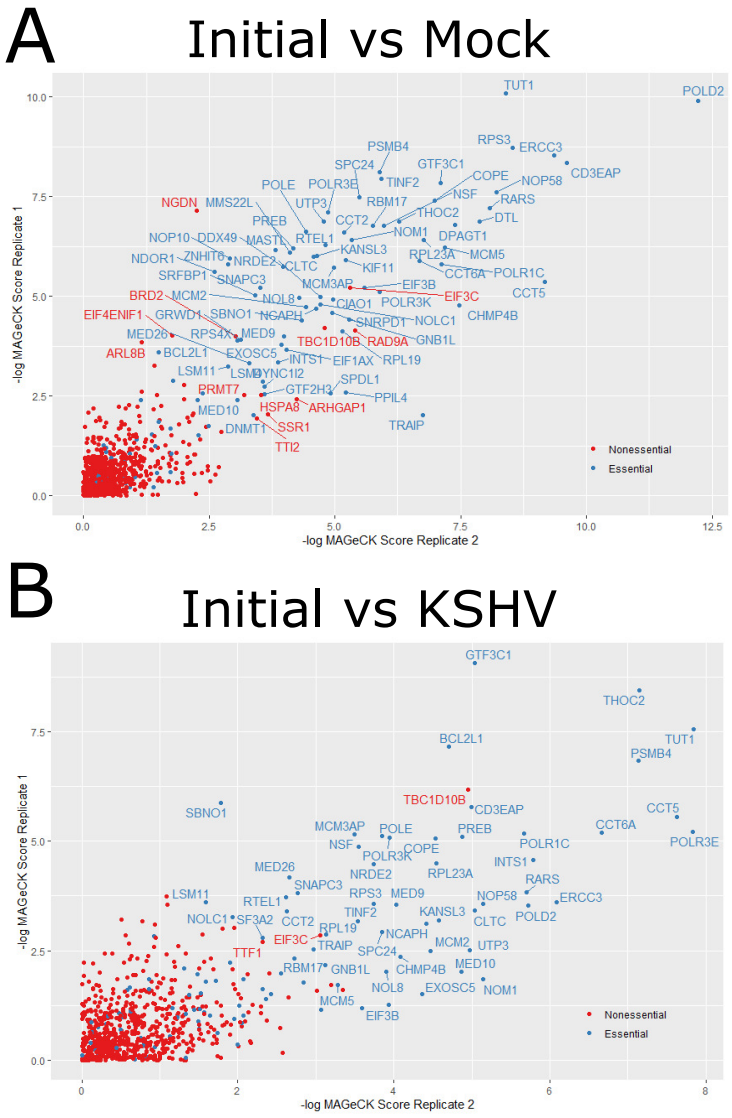

Figure 3.3: Sub-pool Screen Depletion of sgRNAs Targeting Essential Genes: Separation of the target genes in the sgRNA library into either generally essential (blue) or nonessential (red) categories to confirm successful implementation of the CRISPR library and screening protocol. -Log MAGeCK scores for separate replicate experiments are represented on each axis. The final mock population of live cells is compared to the initial population in panel "A" showing selection for essential genes over the course of the 8 day experiment. In panel "B" the final KSHV infected population is compared to the initial population, also showing depletion of generally essential genes while nonessential genes are relatively unchanged over the course of the experiment.

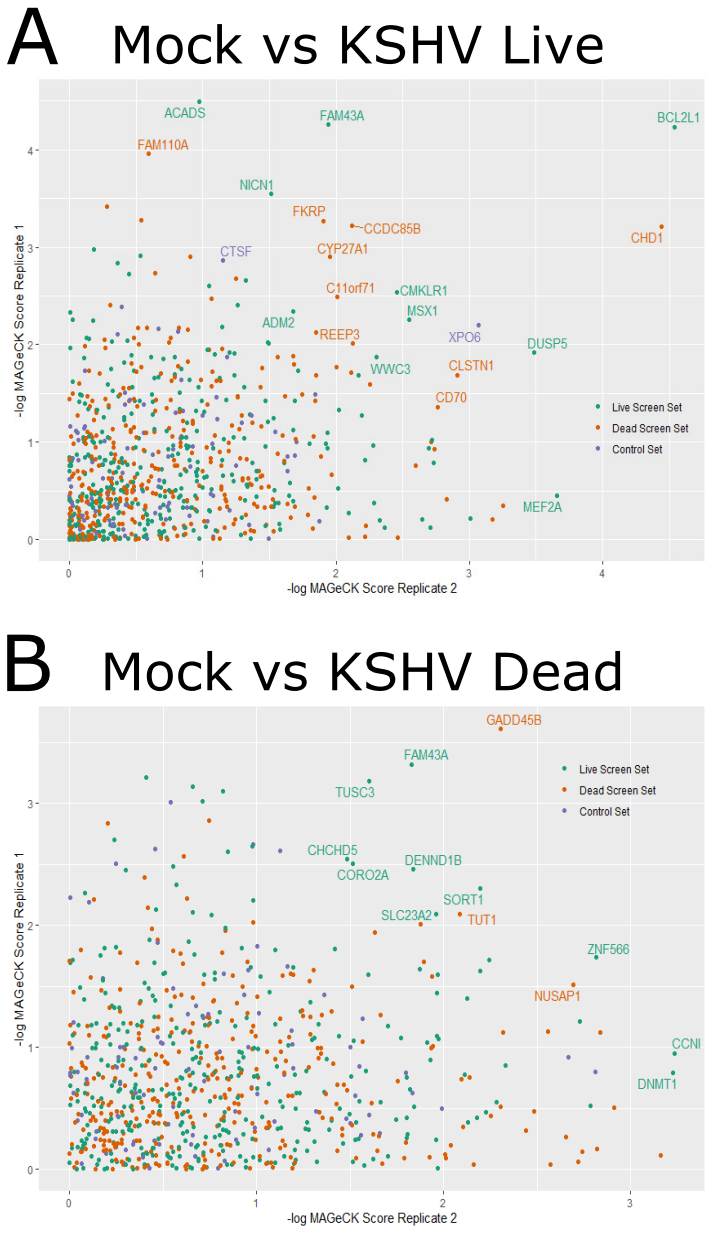

Figure 3.4: Results of the Live Cell and Dead Cell Sub-Pool Screening: Each axis represents -log MAGeCK scores from an independent experiment. Plots examining the correlation between replicates of both the live cell (A) and dead cell (B) screens. Each point represents an individual gene score. Points are colored based on the source of the target gene, with green being from the whole genome live cell screen, orange from the whole genome dead cell screen, and blue from the unchanged control gene set.

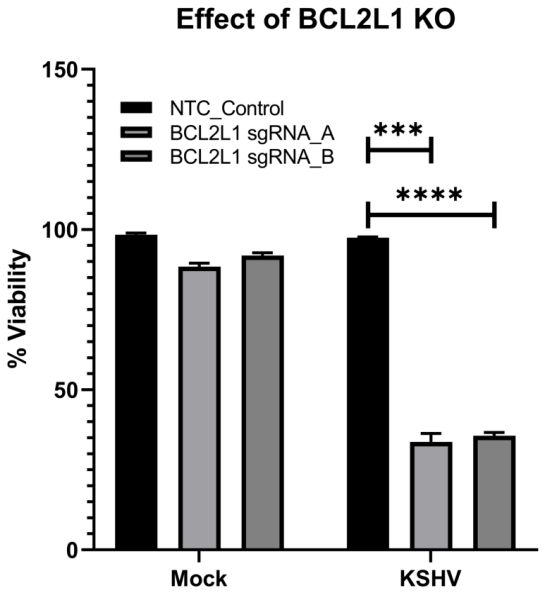

Figure 3.5: BCL2L1 is essential for Infected Endothelial Cells: TIME cells transduced with a non-targeting control (NTC) sgRNA or one two sgRNAs from the sub-pool library targeting BCBL1 were infected and cell viability was measured after 48 hours using trypan blue staining.(Paired t-test, ***P ¡0.001, ****P ¡0.0001, n=3

of the initial screen, and instead to use the results of the first screen to generate a second, smaller library for more powerful determination of essentiality during KSHV infection. While the initial screen was sufficient for the generation of useful hypotheses, including mitochondrial translation which is the subject of chapter 4, sub-pool screening illuminated the short comings of the whole genome screen and pinpointed a few targets on which KSHV infected endothelial cells are more likely to be dependent.

Table 3.2: List of Genes Depleted In Subpool Screening

Gene Symbol	sgRNAs	FDR	Rank	sgRNAs Depleted	Median Log FC
DUSP5	11	0.011719	1	9	-0.48799
FAM43A	12	0.052734	2	11	-0.41284
CHD1	12	0.061198	3	9	-0.38813
ACADS	12	0.07666	4	11	-0.28479
BCL2L1	12	0.07666	5	10	-1.1755
CYP27A1	12	0.07666	6	10	-0.38773
YLPM1	13	0.07666	8	4	-0.46381
ZNF579	12	0.136719	9	7	-0.49551
CCDC85B	12	0.145703	10	9	-0.46149
CMKLR1	12	0.154474	11	9	-0.33901
FKRP	11	0.170373	12	10	-0.4214
SH2D5	13	0.170373	13	10	-0.31978
NECAP2	11	0.182199	14	9	-0.41605
MSX1	11	0.189844	15	9	-0.35147
XPO6	13	0.195068	16	9	-0.37927
WWC3	13	0.224609	17	9	-0.4009
SCAF1	13	0.224609	18	4	-0.369
CERK	10	0.224712	19	5	-0.74361

Chapter 4

THE ESSENTIALITY OF MITOCHONDRIAL TRANSLATION DURING LATENT KSHV INFECTION

This chapter is adapted from a manuscript in preparation [57]

4.1 Abstract

Among the many host genes identified in our whole genome CRISPR/Cas9 Screen, there was an enrichment in genes localizing to the mitochondria, including genes involved in mitochondrial translation. Antibiotics which inhibit bacterial and mitochondrial translation specifically inhibited the expansion of latently infected endothelial cells and caused increased cell death in patient derived PEL cell lines. Direct inhibition of mitochondrial respiration or ablation of mitochondrial genomes induced increased death in latently infected cells. KSHV latent infection decreases mitochondrial numbers but there are increases in mitochondrial size, genome copy number, and transcripts. However, there is no increase in mitochondrial protein levels. The latent locus alone is sufficient to suppress mitochondrial translation and multiple gene products of the latent locus at least partially localize to the mitochondria when exogenously expressed. During latent infection, KSHV significantly alters mitochondrial biology leading to enhanced sensitivity to the inhibition of mitochondrial respiration, providing a potential therapeutic avenue for KSHV associated cancers.

4.2 Introduction

The observation of increased glycolysis and decreased aerobic respiration in cancer cells relative to normal tissue was first observed by Otto Warburg in the early 20th Century [134]. Warburg's findings led him to hypothesize that cancer is a metabolic disease which is driven by mitochondrial dysfunction [135]. Contradictory to Warburg's hypothesis, it is now thought that the metabolic changes observed during cancer metabolism are a phenotype observed in proliferating cells, whether transformed or not [104]. Additionally, mitochondrial function is often essential for the proliferative success of cancer cells [122]. The induction of metabolic changes during viral infection, including infection by oncogenic viruses, has been well studied over the past 15 years [109, 99]. Since mitochondria serve central roles in metabolism, apoptosis, and innate immunity, a number of viruses encode proteins which localize to mitochondria and many of them alter mitochondrial function. While alteration of metabolic function is important for virus production, the role of altered metabolism during latent infection is less clear. Oncogenic viruses provide a unique context to study alteration of metabolism in the absence of somatic mutations.

4.3 Results

4.3.1 Components of the Mitochondrial Translation Machinery are Essential for Latent KSHV Infection

Approximately 10% of the genes depleted from our live cell screen encode proteins that localize to the mitochondria (Figure 3.1B, red labeled genes). This represents an enrichment from ~6% of the total nuclear genes whose products localize to the mitochondria. The largest subset of mitochondrial genes identified in the screen have functions in mitochondrial translation and respiration (Figure 4.1A). The mitochondrial ribosomal subunits MRPS39 and MRPL40 had mean counts roughly four times lower in the KSHV infected population

relative the uninfected control in the live cell screen (Figure 4.1B). The mitochondrial ribosomal subunits MPRS34, MRPL20, and MRPL41 were counted in our dead cell screen while having little to no counts in our mock infected population (Figure 4.1C). In an independent set of experiments, two sgRNAs targeting MRPS34 were able to knock-out MRPS34, and lead to a reduction in protein levels of a mitochondrial genome encoded gene COXII (Figure 4.1D). TIME cells lacking MRPS34 displayed reduced proliferation during KSHV infection when compared to TIME cells transduced with a non-targeting control (NTC) sgRNA at 72 hours post infection (Figure 4.1E). Overall, the screen implicated mitochondrial translation as a potential vulnerability which can be used to inhibit the proliferation and survival of latently infected TIME cells.

4.3.2 Antibiotics Interfere with Proliferation and Survival of KSHV Infected Cells

Since mitochondrial ribosomes are structurally more closely related to bacterial ribosomes than eukaryotic ribosomes, antibiotics which target bacterial ribosomes can be used to selectively inhibit mitochondrial translation [20]. To test for sensitivity to antibiotics that inhibit mitochondrial translation also inhibit cells latently infected with KSHV, chloramphenicol, which interferes with the large mitochondrial ribosomal subunit, and tigecycline, which inhibits the small subunit were used to treat latently infected cells. KSHV infected TIME cells showed a dose-dependent decrease in cell confluence relative to mock infected controls for both chloramphenicol (Figure 4.2A) and tigecycline (Figure 4.2B) after 48 hours of treatment. Therefore, treatment of infected TIME cells with tigecycline or chloramphenicol leads to an inhibition of cell expansion. To determine if this sensitivity is unique to infected endothelial cells, KSHV negative and KSHV positive B-cell lymphomas were also tested for sensitivity. KSHV positive B-cells show a dose dependent sensitivity to treatment with either antibiotic at 48 hours post treatment (Figure 4.2C&D). The B-cells show a strong induction of cell death, not just limitation of proliferation. To confirm that the antibiotic is having the

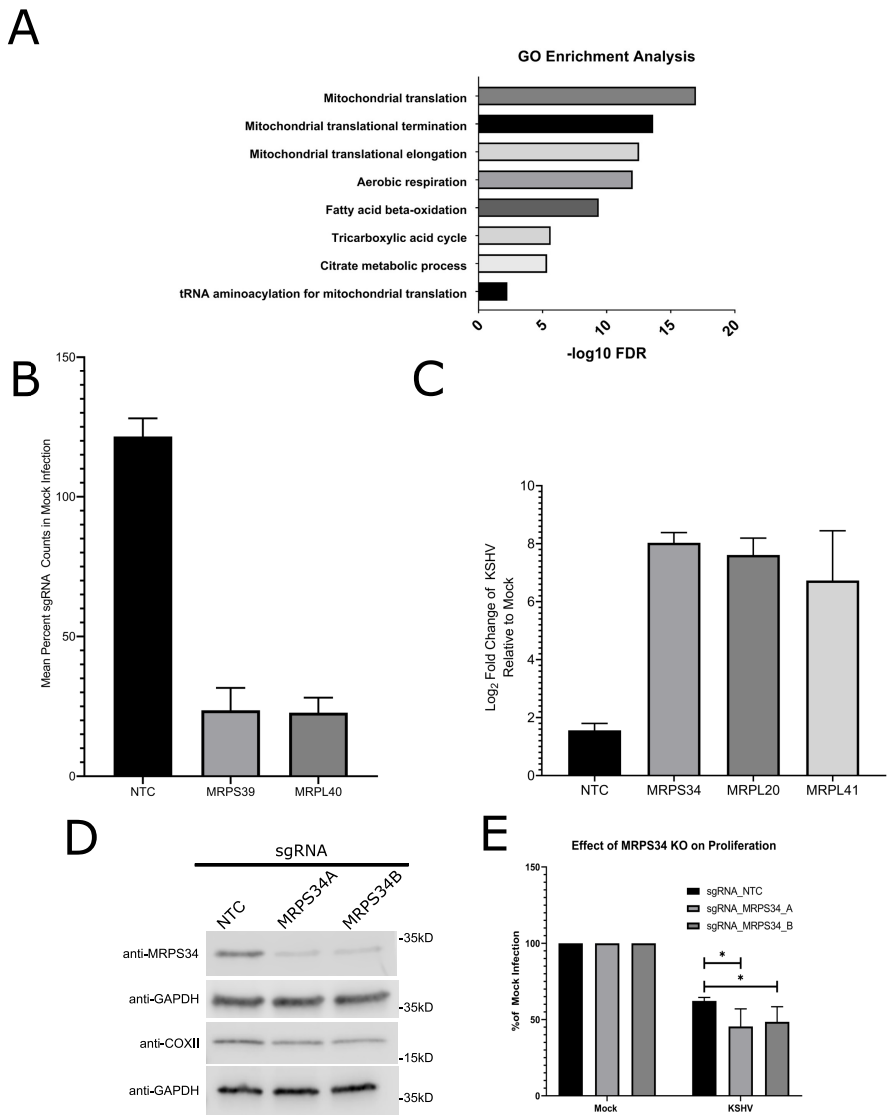

Figure 4.1: CRISPR/Cas9 Screen Identifies Mitochondrial Translation as an Essential Process for KSHV Infected Endothelial Cells: (A) Gene set enrichment analysis for the mitochondrial localizing genes from the live cell CRISPR/Cas9 screen in chapter 3. Average sgRNA values relative to mock infection were plotted for non targeting controls (NTCs) and guides targeting MRPS39 and MRPL40 from the live cell screen (B) and MRPS34, MRPL20, and MRPL41 from the dead cell screen (C). Western blot showing depletion of MRPS34 with two separate sgRNAs and simultaneous reduction in COXII expression (D), GAPDH shown for loading control on two separate blots). The transduced cell lines from D have suppressed growth rates during KSHV infection relative to mock infection (E)

expected effect at the given concentrations, we performed a western blot comparing levels of nuclear and mitochondrial encoded gene products with and without treatment with either chloramphenicol or tigecycline. At 36 hours post treatment, before large scale cell death is observed, there is a visible suppression of COXII by antibiotics selectively in the KSHV infected B-cells but not a substantial decrease in the nuclear encoded mitochondrial proteins (Figure 4.3A&B).

4.3.3 Mitochondrial Respiratory Function is an Essential Process During Latent KSHV Infection

If suppression of mitochondrial translation is essential due to the loss of expression of respiratory complex components, then inhibitors of respiration should also lead to increased cell death and decreased proliferation in KSHV infected cells. KSHV infected TIME cells were treated with the complex I inhibitor rotenone but showed no difference in cellular proliferation when compared to uninfected controls (Figure 4.5). However, endothelial cell media contains pyruvate, which is known to rescue cells from rotenone sensitivity and there is no available pyruvate free endothelial media [70]. Therefore, we tested KSHV infected PELs in media lacking pyruvate and found a dose-dependent increase in cell death (Figure 4.4A), similar to the increase in cell death from chloramphenicol and tigecycline treatment. As an alternative way to test for the essentiality of respiration during KSHV infection of endothelial cells, mitochondrial genomes were eliminated from TIME cells using a genetic, inducible mutagenesis system [115]. The mutagenesis system use a mutant uracil N-glycosylase (mtUNG) which removes thymine from DNA. The enzyme has a mitochondrial targeting sequence added and is placed under the control of a tet-inducible promoter. As a control, the wild type enzyme (wtUNG) which can only remove uracil from RNA is placed in an identical expression system. After two weeks of induction, cells were removed from doxycycline and loss of expression of the mitochondrial genome encoded COXII was confirmed by western blot (Figure 4.6A).

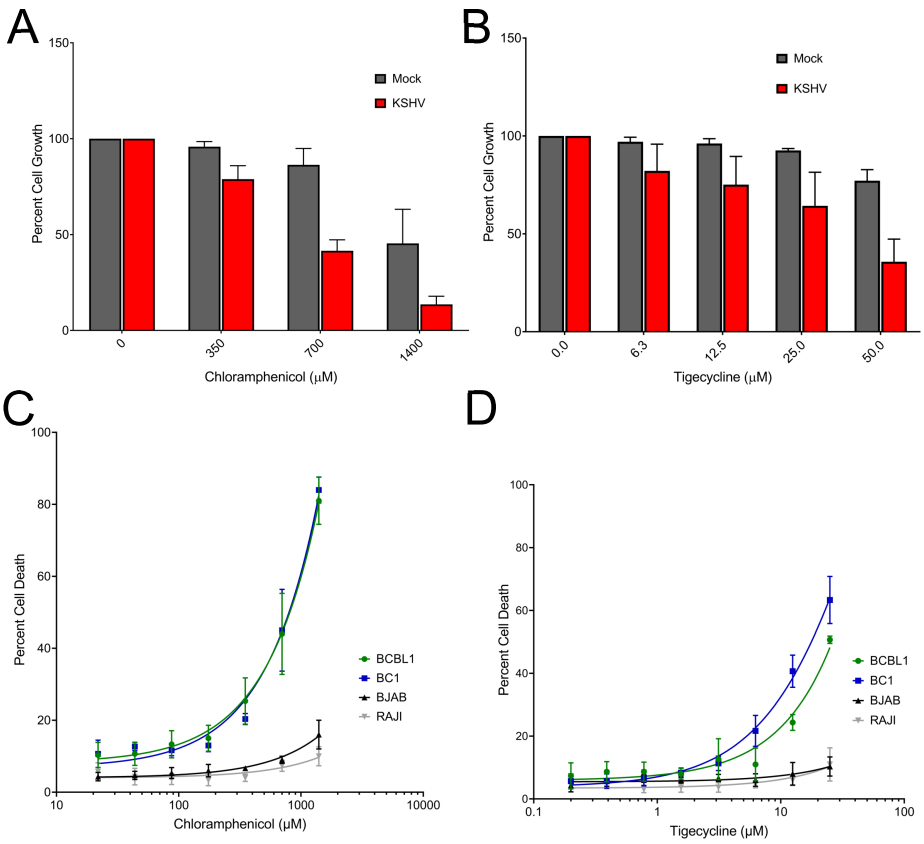

Figure 4.2: Antibiotics Targeting Bacterial Translation Inhibit the Growth and Survival of Cells Latently Infected with KSHV: Treatment of KSHV infected TIME cells suppresses cell growth in a dose dependent manner with both chloramphenicol (A) and tigecycline (B) (Mean with SEM of 3 replicate experiments). KSHV Infected PELs exhibit a dose-dependent induction of cell death for both chloramphenicol (C) and tigecycline (D) which is not seen in B-cell lymphomas lacking KSHV (BJAB and RAJI).

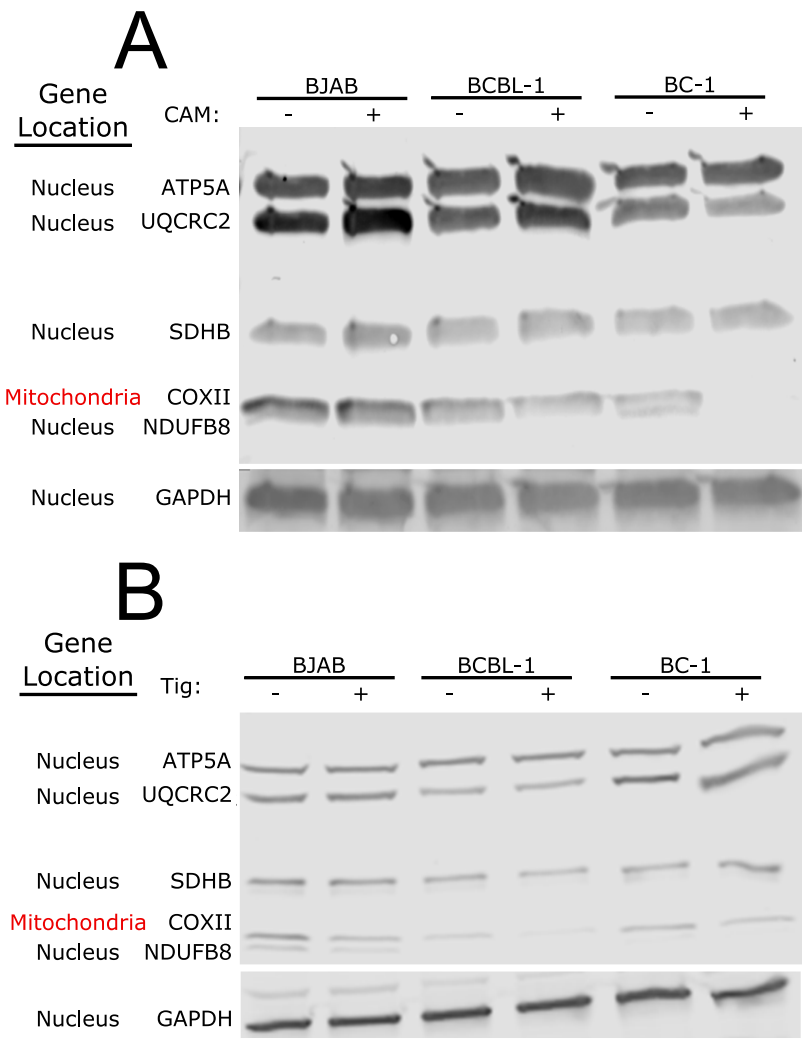

Figure 4.3: Antibiotic Treatment Suppresses Expression of Mitochondrial Encoded Genes: KSHV negative (BJAB) B cell lymphoma is compared to two KSHV positive PELs (BCBL-1 and BC-1) after treatment with either chloramphenicol (A) or Tigecycline (B). Cells were lysed 36 hours post treatment and lysates ananlyed by western blot for mitochondrial proteins. COXII (in red) is encoded in the mitochondiral genome, and its suppressed by antibiotic treatment in all cells, but the levels of the protein are the lowest in treated KSHV infected B cells.

Cell proliferation was compared between cells with intact mitochondria and those without functioning mitochondrial genomes in both the presence and absence of KSHV infection. Cells were plated to 24 well plates an imaged on an Incucyte for 6 days with media changes every two days. The resulting curves show that depletion of mitochondrial genomes leads to a decrease in proliferation during KSHV infection (Figure 4.4B) and an increase in log phase doubling time (Figure 4.6B). Additionally, KSHV infection selectively induces death in cells lacking functional mitochondrial when compared to mock infected controls (Figure 4.4C). Taken together, these results show that inhibitors of respiration or elimination of functional mitochondrial genomes from cells leads to inhibition of cellular proliferation in the case of TIME cells, and induction of cell death in KSHV infected PELs. These results suggest that inhibition of mitochondrial respiration is required for the proliferation and survival of cells latently infected with KSHV.

4.3.4 Latent KSHV Infection Increases Mitochondrial Transcripts and Genome Copy Number

Previous work from our lab established that mitochondrial function is decreased during KSHV infection [25]. One possible explanation which is consistent with both the decreased mitochondrial function and sensitivity to antibiotic treatment is that mitochondria are physically defective in cells latently infected with KSHV. Defects in mitochondrial function can lead to a fragmented mitochondrial network, a previously observed characteristic of certain cancers exhibiting Warburg metabolism [38]. To better characterize the state of the mitochondrial network during KSHV infection, mock and KSHV infected and mock infected endothelial cells were fixed to slides and probed for COXIV as a marker for mitochondria. Images were analyzed using an ImageJ plugin for examining mitochondrial networks [91]. There was a decrease in the average number of mitochondria per cell (effect size of ~47.9), and increases in the average size and length of mitochondria (effect sizes of 38.6% and 25.1%

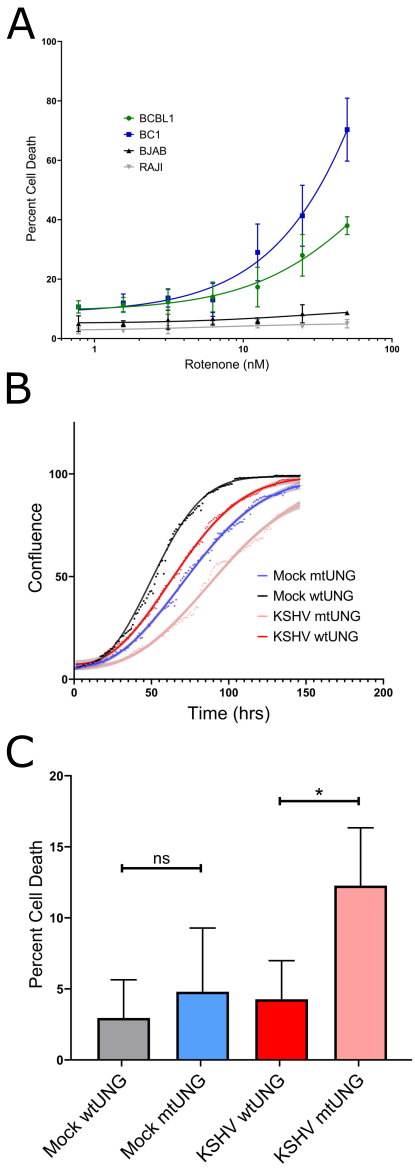

Figure 4.4: Inhibition of Respiration or Loss of Mitochondrial Genomes Suppresses Proliferation and Survival of KSHV Infected Cells: (A) Rotenone induces cell death in PELs in a dose-dependent manner while BJAB and RAJI cells show no sensitivity at the tested concentrations. (B) After ablation of functional mitochondrial genomes, KSHV infected cells lacking mitochondria grow at a slower rate when compared to mock infected cells lacking mitochondria. (C) Additionally, KSHV infected cells lacking mitochondrial show an induction in cell death upon infection relative to controls (Paired t-test *P <0.05, n=3).

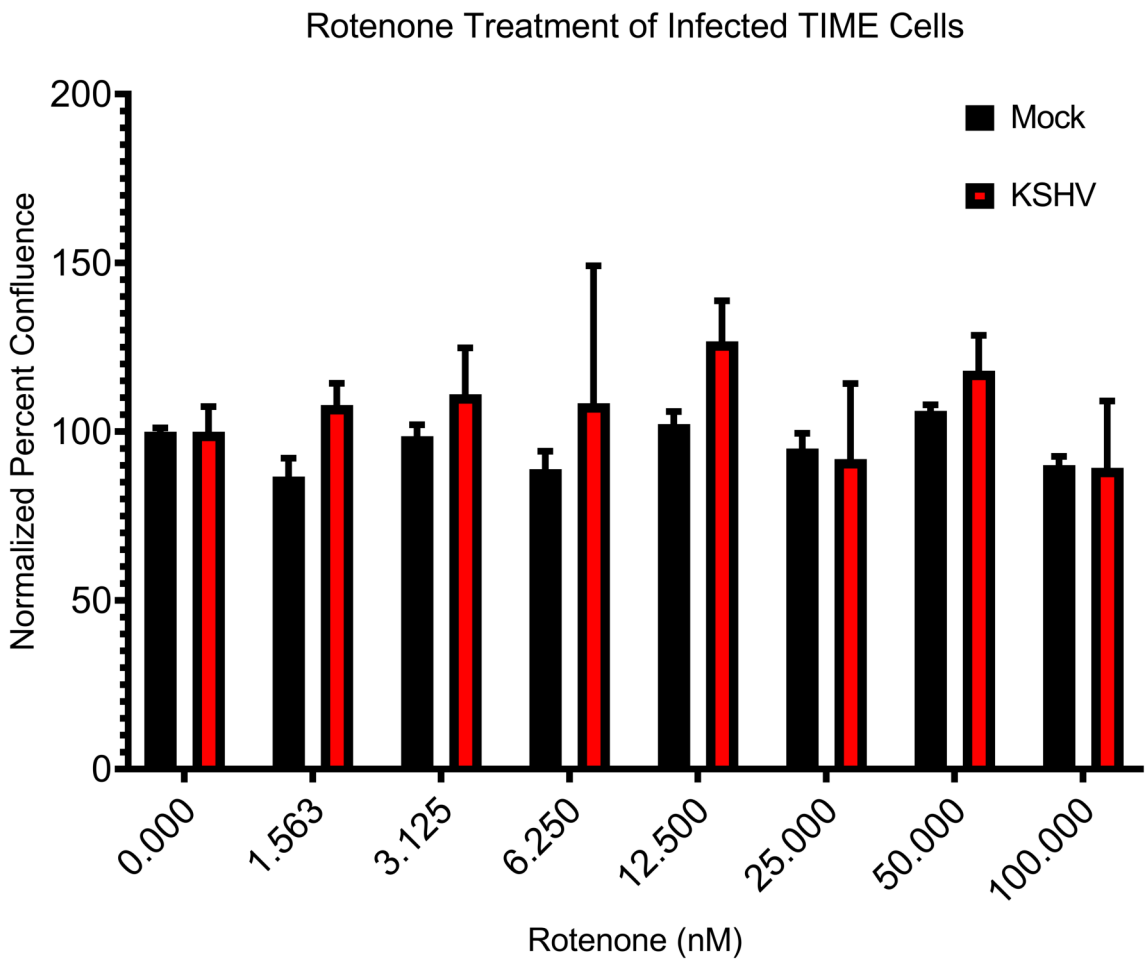

Figure 4.5: KSHV Infected TIME Cells are insensitive to Rotenone Treatment: TIME cells latently infected with KSHV were treated with increasing concentrations of rotenone from 24 to 72 hours post infection. They were then fixed stained with crystal violet and the dye was re-suspended and read on a plate reader to quantify changes in cellular proliferation.

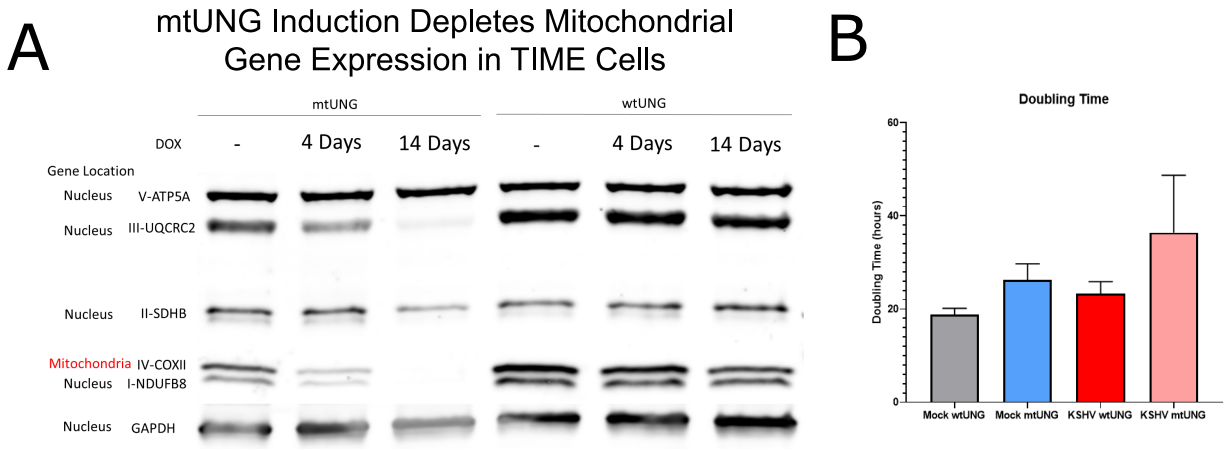

Figure 4.6: Loss of Mitochondrial DNA Eliminates Expression of Mitochondrial Genes and Increases Doubling Time During Infection: Two weeks of induction using a mutagenesis system to catastrophically mutate michondiral genomes eliminates expression of cells expressing mtUNG, but not the control wtUNG (A). Infection of the cells lacking mitochondrial genomes increases the cellular log phase doubling time relative to controls (B).

in KSHV infected cells relative to mock cells, respectively) (Figure 4.7A-C).

Mitochondrial function can be altered at the level of mitochondrial gene transcription. Our previously published RNA-Seq data set [121] was analyzed to look at average gene expression across each chromosome, including the mitochondrial chromosome. While the mean change in transcript level for all genes on a given chromosome was near zero for every nuclear chromosome, the mitochondrial genome showed a ~1.29 fold average increase during KSHV infection (Figure 4.8A). This increase in expression is primarily from tRNAs (Figure 4.8, which are the only transcripts stabilized by polyadenylation in mitochondria and our cDNA library was poly-dT primed. To confirm that transcription of the entire mitochondrial genome is increased during KSHV infect, RT-qPCR primed with random primers showed that transcripts of both strands of the mitochondrial genome are increased during KSHV infection (Figure 4.7). To determine if the increase in transcript levels was related to genome copy number, qPCR of mitochondrial genome copy number showed that KSHV

infected TIME cells possess approximately twice as many mitochondrial genomes as mock infected cells (Figure 4.7). Overall, KSHV infection of TIME cells leads to an increase in the size, length, transcript levels, and genome copies per cell of mitochondria, while decreasing the overall number of mitochondria. These results are not consistent with defective mitochondria, therefore the reduction in oxygen consumption observed during KSHV infection is independent of mitochondrial network structure, mitochondrial transcription, and mitochondrial genome copy number.

4.3.5 KSHV Latent Locus Decreases Expression of a Mitochondrial Genome Encoded Protein

To determine if increased levels of mitochondrial genomes per cell and transcript lead to increased protein levels, the levels of mitochondrial encoded protein cytochrome C oxidase II (COXII) were checked by western blot of cell lysates alongside human genome encoded proteins which localize to the mitochondria. TIME cells infected with wild type KSHV derived from BCBL-1 cells showed no significant decrease in COXII expression compared to mock infected TIME cells (Figure 4.9A). It is possible that an increase in mitochondrial copy number and transcript levels is counteracted by another mechanism suppressing expression of mitochondrial proteins during infection. To test for suppression of mitochondrial proteins, 293T cells were infected with BAC16 derived deletion viruses and compared to mock and wild type infected 293T cells to find changes in COXII expression. While wild type BAC16 KSHV shows a similar slight suppression of COXII compared to mock infection, deletion viruses lacking vFLIP show an increase in COXII expression relative to mock infected cells (Figure 4.9B). Importantly, the increase in COXII expression observed is similar to the roughly 30% increase observed in mitochondrial transcript levels. To test if the latent locus of KSHV is sufficient for suppression of COXII, a plasmid carrying the entire latent locus was transfected into 293T cells at increasing concentrations and cells were harvested for

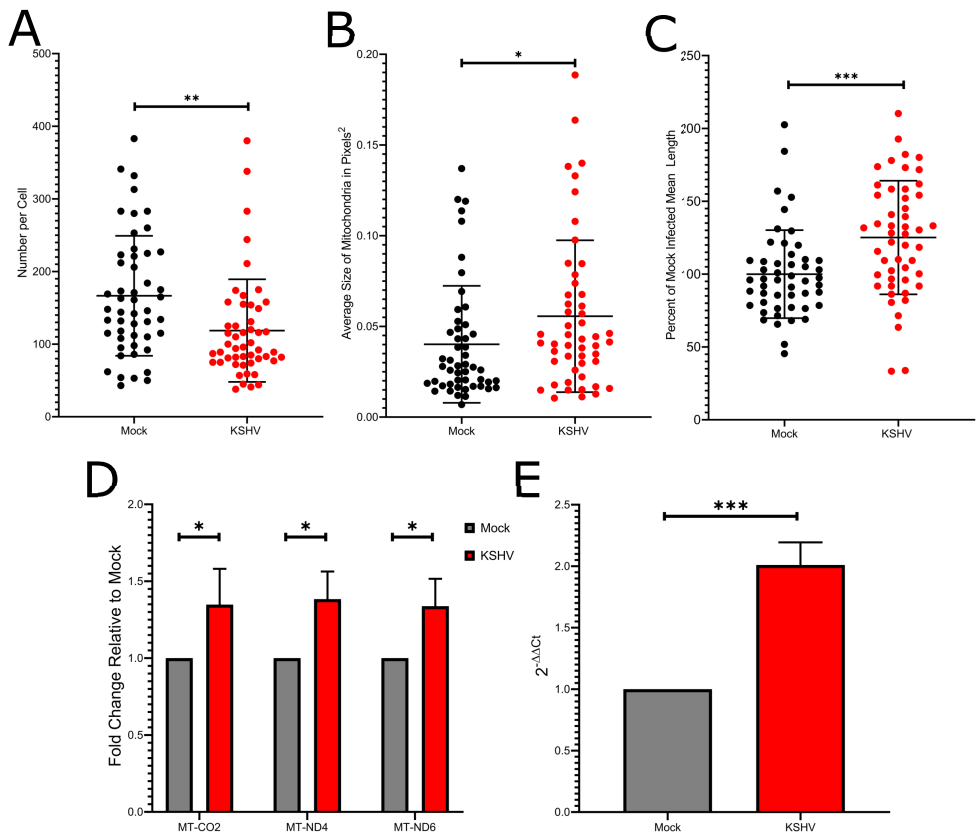

Figure 4.7: KSHV Infection Induces Changes in the Mitochondrial Network and Increases Mitochondrial Transcription and Genome Copy Number: KSHV infected cells were analyzed by immunofluorescence for changes in the mitochondrial network in single cells. The average mitochondrial number decreased per cell (A) while the average area (B) and length (C) of mitochondrial increased (Unpaired t-test * <0.05, **<0.01, **<0.001, n=50 per sample). (D) RT-qPCR shows that transcript levels from the mitochondrial genome increase during KSHV infection (Paired t-test *P <0.05, n=3). (E) qPCR for mitochondrial genome copies relative to host genome copies shows an increase in mitochondrial genome copy number during KSHV infection of TIME cells (Paired t-test ***P <0.001, n=6).

A

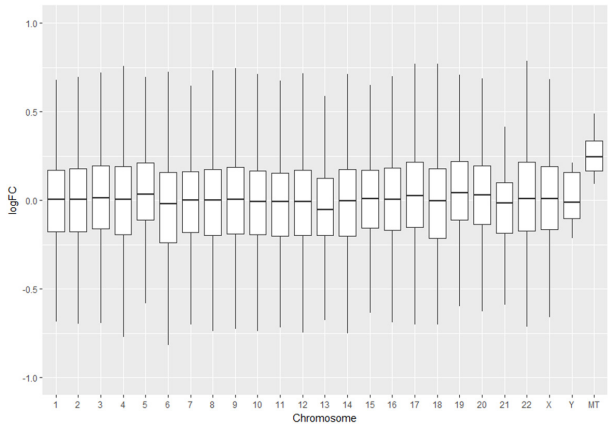

B

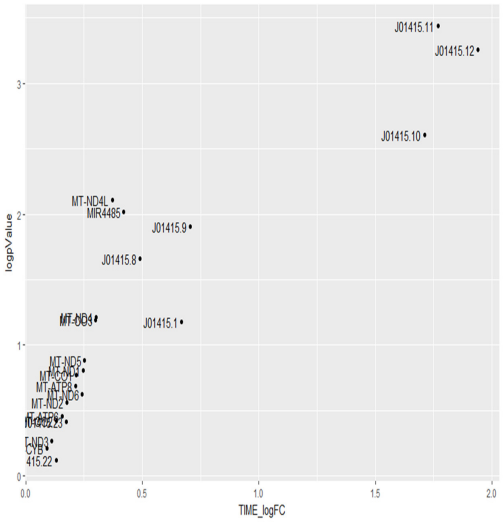

Gene	Description
J01415.12	Mitochondrially Encoded TRNA Serine 1 (UCN)
J01415.11	Mitochondrially Encoded TRNA Tyrosine
J01415.10	Mitochondrially Encoded TRNA Cysteine
J01415.9	Mitochondrially Encoded TRNA Asparagine
J01415.1	Mitochondrially Encoded TRNA Leucine 1 (UUA/G)
J01415.8	Mitochondrially Encoded TRNA Alanine
MIR4485	16S rRNA, apoptosis inhibitor
MT-ND4L	NADH dehydrogenase, subunit 4L (complex I)
MT-ND4	NADH dehydrogenase, subunit 4 (complex I)
MT-CO3	cytochrome c oxidase III

Figure 4.8: RNA-Seq Reveals Mitochondrial Transcription to be Increased: Average log fold change expression levels across all genes is plotted for each chromosome, showing mitochondrial transcription to be elevated (A). The genes increasing the average transcription level are mostly tRNA genes, which are the only mitochondrial transcripts stabilized by polyadenylation (B).

western blot after selection. There is dose-dependent decrease in COXII expression relative to transfection of a control plasmid (Figure 4.9C). However, single gene over-expression in 293T cells did not show suppression of COXII with the possible exception of expression of a codon-optimized vFLIP (vFLIP_HS) that expresses vFLIP to high levels (Figure 4.10A). However, expression of vFLIP_HS alone using a lentivirus construct was not sufficient, even when a strong mitochondrial targeting sequence (MTS) was added to the N-terminal end of the protein (Figure 4.10B). Taken together, it appears that no single latent gene is sufficient to reduce expression of COXII. These results demonstrate that the KSHV latent locus is sufficient to suppress expression of mitochondrial proteins, but it is possible that increased mitochondrial genome number overcomes this suppression during infection.

4.3.6 KSHV Latency Gene Products Localize to Mitochondrial Fractions

To determine if any KSHV latent genes could play a direct role in the alteration of mitochondrial biology, the localization of latent proteins to the mitochondria was examined. Plasmids for transient overexpression of each of the latent proteins with 3xFLAG tag on the N-terminal end were transfected into 293T cells. 48 hours later, the cytoplasmic and mitochondrial fractions of the cells were separated using differential centrifugation. Western blot analysis of whole cell lysates and the mitochondrial and cytoplasmic fractions of the cells was used to identify localization of the viral proteins. GAPDH was used as a marker for the cytoplasmic fraction and ATP5A as a marker for the mitochondria. Kaposin B was present at low levels in the mitochondrial fraction as well as the cytoplasmic fraction and a small portion of the vCyc was also present in the mitochondrial fraction. The vFLIP construct with an N-terminal tag could not be detected. However, a lentiviral based vector with a C-terminal V5 tag was detected and indicated a proportion of vFLIP localizes to the mitochondrial fraction. Kaposin C and LANA did not display localization to the mitochondrial fraction (Figure 4.11). The presence of multiple latent genes in the mitochondrial fraction is consistent with the

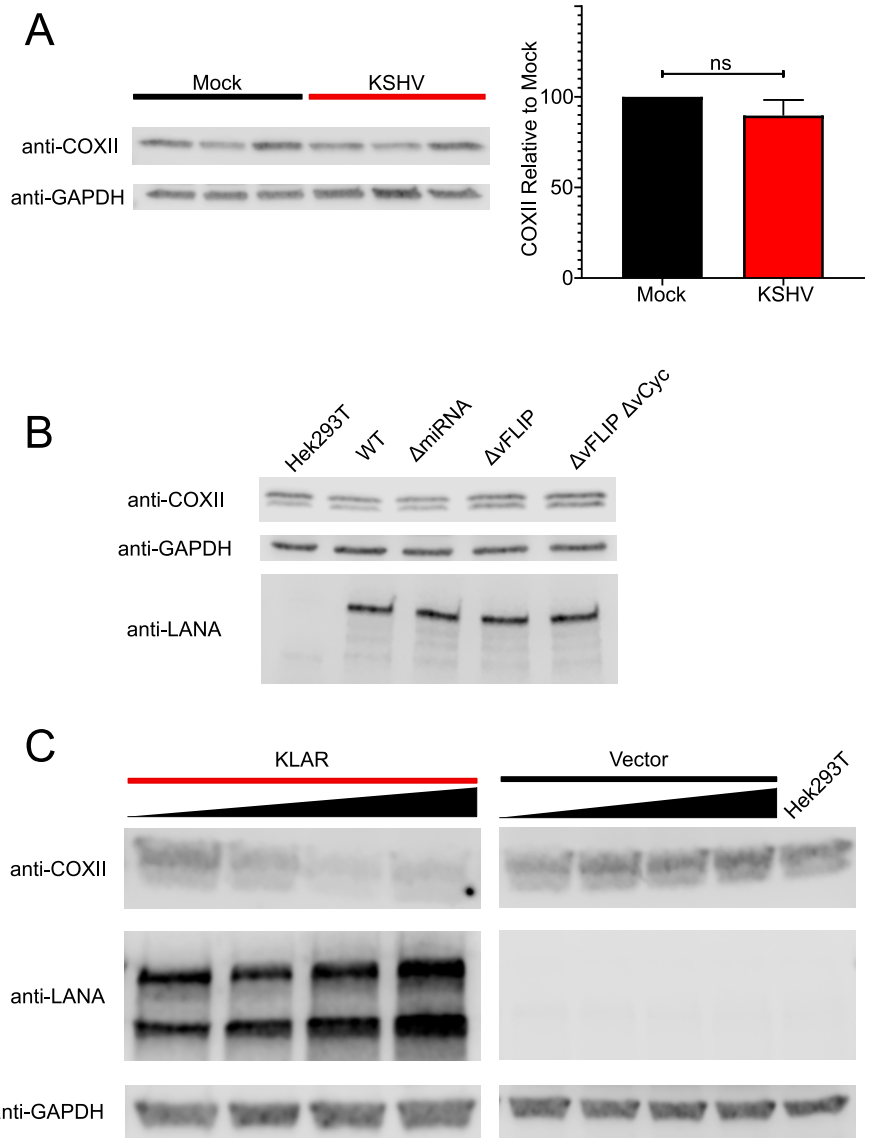

Figure 4.9: KSHV Infection Does Not Lead to a Significant Change in Mitochondrial Protein Levels: (A) COXII levels are not significantly changed during KSHV infection of TIME cells when assessed by western blot (Paired t-test, n=3). (B) Infection of 239T cells with BAC16 derived viruses displayed a similar phenotype as BCBL-1 derived virus in panel A. Deletion viruses lacking vFLIP showed a moderate increase in COXII expression. (C) Expression of the latent locus from a plasmid in 293T cells shows a dose-dependent decrease in COXII expression relative to a control plasmid.

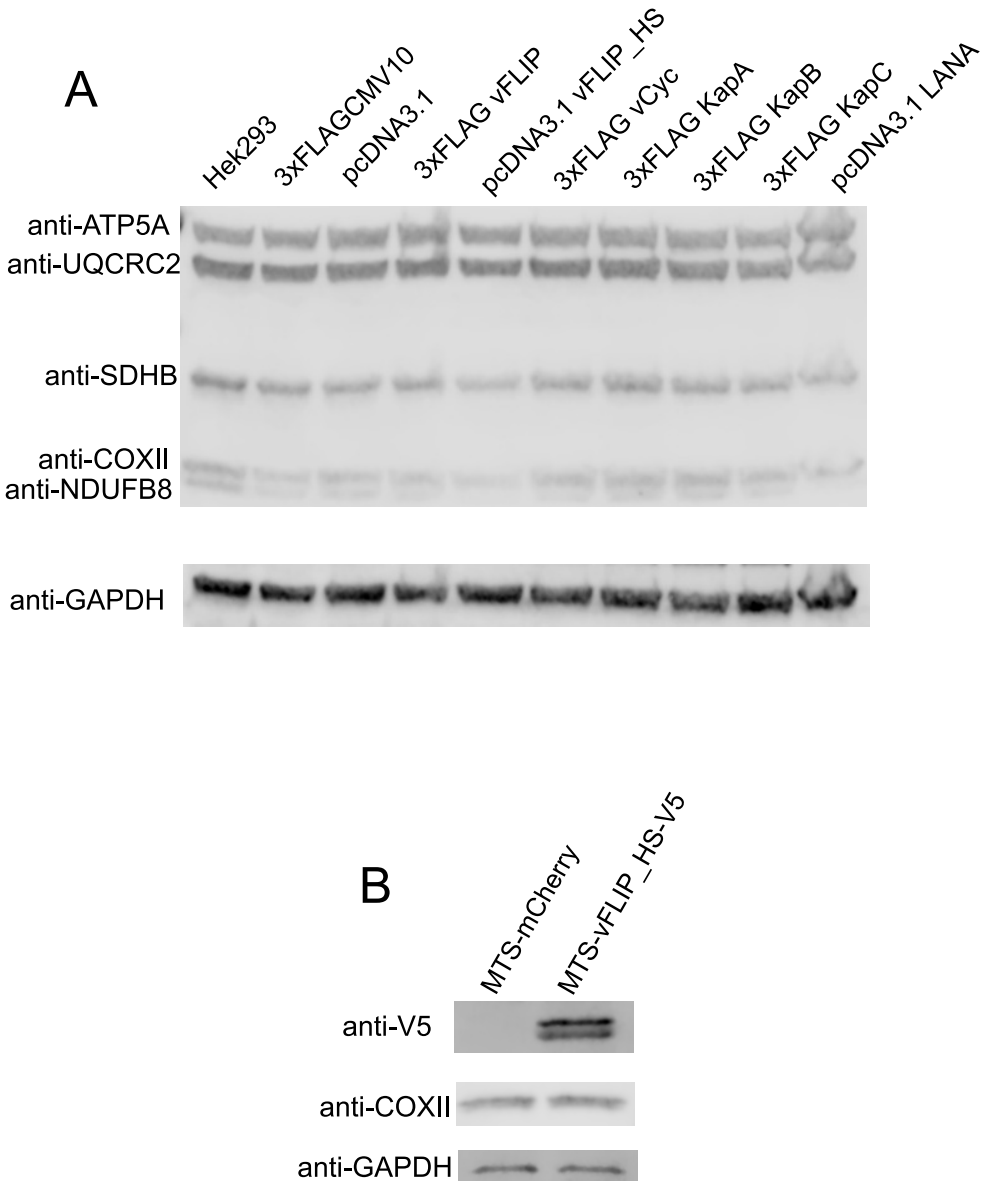

Figure 4.10: No Single Latent Gene is Sufficent for COXII Suppression: Individual genes expressed in Hek293 cells and selected, produced no obvious changes in COXII expression (A). Over-expression of a codon-optimized vFLIP with a strong targeting peptide localizing the protein to the mitochondrial matrix was also unable to suppress COXII expression (B).

ability of the entire latent locus to suppress COXII expression, while none of the individual proteins can suppress COXII expression in isolation.

4.4 Discussion

A large number of genes identified by our live cell screen encode proteins that localize to the mitochondria, leading to the hypothesis that mitochondrial translation is essential for proliferation or survival of cells latently infected with KSHV. Mitochondrial ribosomes can be targeted therapeutically using antibiotics due to the shared ancestry between bacterial ribosomes and eukaryotic mitochondrial ribosomes. This aspect of mitochondrial biology has been exploited for other cancers [67, 75]. Importantly, many of these antibiotics are readily available and on the WHO List of Essential Medicines [136]. We showed that both chloramphenicol and tigecycline are able to suppress proliferation of infected endothelial cells and induce cell death in KSHV infected B-cells. The effective doses of chloramphenicol used are roughly ten times higher than serum levels where serious adverse effects, such as aplastic anemia, begin to occur [144]. Similarly, the effective doses of tigecyline are greater than 15 times the maximum observed serum levels during treatment of bacterial infections [118]. While these antibiotics themselves are not likely therapeutic candidates, their effectiveness highlights a previously underappreciated requirement for mitochondrial function during KSHV infection. Since the mitochondrial ribosome is primarily responsible for synthesizing components of the respiratory chain, our findings suggest that KSHV infected cells require some mitochondrial function despite having lower basal levels of mitochondrial function. Interestingly, while antibiotics inhibited both endothelial cells latently infected with KSHV and PELs, there were slightly different outcomes. The infected endothelial cells were unable to reach confluence as quickly as mock infected controls but there was not obvious large-scale cell death while in the PELs there was wide-spread cell death. It is unknown why latent infection in endothelial cells versus B-cells produce different effects but

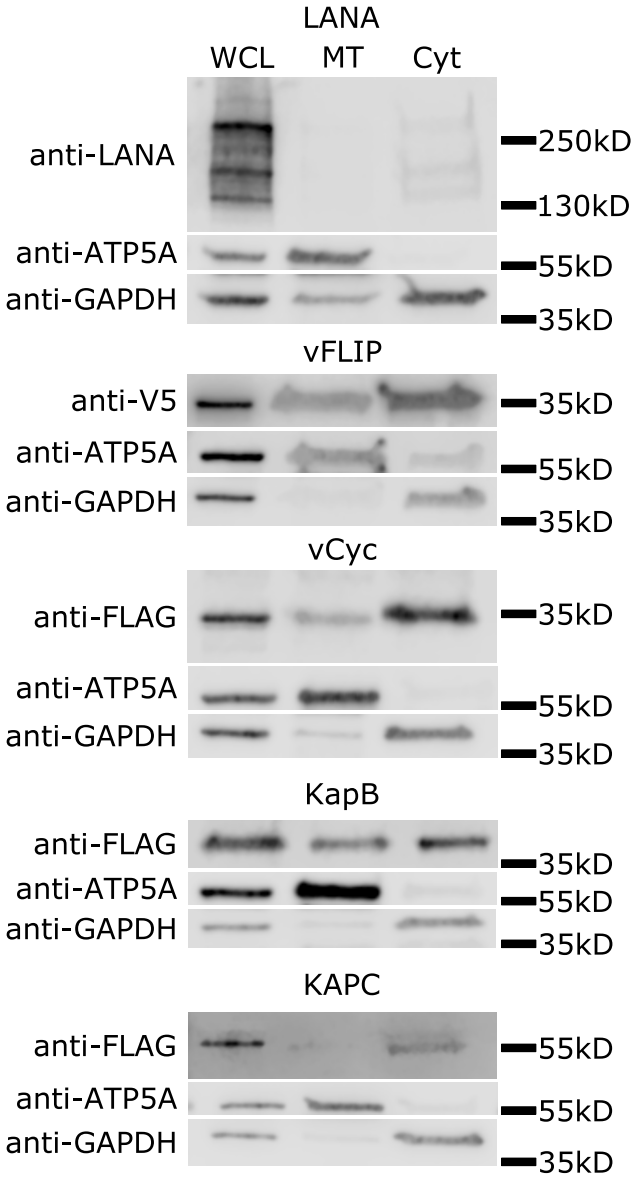

Figure 4.11: KSHV Latent Proteins Localize to the Mitochondrial Fraction: Mitochondrial fractionation by differential centrifugation was used to separate cytosolic and mitochondrial fractions of 293T cells 48 hours after transfection (in the case of all but vFLIP where lentivirus transduction was used). Whole cell lysates were run along with the reduced cytosolic and mitochondrial fractions. Blots were probed for the indicated tag depending on the construct as well as ATP5A and GAPDH. vCyc, vFLIP, and KapB are partially localized to the mitochondria, while LANA and KapC are absent.

could be due to the presence of pyruvate in the endothelial cell media that rescues TIME cells from cell death due to loss of mitochondrial function, but fails to make up for the loss of cellular proliferation.

Our lab and others have shown that KSHV infected cells display characteristics of Warburg metabolism [25, 8, 142, 84]. The KSHV induced metabolic changes include increased glucose consumption, increased production of lactate, and decreased oxygen consumption [134]. These metabolic characteristics are consistent with the presence of mitochondrial defects within cells, which is an observation made by Otto Warburg himself [135]. We sought to confirm the presence of mitochondrial defects by looking for changes in mitochondrial network structure, transcript levels, genome copy number, and protein levels in infected endothelial cells. However, the changes we observed in network structure, transcripts, and genomes were not consistent with mitochondrial dysfunction which usually produces fractured mitochondrial networks, fewer genomes, and lower RNA levels [125, 100]. While the level of a mitochondrial DNA encoded protein was not significantly changed during infection, there was an increase in the mitochondrial DNA copy number and transcript levels. These data suggest that mitochondrial translation is suppressed during latent infection in the presence of increased transcript levels. Interestingly, despite the increase in mitochondrial DNA copy number and transcript levels, there was a decrease in overall mitochondrial number in latently infected endothelial cells. At the same time, there was an increase in mitochondrial size. These results are consistent with, but not definitive proof of, increased mitochondrial fusion. Further experiments will be needed to examine changes in mitochondrial fusion dynamics during KSHV infection and determine the role latent genes might be playing to facilitate or counteract mitochondrial changes during latently infection of human endothelial cells.

Many viruses encode proteins which modify mitochondrial function for a variety of different reasons. Among the observed functions are preventing apoptosis, inducing changes in

metabolism, and avoiding innate immune activation. Some viruses encode proteins which interact with mitochondrial ribosomes in large-scale protein interaction studies. These include the capsid proteins of flaviviruses [113], and Nsp8 of MERS-CoV-2 [41]. A previously published KSHV protein interaction network identified potential interactions between KSHV latent genes and mitochondrial proteins [23]. 92 mitochondrial genes were within vFLIP's interaction network, representing 19.1% of all proteins in the interaction network. 5% of vFLIP's interaction network is made up of proteins involved in mitochondrial translation. Consistent with these findings, we found that vFLIP physically localizes to the mitochondria, and overexpression of the latent locus of KSHV can suppress expression of a mitochondrial genome encoded protein. However, we were unable to demonstrate sufficiency with individual KSHV protein expression. Further studies expressing combinations of proteins will be necessary to determine which proteins are sufficient for KSHV alteration of mitochondrial biology.

While KS is a multi-factorial disease, the fact that the proliferating component is a latently infected endothelial cell has prevented direct targeting of the viral infection. Identifying host genes whose inhibition can selectively eliminate KSHV infected cells has potential for clinical application. While previous work has demonstrated that specific metabolic processes can be used to kill latently infected cells, the central nature of many of the those metabolic pathways limits their utility. Narrowing of the target range to even more specific cellular pathways can make a therapeutic more attractive than broad metabolic inhibitors. While inhibition of mitochondrial translation is an intriguing possibility, the concentrations of antibiotics used in this study to inhibit KSHV infected cell proliferation were relatively high. Future work will determine if antibiotic combination or other antibiotics known to interfere with the mitochondria better than chloramphenicol and tigecycline could identify effective treatments at more reasonable concentrations of antibiotic. While targeting mitochondrial translation is likely still problematic, this work encompasses a step towards gaining

a better understanding of viral alteration of a cellular metabolic hub which can then enable targeting more precise pathways.

Chapter 5

CONDITIONAL LETHALITY FOR METABOLIC PATHWAYS DURING KSHV INFECTION

Daniel L. Holmes, Jie Yin, Michael Lagunoff

Department of Microbiology, University of Washington, Seattle, Washington, USA.

5.1 Abstract

Many viruses induce dramatic changes in cellular metabolism for replication, however, we have shown that Kaposi's Sarcoma-associated Herpes Virus (KSHV) induces cancer-like metabolic changes during latent infection. The proliferating component of KS tumors is a cell of endothelial origin, termed the spindle cell. Over 90% of spindle cells are latently infected, with only a small fraction of cells expressing lytic transcripts. In culture of human endothelial cells, latent infection leads to increased glycolysis, decreased oxidative phosphorylation, and increased accumulation of fatty acids in lipid droplets. Importantly, chemical inhibition of glycolysis, glutaminolysis, and fatty acid synthesis leads to higher cell death in latently infected cells than in mock infected controls. We recently found that KSHV latent infection is sensitive to chemical inhibition of lipid droplet formation. Interestingly, a bacterial artificial chromosome (BAC) derived virus lacking the 3kb latent miRNA cluster loses the requirement for lipid droplet formation while retaining the requirement of glycolysis, glutaminolysis, and fatty acid synthesis. As the miRNA cluster has previously been shown to be sufficient for induction of glycolysis, these results suggest conditional lethality for lipid droplet synthesis for infected cells in response to induction of glycolysis. Therefore,

we propose that glycolysis, glutaminolysis, and fatty acid synthesis are essential for survival of latently infected cells due to requirements for specific products of those reactions, while lipid droplet synthesis is essential to ameliorate the effects of increased glycolysis during infection. As lipid droplets are required in situations of increased lipid accumulation, the loss of sensitivity to this pathway suggests that increased glycolysis is directly or indirectly facilitating the accumulation of lipids during latent KSHV infection. Future experiments are focused on coupling the requirements for metabolic pathways to identify why specific metabolic changes are required for the survival of latently infected cells.

5.2 Introduction

The nature of viruses as obligate intracellular parasites necessitates appropriating many host pathways for viral persistence. Kaposi's Sarcoma-associated herpes virus (KSHV) is the etiologic agent of a highly vascularized endothelial cell tumor termed Kaposi's Sarcoma (KS) in immunocompromised patients [18]. KSHV has both latent and lytic life cycles, but latency is the primary program carried out in cells within a KS tumor, as well as in cultured endothelial cells. KSHV induces metabolic changes during latent infection which are considered a hallmark of cellular transformation into cancer [50]. While most tumor cells express only latent programs, a small fraction of cells display expression of lytic genes in vivo and in culture. While both latent and lytic genes play a role in the pathogenesis of KSHV, the concurrent presence of cells displaying one program or the other has made it difficult to identify which genes are responsible for specific phenotypes. As latency is predominant in spindle cells, this chapter focuses on the latent program to identify the viral determinants of oncogenic phenotypes. The latent locus consists of the genes vFLIP, vCyc, LANA, and the Kaposins. Additionally, there is a cluster of 12 miRNAs expressed during latency [108]. Reconfiguration of host metabolism is a common characteristic of viral infection which is observed across many virus families, including the herpes viruses [110]. Our lab previously

found that endothelial cells which are latently infected with KSHV display increased glycolysis in the presence of oxygen, termed aerobic glycolysis, and increased production of lactate [25]. This alteration in metabolism is observed in many cancers and is referred to as the Warburg effect. Following up on this discovery, another group found that the cluster of latently expressed miRNAs is sufficient for the induction of the Warburg effect in human endothelial cells [142]. To better characterize these metabolic changes on a global scale, we carried out a global metabolomics screen during KSHV infection [26]. Over 50% of the fatty acids identified were significantly increased during infection while none were decreased. Additionally, we observed the increased formation of lipid storage organelles called lipid droplets during infection. The lab went on to show that chemical inhibitors of fatty acid synthesis induce apoptosis in KSHV infected cells, but not uninfected controls. Alterations in fatty acid metabolism are increasingly recognized as important aspects of cancer biology and viral infection. However, the reasons for the requirement of fatty acids for the survival of KSHV latently infected cells remain unclear. We found that the latent locus of KSHV is sufficient for the accumulation of lipid droplets during latent KSHV infection of human endothelial cells. Additionally, we show that latent KSHV infection actually requires the accumulation of lipid droplets, but this requirement is dependent on the presence of the miRNA cluster. Interestingly, we did not observe a complete loss of the requirement for lactate synthesis, fatty acid synthesis or glutaminolysis. Taken together, these results suggest that lipid droplet accumulation exists to ease stress put on the cell by Warburg induction, but the other three pathways are required independent of Warburg status. Lastly we found that the BAC16 derived KSHV lacking the latent miRNA cluster has defects in the expression of the other genes in the latent locus, complicating the interpretation of our results.

5.3 Results

5.3.1 The Latent Locus of KSHV is Sufficent for the Accumulation of Lipid Droplets in Human Endothelial cells

To determine if the latent locus of KSHV (KLAR) is sufficient for lipid droplet accumulation, we used a gutted adenovirus vector, which expresses no adenovirus genes, to exogenously express the 13kbp latent locus in TIME cells. TIME cells were separately treated with wild-type KSHV, the KLAR adenovirus, and a mock infection control. After 48 hours the cells were fixed and stained using the Lipid Droplets Fluorescence Assay Kit (Cayman Chemical). The fixed and stained cells were run on an LSRII flow cytometer (BD) to measure fluorescence. Wild-type KSHV displayed a higher level of lipid droplet accumulation when compared to mock infection. The KLAR adenovirus showed an accumulation of lipid droplets similar to what was observed in wild-type infection (Figure 5.1). This was repeated three times and the geometric means for all three experiments were plotted. While it was previously shown that KSHV infection increased the volume of lipid droplets in endothelial cells, I found that the latent region alone is sufficient for the accumulation of lipid droplets.

5.3.2 Lipid Droplet formation is Essential in Latently Infected Endothelial Cells but dependent on the Latent miRNA Cluster

It was previously established that KSHV requires fatty acid synthesis for cellular survival during latency, and cell death from chemical inhibition can be partially rescued by treatment with the long chain fatty acid palmitate. However, why fatty acids are essential to cellular survival remains unclear. We hypothesized that lipid droplets themselves might be important for the survival of latently infected cells. To test for the requirement of lipid droplets, we used the long chain fatty acyl CoA synthetase inhibitor triacsin C on TIME cells from 48 to 96 hours after KSHV infection. After 72 hours cells were stained with trypan blue and

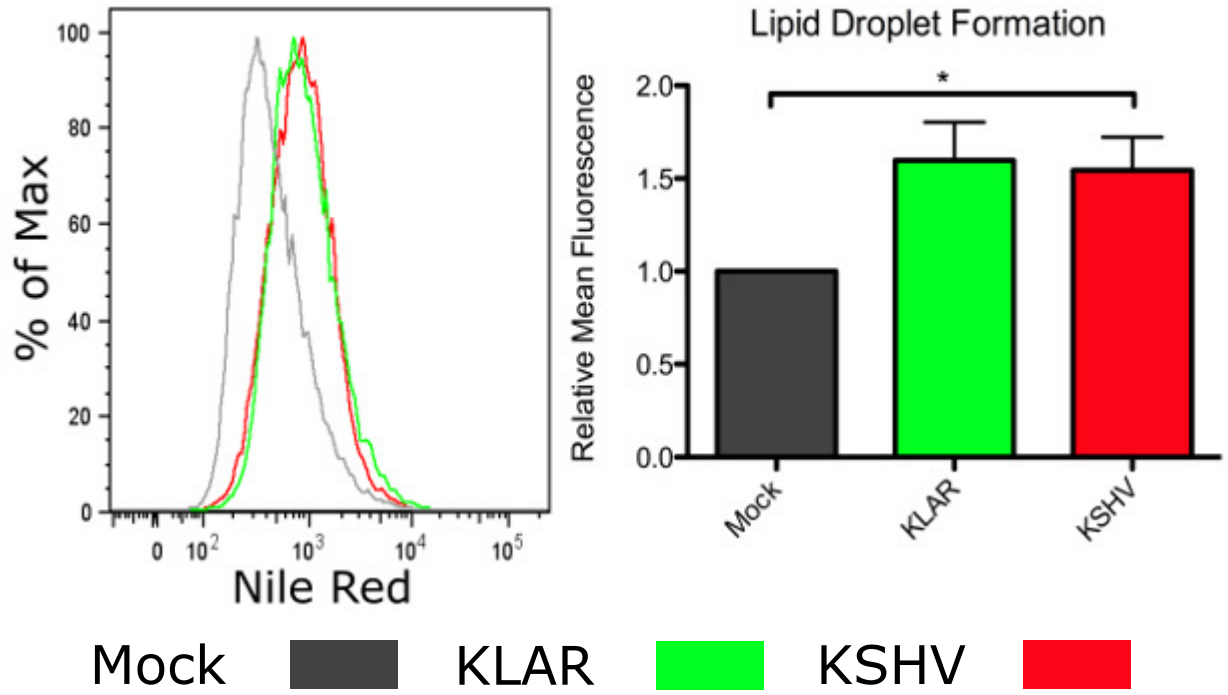

Figure 5.1: KSHV Latent Locus is Sufficient for Lipid Droplet Accumulation: TIME cells were infected with either PEL produced KSHV (red) or helper-dependent Ad5 expressing KLAR (green) and compared to mock infection (black) at 48 hours post infection. A single representative histogram is pictured on the left, on the right is the average of the geometric means from three experiments (paired t-test n=3, * p <0.05)

counted for cell viability. We found that latently infected cells require lipid droplet formation for survival (Figure 5.2). This requirement adds an additional, essential step in the synthesis and storage of fatty acids during KSHV infection.

In light of another group's work demonstrating that the miRNA cluster in the latent locus is responsible for induction of the Warburg effect in endothelial cells, metabolic inhibitors were tested in the presence and absence of the miRNA cluster. A bacterial artificial chromosome based recombinant KSHV (BAC16) [15, 60] lacking a 3 kpb segment of the latent locus which contains 10 of the 12 miRNAs expressed during latency was used to examining the effects of miRNA loss on sensitivity to metabolic inhibitors. Cells infected with this deletion virus lost sensitivity's to triacsin C treatment (Figure 5.2). The loss of sensitivity to triascin C in the absence of the miRNA cluster suggested a previously unknown connection between glucose metabolism and the accumulation of fatty acids in lipid droplets during KSHV infection.

5.3.3 A Deletion Virus Lacking Latent miRNAs retains sensitivity to ACC

We next wanted to examine the requirement for fatty acid synthesis during infection with the ΔmiRNA virus. We hypothesized that the requirement for FAS would also be reduced during infection with the miRNA deletion virus, given that the two enzymes are in the same pathway. TIME cells were infected with the parent, wild-type BAC16 KSHV (WT) or the ΔmiRNA BAC16 KSHV (ΔmiR) and were treated with and acetyl-CoA carboxylase inhibitor TOFA from 48 to 96 hours post infection. WT infection displayed the same sensitivity previously shown to TOFA treatment (Figure 5.3). Interestingly, the ΔmiR infected TIME cells retained sensitivity to TOFA treatment. The precise reason for the genetically separable difference between the requirement for FAS and the requirement for lipid droplets is unclear. A reasonable interpretation is that latent KSHV infection only requires lipid droplets in the presence of Warburg metabolism, but latent cells require a product of FAS

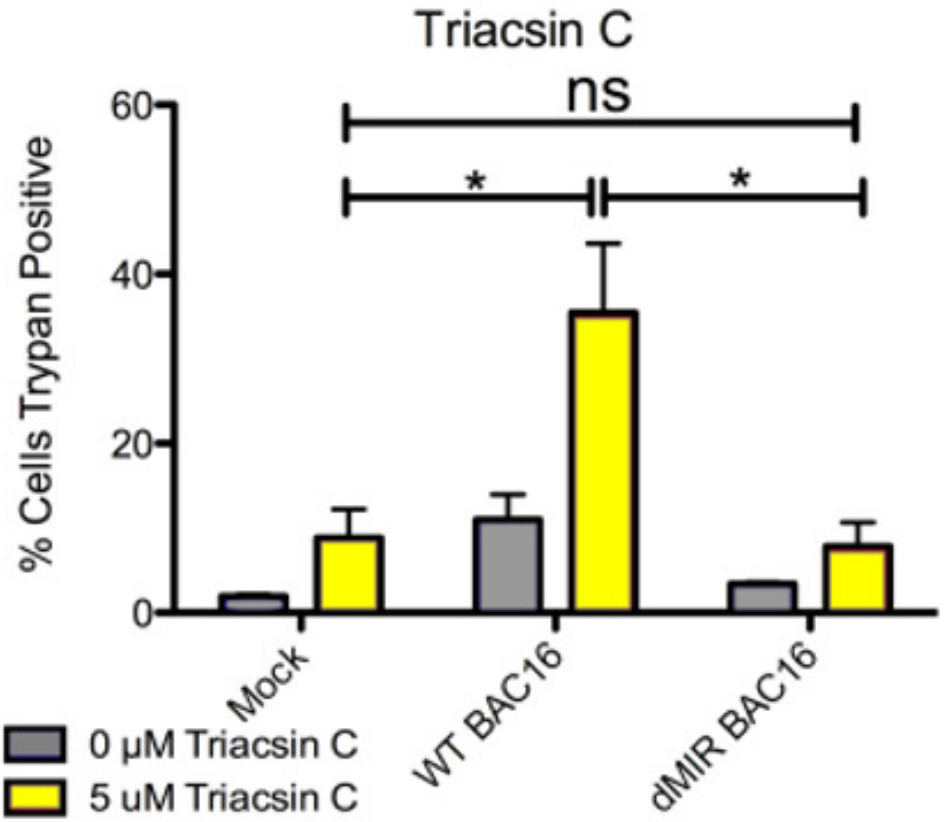

Figure 5.2: Sensitivity to Inhibition of Lipid Droplet Formation is Dependent on the miRNA Cluster: TIME cells were infected with either WT BAC16 or ΔmiRNA BAC16 and compared to mock infection. The cells were treated at 48 hours post infection and counted with trypan blue 48 hours later (paired t-test, * $p < 0.05$).

for an independent, as yet unidentified reason.

5.3.4 ΔmiRNA Virus Infected Cells Retain Addiction to Lactate Production but Lose Addiction to Glutaminolysis

Previous publications from our lab demonstrated that chemical inhibition of lactate dehydrogenase with oxamate and chemical inhibition of glutaminase with BPTES selectively killed KSHV infected TIME cells. The requirement for these two pathways is thought to be in support of Warburg metabolism by regeneration of NAD+ and restoration of carbon to the TCA cycle, respectively. To determine if the lack of viral miRNA expression in the ΔmiRNA virus changes responses to both of these drugs, we confirmed sensitivity during wild-type BAC16 infection and compared those responses to treatment during deletion virus infection. We found that ΔmiRNA virus infection retains at least some sensitivity to the inhibition of lactate production. Glutaminolysis inhibition also showed an intermediate phenotype and ΔmiRNA virus infection appears to retain at least some sensitivity. These results suggest that the reliance on these two pathways is not simply just supporting Warburg metabolism and that the products of these reactions are required for survival of latently infected cells.

5.3.5 KSHV Infected Cells are not Addicted to the Mevalonate Pathway

Since fatty acid metabolism is essential regardless of the supposed Warburg status of the cell, we hypothesized that cholesterol metabolism, more formally know as the mevalonate pathway, was related to the essentiality of FAS. The potential requirement of the mevalonate pathway is supported by the sensitivity of a number of viruses to treatment with statins [141, 130], which inhibit HMG-CoA reductase. We treated TIME cells with pravastatin 24 hours post infection and measured cell death 48 hours after treatment. KSHV infected cells showed only a slight, non-significant increase in cell death with pravastatin treatment

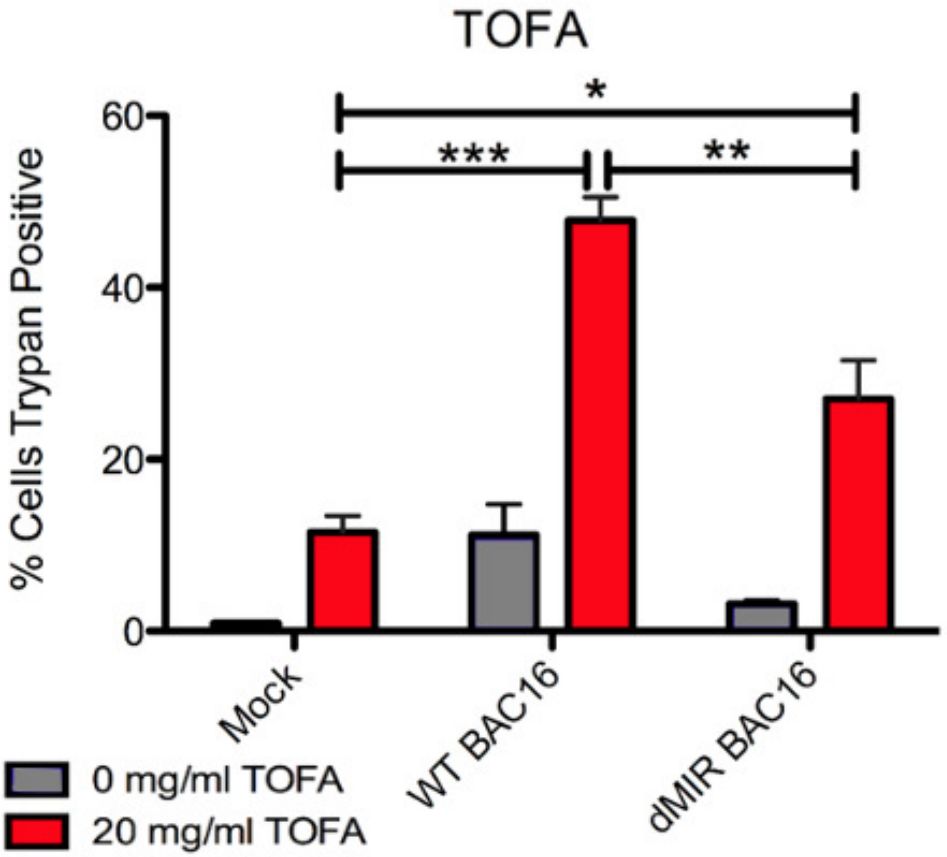

Figure 5.3: ΔmiRNA KSHV Retains Sensitivity to TOFA Treatment: TIME cells were infected with either WT BAC16 or ΔmiRNA BAC16 and compared to mock infection. The cells were treated with at 24 hours post infection and counted with trypan blue 48 hours later (paired t-test, * $p < 0.05$, ** $p < 0.01$, *** $p < 0.001$).

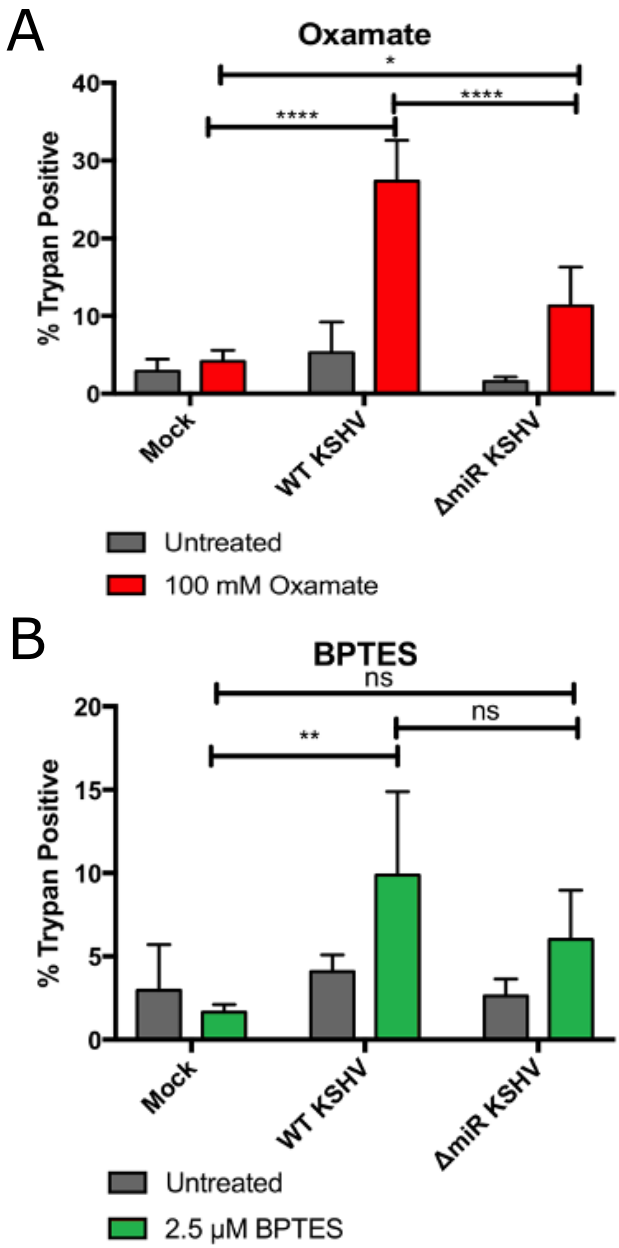

Figure 5.4: Retention of Oxamate and BPTES Sensitivity During ΔmiRNA Virus Infection: TIME cells were infected with either WT BAC16 or ΔmiRNA BAC16 and compared to mock infection. The cells were treated with at 24 hours post infection and counted with trypan blue 48 hours later (paired t-test, * p <0.05, ** p <0.01, **** p <0.0001).

in comparison to mock infected controls (Figure 5.5). This suggests that the mevalonate pathway is a relatively minor contributor to the need for FAS during KSHV infection.

5.3.6 Suppression of Entire Latent Region with miRNA Cluster Deletion

In attempting to confirm the above results, we sought to complement loss of the miRNA cluster. Several different attempts at either whole complement or partial complement with the 3 kbp cluster or fragments of the cluster were not successful (data not shown). To check to make sure that the deletion of the miRNA cluster was not affecting expression of other latent genes, we performed RT-qPCR to analyze transcript level differences between wild type KSHV BAC16 infection, and ΔmiRNA BAC16 infection. Importantly, infection rates were confirmed by IFA and measuring GFP fluorescence to ensure that the levels of cellular infection were close between viruses. We found that levels of transcripts containing the latent protein coding regions were all suppressed during latent KSHV infection (Figure 5.6A&B). This raises problems with the association of the ΔmiRNA virus with the phenotypes above. We can generally associated changes in drug sensitivities above to suppression of the entire latent locus, but individual determinants will need to be found with additional genetic experiments.

5.4 Discussion

The induction of metabolic restructuring in endothelial cells by latent KSHV infection creates exploitable vulnerabilities. Our lab and others have described the alterations by performing detailed metabolomic analyses. These studies identified chemical inhibitors which can be used to selectively target latent infection *in vitro*. However, the potential benefit for these alterations, the mechanism for their induction, and the reason for their essential nature have not been identified. In this chapter, we sought to narrow the genetic determinants around the induction of lipid droplet formation, as well as the determinants of susceptibility

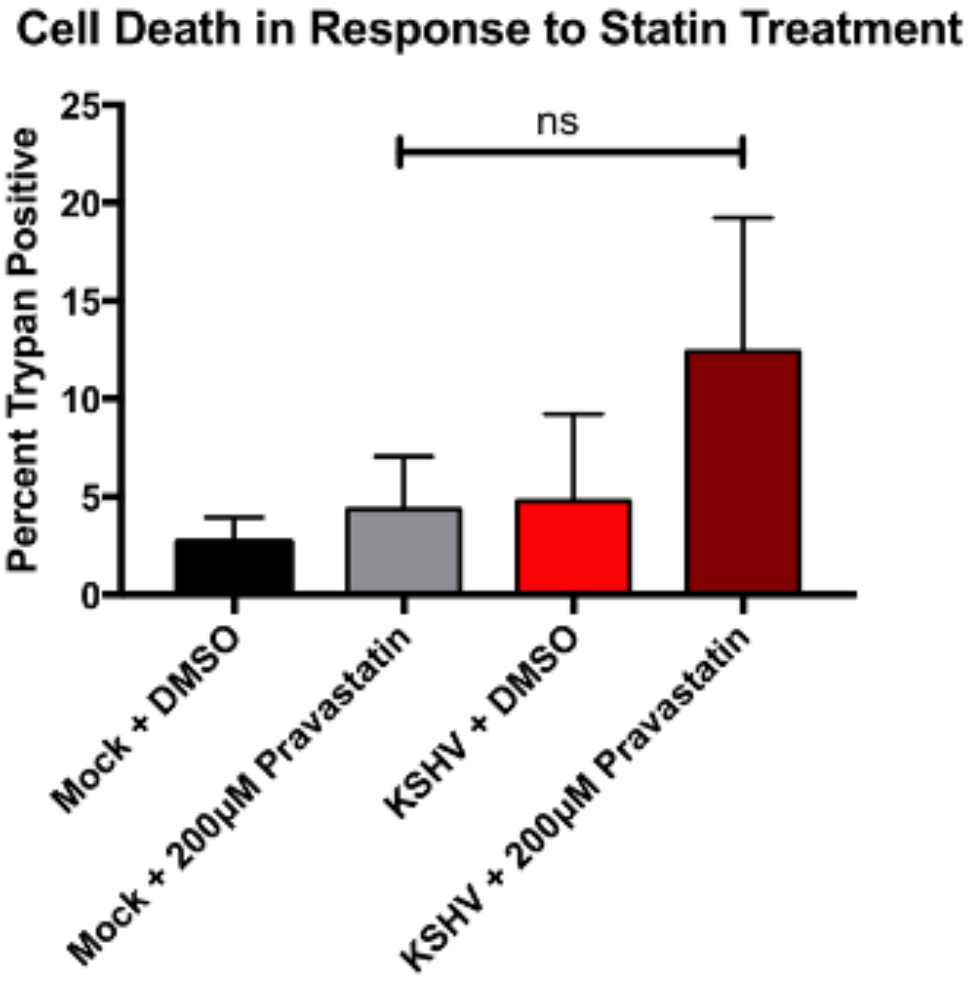

Figure 5.5: The Mevalonate Pathway is not Required for Latent KSHV Infection: TIME cells were either mock infected or infected with wild type KSHV BAC16 and treated with DMSO or pravastatin at 24 hours post infection. Cells were counted for viability with trypan blue at 72 hours post infection. (paired t-test, ns $p > 0.5$)

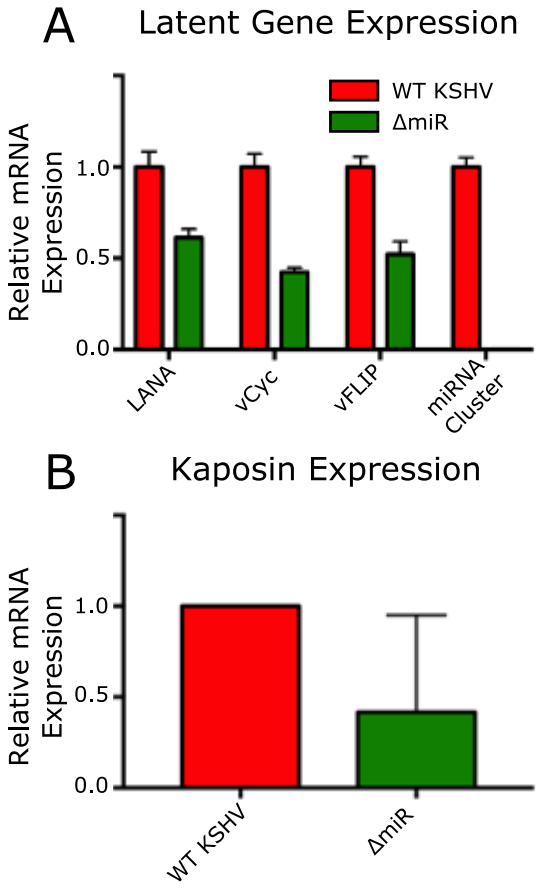

Figure 5.6: miRNA Cluster Deletion Leads to Suppression of Latent Locus Expression: RT-qPCR was used to compare gene expression between wild type KSHV infection and infection with the miRNA deletion virus in TIME cells. (A) includes the LANA, vCyc, and vFLIP which are transcribed from a shared promoter, as well as a pair of primers targeting the miRNA cluster (n=3), (B) uses primers targeting the kaposin locus in a seperate set of experiments (n=3). These experiments were done by Jie Yin.

to chemical inhibition of specific metabolic pathways.

We found that the latent locus of KSHV is sufficient for the accumulation of lipid droplets, and that chemical inhibition of lipid droplet formation during latent KSHV infection leads to cell death. Given the publication that the latent miRNA cluster is sufficient for the induction of the Warburg effect in endothelial cells, we tested a set of metabolic inhibitors to determine the effect of Warburg status on the dependence of other pathways. Perhaps the most surprising finding is that infection with the ΔmiRNA virus loses sensitivity to inhibition of lipid droplet formation while retaining sensitivity to inhibition of fatty acid synthesis. The simplest interpretation of this observation involves the idea of lipotoxicity [54], where the accumulation of fat requires lipid droplets to sequester toxic lipids which would otherwise accumulate in the cytoplasm and kill the cell. However, if fat is not accumulating in a cell, the successful storage of fat in lipids is less important for cell survival. If the miRNA induced Warburg metabolism is stimulating FAS, either by providing carbon and or providing reducing equivalents, then loss of the miRNA cluster would lead to less FAS, and less of a requirement for lipid droplets. It is also interesting that at least some of the requirement for FAS remains, suggesting that there may be a downstream product of FAS which is essential for latent KSHV infection independent of the Warburg effect.

We next tested inhibitors of lactate production (oxamate) and glutaminolysis (BPTES), which are both known to be necessary for amelioration of the consequences of Warburg induction. ΔmiRNA KSHV infected cells showed a decrease in sensitivity to oxamate, but still retains some requirement for the pathway. Glutaminolysis was slightly less clear due to the small effect size, but it appears to be required even in the absence of the miRNA cluster. We also tested the sensitivity of KSHV infected cells to statin treatment. Recent publications suggest that statins might prime cells to respond to viral infections through innate immune pathways [143], and the interferon stimulated gene viperin inhibits infection by a number of viruses by inhibition of an enzyme in the mevalonate pathway [10, 133]. Additionally,

FAS and cholesterol biosynthesis are often linked to one another by transcription activation, and utilize the same substrates in the same cellular compartments [140]. Contrary to our expectations, endothelial cells latently infected with KSHV showed no significant sensitivity to treatment with pravastatin.

Lastly, we sought to complement the loss of the miRNA cluster in triacsin C treatment. However, we were not successful in our attempts to rescue cells by expression of the entire cluster or with parts of the cluster. We were not able to confirm expression of mature miRNAs, but we were using lentiviral constructs similar to those used to demonstrate that the miRNA cluster induces Warburg metabolism. We tested for the possibility that the 3 kbp deletion in the latent locus had negative effects on the expression of the surrounding genes. Using RT-qPCR we found that expression of the rest of the latent locus was reduced to approximately half of the levels observed during wild type KSHV infection. The expression defects caused by the deletion raise the question of whether it is only the loss of miRNA cluster that results in loss of the requirement for lipid droplet formation or if other latent genes may be involved. Future experiments expressing latent genes in isolation and in combination while testing for triacsin C sensitivity will help to inform the above results of this chapter.

Chapter 6
SUMMARY AND FUTURE DIRECTIONS

6.1 Summary

KSHV is the etiological agent of a few forms of cancer, with KS being the most well-known due to its association with the AIDS epidemic [18]. KS incidence has increased with the onset of the AIDS epidemic to the point of becoming one of the most common cancers in Sub-Saharan Africa. While KS can be treated with some success with liposomal anthracyclines [81], disease is not resolved in every patient and the cost of treatment means it is not useful in resource limited environments. Additionally, KSHV also causes PEL, a rare B cell cancer with a typically poor prognosis. There is a need for additional therapeutic targets, preferably with chemical inhibitors that are inexpensive and widely available.

The main proliferating component of KS is the spindle cell. Though the exact origin of the spindle cell is not known, it is currently believed to be of endothelial origin. Within the KS tumor, over 90% of the cells are latently infected. Latency is a cellular state where no virus production occurs and where few viral genes are actually expressed. The lack of viral replication in spindle cells is troubling for intervention as traditional therapies for herpesvirus caused diseases target lytic replication. While lytic replication is also likely important for disease, the predominance of latent cells in a KS tumor suggests identifying targetable functions in latently infected cells are necessary for successful treatment.

Our lab has previously demonstrated that latently infected cells can be selectively killed using inhibitors to specific metabolic pathways. Initial work found that KSHV induces the Warburg effect during latent infection of endothelial cells, which is a state of increased glucose consumption, increased lactic acid production, and decreased oxygen consumption [25].

The Warburg effect is understood to be a general program of metabolism in rapidly proliferating cells which cancer cells co-opt. Of particular interest, the changes in metabolism are targetable vulnerabilities for KSHV infected cells but not uninfected controls. Chemical inhibition of glycolysis at glucose-6-phosphate isomerase with 2-DG or lactate production with oxamate lead to apoptosis during latent KSHV infection. Since the glycolytic changes induced by KSHV aided the identification of new therapies, our lab next published on a large scale metabolomic screen which led to the identification of fatty acid synthesis and glutamine metabolism as significantly altered during latent infection [26, 110]. These pathways provided previously unknown targets for latent infection in fatty acid synthase, acetyl-CoA carboxylase, and glutaminase.

The advent of CRISPR technology in high-throughput screening for essential genes after the metabolomic studies provided a new approach to identifying new therapeutic targets. Even just within the KSHV field, other groups have published on screens in PELs and the murine MM cell line [88, 48]. However, a screen in cells which are relevant to KS spindle cells had not been done prior to the work in this thesis. We performed a single replicate, whole-genome screen using a lentivirus-based CRISPR/Cas9 sgRNA library followed by a two replicate sub-pool screen to identify genes which are essential to latent KSHV infection. In addition to comparing mock and KSHV infected cells at the end of the experiment, we harvested the dead cells in the supernatant from each sample at each passage and sequenced the dead cell pools as well. The rationale for collecting dead cells was to help us differentiate between knockouts which suppress proliferation and knockouts which induce cell death. Our initial screen produced a 146 KSHV essential gene list from the live cell screen and roughly 1600 genes which were enriched in our dead cell screen. Our follow up sub-pool screening used the initial whole genome screen to define a list of high-likelihood targets as well as find controls which are not expected to change. We generated a new library with ~13 sgRNAs targeting each gene in this list and repeated our screening protocol. Overall, we found

a relatively low level of reproducibility from our initial screen to our second, but we have successfully been able to follow up on candidates from our initial screen. The sub-pool screen allowed us to identify genes as essential which were not quite significant in our whole genome screen. The most promising among these so far is the anti-apoptotic protein BCL2L1 (or BCL-xL) which has been validated above using independently cloned sgRNAs in TIME cells. The identification of BCL2L1 is of particular interest to our lab as it has been identified as a sensor for metabolic stress [124]. Our lab's work on the use of metabolic inhibitors during latent infection frequently finds the pathway of cell death to be apoptosis, but the mechanism triggering this response has not yet been identified.

Both the whole genome screen as well as the sub-pool screen contained a number of different genes involved in mitochondrial translation. Because mitochondrial ribosomes have a shared ancestry with bacterial ribosomes, antibiotics which target bacterial translation can also be used to inhibit mitochondrial translation. Other groups have successfully used antibiotics to selectively inhibit the proliferation of cancer cells in culture [75, 67]. Additionally, many antibiotics are widely available and relatively inexpensive. For these reasons we identified mitochondrial translation as a possible pathway for therapeutic intervention. We found that antibiotic treatment lead to the suppression of proliferation in latently infected human endothelial cells, and induced cell death in PEL cell lines while cells lacking KSHV showed reduced responses in both cases. The function of the mitochondrial ribosome is to translate the proteins encoded in the mitochondrial genome which are essential for respiration. To determine if respiration itself is essential, we treated cells with rotenone, an inhibitor of complex I of the electron transport chain (ETC). Rotenone treatment led to the induction of cell death in KSHV PELs, but not in uninfected B-cell lymphomas. Even though TIME cells showed no response to rotenone, testing TIME cells lacking mitochondrial genomes confirmed that these cells need the the entire ETC for optimal proliferation in culture.

We hypothesized that endothelial cells latently infected with KSHV are sensitive to the

inhibition of mitochondrial translation because KSHV itself might be interfering with mitochondrial function. As our lab has previously published that mitochondrial respiration is reduced during KSHV infection [25], induction of mitochondrial defects seemed like a likely possibility. We examined three possible points for the induction of defects in mitochondrial function. The first was mitochondrial network architecture, where dysfunctional mitochondria are expected to present in a fractured structure rather than an interconnected network [115]. The second was mitochondrial transcription, where suppression of the expression of mitochondrial gene expression leads to defective metabolism, known to occur during some immune responses including NF- KB [64]. The last was the possibility that KSHV might be suppressing mitochondrial translation itself. The possibility of KSHV mediated interference with mitochondrial is supported by protein interaction data generated by the Glaunsinger lab which suggested that the latent protein vFLIP has a physical interaction with the large subunit of the mitochondrial ribosome [23]. Contrary to our expectations, we found no indication in any of the above points that KSHV was directly altering mitochondrial function. However, we did find that three of the latent proteins partially localize to the mitochondriaa, leaving the possibility that these genes are having a direct effect on mitochondrial function through a currently unknown mechanism.

The last chapter of this thesis followed up on the requirement for fatty acid synthesis and attempted to examine the relationship between metabolic pathway inhibitors and the presence of the Warburg effect in endothelial cells. Work done by another group showing that the latent miRNA cluster is sufficient for induction of Warburg metabolism in endothelium [142] set the foundation for probing in involvement of KSHV genes in metabolism. We first found that the latent locus is sufficient for inducing the accumulation of lipid droplets to a level similar to KSHV infection. We also found that inhibition of lipid droplet formation with the acyl-CoA synthetase inhibitor triascin C induced cell death in latently infected cells while having little effect during mock infection. We next took advantage of a mutant virus lacking

a 3 kbp region in the latent locus which contains 10 of the 12 miRNA loci. We compared latent infection of endothelial cells with wild type virus to infection with the miRNA mutant virus in regard to susceptibility to metabolic inhibitors. The inhibitors tested included oxamate, TOFA which inhibits acetyl-CoA carboxylase, BPTES which inhibits glutaminase, and triacsin C. We found that cells latently infected with the miRNA virus retained at least some sensitivity to all inhibitors with the exception of triascin C. This suggests that the production of lactate, breakdown of glutamine, and synthesis of fatty acids are essential regardless of the Warburg status of the cell, while lipid droplet formation is essential only in the presence of Warburg induction.

We believe the separation of the requirement of fatty acid synthesis and lipid droplet formation reveals an important aspect of lipid biology during KSHV infection. The hypothesis is that Warburg metabolism supports the accumulation fatty acids during infection, but accumulation of fat in the cytosol results in lipotoxicity when cells can not store fat in lipid droplets. However, if Warburg is not induced, there is less of a requirement for lipid droplet formation. Lastly, after our attempts to complement the loss of triacsin C sensitivity with exogenous expression of the miRNA cluster failed, we examined expression of the transcripts from the latent locus for potential defects in transcription. We found that the transcription of the entire latent locus is suppressed, suggesting that the 3 kbp deletion had a negative effect on the rest of the latent genes. This complicates our findings, however we can attribute the loss of triascin C to the absence of the latent locus.

6.2 Future Directions

6.2.1 CRISPR/Cas9 Screening

There is substantial application for CRISPR/Cas9 screening during KSHV infection. Our lab has established the ability to implement full genome screens as well as carry out custom screens to assay for essential genes during KSHV infection. One observation from

our sub-pool screen was that the sgRNA level results from our whole genome screen were a better predictor of whether or not a particular gene was essential than MAGeCK score. Additional sub-pool screening with genes designed around the most depleted sgRNAs in our original screen is likely to yield additional essential genes. Additional changes to protocols might improve future screening efforts. Increasing the number of replicates where technically possible. The sgRNAs used for our whole genome screen are currently outdated, and using more recent libraries with higher on-target efficiencies will improve essential gene discovery. Finally, there is evidence that histone deacetylase (HDAC) inhibitors can increase editing efficiency and the addition of an HDAC inhibition step may improve the effectiveness of dropout screens [83]. In addition to knock-out screening, CRISPRi and CRISPRa [39] systems can be used to further probe the biology of latency during infection with KSHV. CRISPRi uses catalytically inactive Cas9 fused to a protein which induces heterochromatin formation to silence gene expression. These constructs are targeted to RNA pol II binding sites in the genome where they suppress gene expression. The CRISPRi system can be used to probe the effect of knock-down rather than knock-out during KSHV infection which may yield tractable therapeutic options. CRISPRa also uses catalytically inactive Cas9, but this time it is fused to a strong transactivation domain which drives expression of downstream genes. CRISPRa will enable us to examine the effect of increased expression of virtually every protein coding gene in the human genome on KSHV infection. This will allow us to identify novel restriction factors which may prevent KSHV from infecting certain cell types and offer another potential way of restricting infection. While CRISPR/Cas9 Screening has been far from perfect, it has been fruitful and the large toolbox of different types of systems readily available leaves many new avenues to take where the experimental protocol is essentially identical to the ones used in this thesis.

6.2.2 Mitochondrial Biology

It's clear that endothelial cells latently infected with KSHV and PELs are sensitive to inhibition of mitochondrial translation, but it is still unclear how this is happening and if it is connected to the previously reported metabolic alterations. While the lab has previously published that mitochondrial respiration is decreased during latent KSHV infection, it is not clear if decreased respiration is due to an actual deficit in mitochondrial function or an under-utilization of the cell's mitochondrial capacity. Respiration can be assayed on a Seahorse XF analyzer by measuring oxygen consumption in response to a series of drugs. This will measure how much oxygen is being consumed at a basal level and compare that to the amount of oxygen consumed in the presence of a decoupling agent which disrupts the proton gradient and induces maximum oxygen consumption. If mitochondrial function is indeed disrupted, then the viral genes known to localize to the mitochondria can be tested individually and in combination to identify genes interfering with maximal oxygen consumption. The hope is that with a viral gene identified and mass-spec determined protein interaction networks available for each viral protein, the mechanism of the mitochondrial perturbation will be relatively easy to find. If maximum oxygen consumption is unchanged during KSHV infection, suppressed oxygen consumption is likely being governed by a change in substrate availability. Substrate utilization can be assayed by coupling techniques previously used in our lab to do metabolomics on isolated mitochondria in mock infected cells and cells latently infected with KSHV. Metabolic screening of mitochondria will shed light on possible mechanisms where viral genes interfere with substrate availability. As an example, decreased respiration could be caused by a reduction in mitochondrial NADH. A lack of NADH would suggest a defect in one of the shuttling pathways (e.g. the malate-aspartate shuttle). While the latter direction is more open-ended, both of these alternatives will be useful for informing our understanding of Warburg induction and the possible connection sensitivity to antibiotic treatment during latent KSHV infection.

6.2.3 Metabolic Pathway Inhibition

Work in this chapter made progress in identifying the viral determinant of fatty acid accumulation, but the minimal set of latent genes still needs to be identified. The first step is testing single genes and gene combinations to identify factors needed for lipid droplet formation. One technical hurdle that will need to be addressed is how to express the miRNA cluster. We can express the miRNAs well individually, but the literature suggests that single miRNAs are not sufficient for most phenotypes. We need to develop and validate a better expression system for non-coding RNAs to definitively test the necessity of the entire cluster. We also need to confirm that the miRNA cluster is actually essential for Warburg induction, and not just sufficient. Confirmation of Warburg induction can be done on the Seahorse XF analyzer mentioned above, which our lab has used previously. The metabolic pathway inhibition in chapter 5 only hints at a connection between glycolysis and FAS, but this can be definitively shown using C13 tracing of glucose. C13 labeled glucose will enable the tracing of carbon into specific pathways, including fatty acid synthesis. Because the phenotype of triascin C induced cell death is relatively strong, that assay lends itself to functional analysis. Each of the latent genes should be tested individually and in combination to the ability to restore triacsin C sensitivity in endothelial cells infected with KSHV lacking the miRNA cluster. The above experiments will inform the necessity for the miRNA cluster in Warburg induction and clarify the relationship between the requirements for each of the pathways tested in chapter 5 during Warburg induction.

6.3 Conclusion

CRISPR/Cas9 knock-out screening is a powerful new approach to identifying the genetic requirements of cellular proliferation and survival. Our group and others have successfully used this technology to identify genes which can be targeted to inhibit viral infection. In my thesis, I performed the first of these screens in a human endothelial cell line infected with

KSHV. As KS tumors are predominantly composed of latently infected endothelial cells, this study sought to identify novel targets for potential therapeutic use. The whole genome screen was followed up with sub-pool screening to generate a list of strongly selective hits.

I followed up on some of the suggested targets by focusing on mitochondrial translation. The literature suggested that mitochondrial translation was a reasonable, targetable process due to the shared ancestry between mitochondrial and bacterial ribosomes allowing the use of widely available antibiotics to inhibit mitochondrial function. I found that antibiotics were able to suppress the proliferation of latently infected endothelial cells and induce cell death in latently infected primary effusion lymphomas while controls lacking KSHV were less affected. In an attempt to explain why KSHV infection causes sensitivity to antibiotic treatment, I sought to describe mitochondria during latency. I found that there are fewer mitochondria during latent infection, but mitochondria take up more space in the cell and are longer on average. In addition, I found that transcript levels of mitochondrial genome encoded genes and mitochondrial genome copy numbers are both increased during infection. The state of mitochondria I found is not consistent with mitochondrial dysfunction, though I did not explore all possibilities. To determine if any viral genes were physically locating to the mitochondria I isolated the mitochondria from cells expressing tagged version of latent proteins and found that three of the proteins tested were present in the isolates. This leaves open the possibility that one of these genes may be stressing the mitochondria to the point that the addition of antibiotics is catastrophic.

Lastly, I showed that the latent locus of KSHV is sufficient for the accumulation of lipid droplets, and that chemical inhibition of lipid droplets selectively kills infected cells. I also found that a virus lacking the latent miRNA cluster loses the requirment for lipid droplets requirement while retaining at least some of the requirement for lactate production, glutaminolysis, and FAS. Due to an issue with the mutation in the deletion virus, expression of the rest of the latent locus was suppressed, so it is possible that the phenotypes observed

are not due to the loss of the miRNA cluster. Together, the studies in these chapters identified new targets for KS treatment and provided direction for future inquiries into the changes of cellular metabolism induced by KSHV.

Daniel Holmes

dlholmes@uw.edu

Microbiology, South Lake Union
University of Washington
750 Republican St.

Box 358070
Seattle, WA 98109
(214)-507-2324

Education

University of Washington
Ph.D. Candidate in Microbiology
Anticipated Graduation: September 2020. GPA: 3.7

Rutgers University, B.S.
Microbiology Major, Public Health Minor
Graduated: Fall 2010. GPA: 3.56

Research Experience

University of Washington Medical Center, Department of Microbiology, Seattle, WA

- June 2014-present
- Graduate research assistant
- Studying metabolic alterations of endothelial cells during viral infection
- Identifying viral and cellular determinants of changes in fatty acid metabolism
- CRISPR/Cas9 whole genome and subpool screening for essential host factors during KSHV infection
- Mentoring undergraduate and post-baccalaureate research assistants

University of Texas Southwestern Medical Center, Department of Biochemistry, Dallas, TX

- April 2011-August 2013
- Research technician
- Characterizing the effects of the [MOT3] prion
- Developing a flow cytometry-based assay for prion aggregation
- Cloning, western blots, RNA isolation and RT-PCR among many other techniques
- Managing the purchase and upkeep of lab equipment and supplies
- Training of new lab members

Rutgers University, The Environmental Biophysics & Molecular Ecology Program, New Brunswick, NJ

- February 2010-December 2010
- Undergraduate research
- Studied cell death and viral infection in phytoplankton
- Worked on the purification of virus from culture for genome sequencing

Publications

Holmes DL, Vogt D, Lagunoff M. (2020) A CRISPR/Cas9 screen identifies mitochondrial translation as an essential process in latent KSHV infection of human endothelial cells. *Proceedings of the National Academy of Sciences*. (under revision).

Holmes DL, Hart M, Yie J, Lagunoff M. (2020) Conditional lethality of metabolic pathway inhibition during Warburg induction by KSHV. (in preparation).

Holmes DL, Lancaster AK, Lindquist S, and Halfmann R. (2013). Heritable remodeling of yeast multicellularity by an environmentally responsive prion. *Cell* 153(1), 153-165.

Wang G, Wang X, Yu H, Wei S, Williams N, **Holmes DL**, Halfmann R, Naidoo J, Wang L, Li L, Chen S, Harran P, Lei X, Wang X. (2013). Small-molecule activation of the TRAIL receptor DR5 in human cancer cells. *Nature Chemical Biology* 9, 84–89.

Research Presentations

"A CRISPR/Cas9 screen reveals mitochondrial translation as an essential process for latent KSHV infection"
Public Oral Presentation & Poster: 44th IHW, Knoxville, TN, summer 2019.

"A CRISPR/Cas9 screen reveals mitochondrial translation as an essential process for latent KSHV infection"
Public Oral Presentation: Pathogen-Associated Malignancies Retreat, Seattle, WA, spring 2019.

"A CRISPR/Cas9 screen reveals mitochondrial translation as an essential process for latent KSHV infection"
Poster Presentation: Dept. of Microbiology Retreat, Leavenworth, WA, fall 2018.

"A CRISPR/Cas9 screen reveals mitochondrial translation as an essential process for latent KSHV infection"
Public Oral Presentation: 43rd IHW Gammaherpesvirus Satellite, Vancouver, BC, summer 2018.
Poster Presentation: 43rd IHW, Vancouver, BC, summer 2018.

*"*A CRISPR/Cas9 screen reveals mitochondrial translation as an essential process for latent KSHV infection"
Poster Presentation: Viral Pathogenesis Retreat, Seattle, WA, summer 2018

"Perturbation of host fatty acid metabolism by the KSHV latent region"
Poster Presentation: Dept. of Microbiology Retreat, Leavenworth, WA, fall 2017.

"Conditional lethality for metabolic pathways during Warburg induction by KSHV"
Poster Presentation: Viral Pathogenesis Retreat, Seattle, WA, summer 2017

"Perturbation of host fatty acid metabolism by the KSHV latent region"
Poster Presentation: Dept. of Microbiology Retreat, Leavenworth, WA, fall 2016

"Manipulation of cellular fatty acid metabolism by the KSHV latent region"
Public Oral Presentation: Viral Pathogenesis Retreat, Seattle, WA, summer 2016

"The KSHV latency region stimulates endothelial cells to accumulate fatty acids"
Poster Presentation: Dept. of Microbiology Retreat, Leavenworth, WA, fall 2015
Poster Presentation: Viral Pathogenesis Retreat, Seattle, WA, summer 2015

Honors and Awards

International Herpes Workshop 2019 Merit Award	Summer 2019
Department of Microbiology Retreat Poster Award	Fall 2018
NSF GRFP Honorable Mention	2015
UW Top Scholar Award	Fall 2013

Teaching Experience

Microbiology 402: Fundamentals of General Microbiology Lab: spring 2015

- Laboratory section teaching assistant

Microbiology 411: Bacterial Genetics: winter 2015

- Laboratory section teaching assistant

Meetings Attended

44th Annual International Herpes Workshop: Knoxville, TN, July 20th- July 24th 2019.
43rd Annual International Herpes Workshop: Vancouver, BC, July 21st- July 25th 2018.
18th International Workshop on KSHV and Related Agents: Miami, FL, June 30th- July 3rd 2015.

Funding Sources

UW/FHCRC Viral Pathogenesis Training Grant	June 2014-June 2016
UW Top Scholars Award	Fall 2013

Mentoring and Outreach

Jie Yin: Undergraduate Summer 2016-Sping 2018

- Currently in medical school at Boston University
- Post-baccalaureate program at the NIH beginning Summer 2018
- Husky 100, 2018
- Levinson Emerging Scholars Award, University of Washington, September 2017
- Jacques Chiller Award, Department of Microbiology, University of Washington, May 2017
- Mary Gates Endowment Research Award, University of Washington, May 2017
- Undergraduate Research Award, Department of Microbiology, March 2017

Maddie Hart: Post-baccalaureate Summer 2017-Summer 2018

- Ph.D. student in M3D beginning Fall 2018 at University of Washington

STEM-OUT: Weekly, fall 2014-spring 2015

- Mentoring high-school students at TAF Academy in Federal Way, WA

BIBLIOGRAPHY

[1] Feng-Qi An, Hope Merlene Folarin, Nicole Compitello, Justin Roth, Stanton L. Gerson, Keith R. McCrae, Farnaz D. Fakhari, Dirk P. Dittmer, and Rolf Renne. Long-Term-Infected Telomerase-Immortalized Endothelial Cells: a Model for Kaposi's Sarcoma-Associated Herpesvirus Latency In Vitro and In Vivo. *Journal of Virology*, 80(10):4833–4846, may 2006.

[2] Carolina Arias, Ben Weisburd, Noam Stern-Ginossar, Alexandre Mercier, Alexis S. Madrid, Priya Bellare, Meghan Holdorf, Jonathan S. Weissman, and Don Ganem. KSHV 2.0: A Comprehensive Annotation of the Kaposi's Sarcoma-Associated Herpesvirus Genome Using Next-Generation Sequencing Reveals Novel Genomic and Functional Features. *PLoS Pathogens*, 10(1):e1003847, jan 2014.

[3] Rodolphe Barrangou, Christophe Fremaux, Hélène Deveau, Melissa Richards, Patrick Boyaval, Sylvain Moineau, Dennis A. Romero, and Philippe Horvath. CRISPR provides acquired resistance against viruses in prokaryotes. *Science*, 315(5819):1709–1712, mar 2007.

[4] F. Barré-Sinoussi, J. C. Chermann, F. Rey, M. T. Nugeyre, S. Chamaret, J. Gruest, C. Dauguet, C. Axler-Blin, F. Vézinet-Brun, C. Rouzioux, W. Rozenbaum, and L. Montagnier. Isolation of a T-lymphotropic retrovirus from a patient at risk for acquired immune deficiency syndrome (AIDS). *Science*, 220(4599):868–871, 1983.

[5] Fiona M. Behan, Francesco Iorio, Gabriele Picco, Emanuel Gonçalves, Charlotte M. Beaver, Giorgia Migliardi, Rita Santos, Yanhua Rao, Francesco Sassi, Marika Pinnelli,

Rizwan Ansari, Sarah Harper, David Adam Jackson, Rebecca McRae, Rachel Pooley, Piers Wilkinson, Dieudonne van der Meer, David Dow, Carolyn Buser-Doepner, Andrea Bertotti, Livio Trusolino, Euan A. Stronach, Julio Saez-Rodriguez, Kosuke Yusa, and Mathew J. Garnett. Prioritization of cancer therapeutic targets using CRISPR–Cas9 screens. *Nature*, 568(7753):511–516, apr 2019.

[6] V. Beral, T. A. Peterman, R. L. Berkelman, and H. W. Jaffe. Kaposi's sarcoma among persons with AIDS: a sexually transmitted infection? *The Lancet*, 335(8682):123–128, jan 1990.

[7] Giovanni Bernard, Nadège Bellance, Dominic James, Philippe Parrone, Helder Fernandez, Thierry Letellier, and Rodrigue Rossignol. Mitochondrial bioenergetics and structural network organization. *Journal of Cell Science*, 120(5):838–848, mar 2007.

[8] Aadra P Bhatt, Sarah R Jacobs, Alex J Freemerman, Liza Makowski, Jeffrey C Rathmell, Dirk P Dittmer, and Blossom Damania. Dysregulation of fatty acid synthesis and glycolysis in non-Hodgkin lymphoma. *Proceedings of the National Academy of Sciences of the United States of America*, 109(29):11818–23, jul 2012.

[9] Grace Birungi, Sheryl Meijie Chen, Boon Pheng Loy, Mah Lee Ng, and Sam Fong Yau Li. Metabolomics approach for investigation of effects of dengue virus infection using the EA.hy926 cell line. *Journal of Proteome Research*, 9(12):6523–6534, dec 2010.

[10] Mathieu Blanc, Wei Yuan Hsieh, Kevin A. Robertson, Steven Watterson, Guanghou Shui, Paul Lacaze, Mizanur Khondoker, Paul Dickinson, Garwin Sing, Sara Rodríguez-Martín, Peter Phelan, Thorsten Forster, Birgit Strobl, Matthias Müller, Rudolph Riemersma, Timothy Osborne, Markus R. Wenk, Ana Angulo, and Peter Ghazal. Host Defense against Viral Infection Involves Interferon Mediated Down-Regulation of Sterol Biosynthesis. *PLoS Biology*, 9(3):e1000598, mar 2011.

[11] Francis Blokzijl, Joep De Ligt, Myrthe Jager, Valentina Sasselli, Sophie Roerink, Nobuo Sasaki, Meritxell Huch, Sander Boymans, Ewart Kuijk, Pjotr Prins, Isaac J. Nijman, Inigo Martincorena, Michal Mokry, Caroline L. Wiegerinck, Sabine Middendorp, Toshiro Sato, Gerald Schwank, Edward E.S. Nieuwenhuis, Monique M.A. Verstegen, Luc J.W. Van Der Laan, Jeroen De Jonge, Jan N.M. Ijzermans, Robert G. Vries, Marc Van De Wetering, Michael R. Stratton, Hans Clevers, Edwin Cuppen, and Ruben Van Boxtel. Tissue-specific mutation accumulation in human adult stem cells during life. *Nature*, 538(7624):260–264, 2016.

[12] Veronika Boczonadi and Rita Horvath. Mitochondria: Impaired mitochondrial translation in human disease, mar 2014.

[13] Alexander Bolotin, Benoit Quinquis, Alexei Sorokin, and S. Dusko Ehrlich. Clustered regularly interspaced short palindrome repeats (CRISPRs) have spacers of extrachromosomal origin. *Microbiology*, 151(8):2551–2561, aug 2005.

[14] Stan J.J. Brouns, Matthijs M. Jore, Magnus Lundgren, Edze R. Westra, Rik J.H. Slijkhuis, Ambrosius P.L. Snijders, Mark J. Dickman, Kira S. Makarova, Eugene V. Koonin, and John Van Der Oost. Small CRISPR RNAs guide antiviral defense in prokaryotes. *Science*, 321(5891):960–964, aug 2008.

[15] Kevin F Brulois, Heesoon Chang, Amy Si-Ying Lee, Armin Ensser, Lai-Yee Wong, Zsolt Toth, Sun Hwa Lee, Hye-Ra Lee, Jinjong Myoung, Don Ganem, Tae-Kwang Oh, Jihyun F Kim, Shou-Jiang Gao, and Jae U Jung. Construction and manipulation of a new Kaposi's sarcoma-associated herpesvirus bacterial artificial chromosome clone. *Journal of virology*, 86(18):9708–20, sep 2012.

[16] Xuezhong Cai, Shihua Lu, Zhihong Zhang, Carlos M. Gonzalez, Blossom Damania, and Bryan R. Cullen. Kaposi's sarcoma-associated herpesvirus expresses an array of

viral microRNAs in latently infected cells. *Proceedings of the National Academy of Sciences of the United States of America*, 102(15):5570–5575, apr 2005.

[17] Ethel Cesarman, Yuan Chang, Patrick S. Moore, Jonathan W. Said, and Daniel M. Knowles. Kaposi's sarcoma-associated herpesvirus-like DNA sequences in AIDS-related body-cavity-based lymphomas. *New England Journal of Medicine*, 332(18):1186–1191, may 1995.

[18] Ethel Cesarman, Blossom Damania, Susan E. Krown, Jeffrey Martin, Mark Bower, and Denise Whitby. Kaposi sarcoma. *Nature Reviews Disease Primers*, 5(1):9, dec 2019.

[19] Y Chang, E Cesarman, M. Pessin, F Lee, J Culpepper, D. Knowles, and P. Moore. Identification of herpesvirus-like DNA sequences in AIDS-associated Kaposi's sarcoma. *Science*, 266(5192):1865–1869, dec 1994.

[20] Bruce H. Cohen and Russell P. Saneto. Mitochondrial translational inhibitors in the pharmacopeia, sep 2012.

[21] Le Cong, F. Ann Ran, David Cox, Shuailiang Lin, Robert Barretto, Naomi Habib, Patrick D. Hsu, Xuebing Wu, Wenyan Jiang, Luciano A. Marraffini, and Feng Zhang. Multiplex genome engineering using CRISPR/Cas systems. *Science*, 339(6121):819–823, feb 2013.

[22] Erin Currie, Almut Schulze, Rudolf Zechner, Tobias C. Walther, and Robert V. Farese. Cellular fatty acid metabolism and cancer, aug 2013.

[23] Zoe H. Davis, Erik Verschueren, Gwendolyn M. Jang, Kevin Kleffman, Jeffrey R. Johnson, Jimin Park, John VonDollen, M. Cyrus Maher, Tasha Johnson, William Newton, Stefanie Jäger, Michael Shales, Julie Horner, Ryan D. Hernandez, Nevan J. Krogan,

and Britt A. Glaunsinger. Global mapping of herpesvirus-host protein complexes reveals a transcription strategy for late genes. *Molecular Cell*, 57(2):349–360, jan 2015.

[24] Ralph J. DeBerardinis, Anthony Mancuso, Evgueni Daikhin, Ilana Nissim, Marc Yudkoff, Suzanne Wehrli, and Craig B. Thompson. Beyond aerobic glycolysis: Transformed cells can engage in glutamine metabolism that exceeds the requirement for protein and nucleotide synthesis. *Proceedings of the National Academy of Sciences of the United States of America*, 104(49):19345–19350, dec 2007.

[25] Tracie Delgado, Patrick A Carroll, Almira S Punjabi, Daciana Margineantu, David M Hockenbery, and Michael Lagunoff. Induction of the Warburg effect by Kaposi's sarcoma herpesvirus is required for the maintenance of latently infected endothelial cells. *Proceedings of the National Academy of Sciences of the United States of America*, 107(23):10696–701, jun 2010.

[26] Tracie Delgado, Erica L Sanchez, Roman Camarda, and Michael Lagunoff. Global metabolic profiling of infection by an oncogenic virus: KSHV induces and requires lipogenesis for survival of latent infection. *PLoS pathogens*, 8(8):e1002866, jan 2012.

[27] Elitza Deltcheva, Krzysztof Chylinski, Cynthia M. Sharma, Karine Gonzales, Yanjie Chao, Zaid A. Pirzada, Maria R. Eckert, Jörg Vogel, and Emmanuelle Charpentier. CRISPR RNA maturation by trans-encoded small RNA and host factor RNase III. *Nature*, 471(7340):602–607, mar 2011.

[28] Dirk Dittmer, Michael Lagunoff, Rolf Renne, Katherine Staskus, Ashley Haase, and Don Ganem. A Cluster of Latently Expressed Genes in Kaposi's Sarcoma-Associated Herpesvirus. *Journal of Virology*, 72(10):8309–8315, oct 1998.

[29] John G. Doench, Nicolo Fusi, Meagan Sullender, Mudra Hegde, Emma W. Vaimberg, Katherine F. Donovan, Ian Smith, Zuzana Tothova, Craig Wilen, Robert Orchard,

Herbert W. Virgin, Jennifer Listgarten, and David E. Root. Optimized sgRNA design to maximize activity and minimize off-target effects of CRISPR-Cas9. *Nature Biotechnology*, 34(2):184–191, feb 2016.

[30] J. J.Gomes D'oliveira and F. Oliveira Torres. Kaposi's sarcoma in the bantu of mozambique. *Cancer*, 30(2):553–561, 1972.

[31] Lan Feng Dong, Jaromira Kovarova, Martina Bajzikova, Ayenachew Bezawork-Geleta, David Svec, Berwini Endaya, Karishma Sachaphibulkij, Ana R. Coelho, Natasa Sebkova, Anna Ruzickova, An S. Tan, Katarina Kluckova, Kristyna Judasova, Katerina Zamecnikova, Zuzana Rychtarcikova, Vinod Gopalan, Ladislav Andera, Margarita Sobol, Bing Yan, Bijay Pattnaik, Naveen Bhatraju, Jaroslav Truksa, Pavel Stopka, Pavel Hozak, Alfred K. Lam, Radislav Sedlacek, Paulo J. Oliveira, Mikael Kubista, Anurag Agrawal, Katerina Dvorakova-Hortova, Jakub Rohlena, Michael V. Berridge, and Jiri Neuzil. Horizontal transfer of whole mitochondria restores tumorigenic potential in mitochondrial DNA-deficient cancer cells. *eLife*, 6, feb 2017.

[32] Aurélia Faure, Mitch Hayes, and Bill Sugden. How Kaposi's sarcoma-associated herpesvirus stably transforms peripheral B cells towards lymphomagenesis. *Proceedings of the National Academy of Sciences of the United States of America*, 116(33):16519–16528, aug 2019.

[33] Nigel Field, Walter Low, Mark Daniels, Steven Howell, Laurent Daviet, Chris Boshoff, and Mary Collins. KSHV vFLIP binds to IKK-γ to activate IKK. *Journal of Cell Science*, 116(18):3721–3728, sep 2003.

[34] Mike Flint, Payel Chatterjee, David L. Lin, Laura K. McMullan, Punya Shrivastava-Ranjan, Éric Bergeron, Michael K. Lo, Stephen R. Welch, Stuart T. Nichol, Andrew W. Tai, and Christina F. Spiropoulou. A genome-wide CRISPR screen identifies

N-acetylglucosamine-1-phosphate transferase as a potential antiviral target for Ebola virus. *Nature Communications*, 10(1):1–13, dec 2019.

[35] Jacques Friborg, Wing Pul Kong, Michael O. Hottlger, and Gary J. Nabel. p53 Inhibition by the LANA protein of KSHV protects against cell death. *Nature*, 402(6764):889–894, dec 1999.

[36] Don Ganem. KSHV INFECTION AND THE PATHOGENESIS OF KAPOSI'S SARCOMA. *Annual Review of Pathology: Mechanisms of Disease*, 1(1):273–296, feb 2006.

[37] Anastasia Gelgor, Inna Kalt, Shir Bergson, Kevin F. Brulois, Jae U. Jung, and Ronit Sarid. Viral Bcl-2 Encoded by the Kaposi's Sarcoma-Associated Herpesvirus Is Vital for Virus Reactivation. *Journal of Virology*, 89(10):5298–5307, may 2015.

[38] An Hoa Giang, Tamara Raymond, Paul Brookes, Karen De Mesy Bentley, Edward Schwarz, Regis O'Keefe, and Roman Eliseev. Mitochondrial dysfunction and permeability transition in osteosarcoma cells showing the warburg effect. *Journal of Biological Chemistry*, 288(46):33303–33311, nov 2013.

[39] Luke A. Gilbert, Max A. Horlbeck, Britt Adamson, Jacqueline E. Villalta, Yuwen Chen, Evan H. Whitehead, Carla Guimaraes, Barbara Panning, Hidde L. Ploegh, Michael C. Bassik, Lei S. Qi, Martin Kampmann, and Jonathan S. Weissman. Genome-Scale CRISPR-Mediated Control of Gene Repression and Activation. *Cell*, 159(3):647–661, oct 2014.

[40] Priscila H. Gonçalves, Thomas S. Uldrick, and Robert Yarchoan. HIV-associated Kaposi sarcoma and related diseases, sep 2017.

[41] David E. Gordon, Gwendolyn M. Jang, Mehdi Bouhaddou, Jiewei Xu, Kirsten Obernier, Kris M. White, Matthew J. O'Meara, Veronica V. Rezelj, Jeffrey Z. Guo,

Danielle L. Swaney, Tia A. Tummino, Ruth Hüttenhain, Robyn M. Kaake, Alicia L. Richards, Beril Tutuncuoglu, Helene Foussard, Jyoti Batra, Kelsey Haas, Maya Modak, Minkyu Kim, Paige Haas, Benjamin J. Polacco, Hannes Braberg, Jacqueline M. Fabius, Manon Eckhardt, Margaret Soucheray, Melanie J. Bennett, Merve Cakir, Michael J. McGregor, Qiongyu Li, Bjoern Meyer, Ferdinand Roesch, Thomas Vallet, Alice Mac Kain, Lisa Miorin, Elena Moreno, Zun Zar Chi Naing, Yuan Zhou, Shiming Peng, Ying Shi, Ziyang Zhang, Wenqi Shen, Ilsa T. Kirby, James E. Melnyk, John S. Chorba, Kevin Lou, Shizhong A. Dai, Inigo Barrio-Hernandez, Danish Memon, Claudia Hernandez-Armenta, Jiankun Lyu, Christopher J.P. Mathy, Tina Perica, Kala Bharath Pilla, Sai J. Ganesan, Daniel J. Saltzberg, Ramachandran Rakesh, Xi Liu, Sara B. Rosenthal, Lorenzo Calviello, Srivats Venkataramanan, Jose Liboy-Lugo, Yizhu Lin, Xi Ping Huang, Yong Feng Liu, Stephanie A. Wankowicz, Markus Bohn, Maliheh Safari, Fatima S. Ugur, Cassandra Koh, Nastaran Sadat Savar, Quang Dinh Tran, Djoshkun Shengjuler, Sabrina J. Fletcher, Michael C. O'Neal, Yiming Cai, Jason C.J. Chang, David J. Broadhurst, Saker Klippsten, Phillip P. Sharp, Nicole A. Wenzell, Duygu Kuzuoglu-Ozturk, Hao Yuan Wang, Raphael Trenker, Janet M. Young, Devin A. Cavero, Joseph Hiatt, Theodore L. Roth, Ujjwal Rathore, Advait Subramanian, Julia Noack, Mathieu Hubert, Robert M. Stroud, Alan D. Frankel, Oren S. Rosenberg, Kliment A. Verba, David A. Agard, Melanie Ott, Michael Emerman, Natalia Jura, Mark von Zastrow, Eric Verdin, Alan Ashworth, Olivier Schwartz, Christophe D'Enfert, Shaeri Mukherjee, Matt Jacobson, Harmit S. Malik, Danica G. Fujimori, Trey Ideker, Charles S. Craik, Stephen N. Floor, James S. Fraser, John D. Gross, Andrej Sali, Bryan L. Roth, Davide Ruggero, Jack Taunton, Tanja Kortemme, Pedro Beltrao, Marco Vignuzzi, Adolfo García-Sastre, Kevan M. Shokat, Brian K. Shoichet, and Nevan J. Krogan. A SARS-CoV-2 protein interaction map reveals targets for drug repurposing. *Nature*, 583(7816):459–468, jul 2020.

[42] G. J. Gottlieb, A. Ragaz, J. V. Vogel, A. Friedman-Kien, A. M. Rywlin, E. A. Weiner, and A. B. Ackerman. A preliminary communication on extensively disseminated Kaposi's sarcoma in young homosexual men. *American Journal of Dermatopathology*, 3(2):111–114, 1981.

[43] Eva Gottwein. Kaposi's sarcoma-associated herpesvirus microRNAs, may 2012.

[44] Eva Gottwein, Neelanjan Mukherjee, Christoph Sachse, Corina Frenzel, William H. Majoros, Jen Tsan A. Chi, Ravi Braich, Muthiah Manoharan, Jürgen Soutschek, Uwe Ohler, and Bryan R. Cullen. A viral microRNA functions as an orthologue of cellular miR-155. *Nature*, 450(7172):1096–1099, dec 2007.

[45] Stéphanie Grandemange, Sébastien Herzig, and Jean Claude Martinou. Mitochondrial dynamics and cancer, feb 2009.

[46] Michael W. Gray, Gertraud Burger, and B. Franz Lang. Mitochondrial evolution, mar 1999.

[47] Claudia Grossmann, Simona Podgrabinska, Mihaela Skobe, and Don Ganem. Activation of NF-κB by the Latent vFLIP Gene of Kaposi's Sarcoma-Associated Herpesvirus Is Required for the Spindle Shape of Virus-Infected Endothelial Cells and Contributes to Their Proinflammatory Phenotype. *Journal of Virology*, 80(14):7179–7185, jul 2006.

[48] Marion Gruffaz, Hongfeng Yuan, Wen Meng, Hui Liu, Sangsu Bae, Jin Soo Kim, Chun Lu, Yufei Huang, and Shou Jiang Gao. CRISPR-Cas9 screening of Kaposi's sarcoma-associated herpesvirus-transformed cells identifies XPO1 as a vulnerable target of cancer cells. *mBio*, 10(3), may 2019.

[49] Ilaria Guasparri, Shannon A. Keller, and Ethel Cesarman. KSHV vFLIP Is Essential for the Survival of Infected Lymphoma Cells. *Journal of Experimental Medicine*, 199(7):993–1003, apr 2004.

[50] Douglas Hanahan and Robert A Weinberg. Hallmarks of cancer: the next generation. *Cell*, 144(5):646–74, mar 2011.

[51] Traver Hart, Megha Chandrashekhar, Michael Aregger, Zachary Steinhart, Kevin R. Brown, Graham MacLeod, Monika Mis, Michal Zimmermann, Amelie Fradet-Turcotte, Song Sun, Patricia Mero, Peter Dirks, Sachdev Sidhu, Frederick P. Roth, Olivia S. Rissland, Daniel Durocher, Stephane Angers, and Jason Moffat. High-Resolution CRISPR Screens Reveal Fitness Genes and Genotype-Specific Cancer Liabilities. *Cell*, 163(6):1515–1526, dec 2015.

[52] Traver Hart, Amy Hin Yan Tong, Katie Chan, Jolanda Van Leeuwen, Ashwin Seetharaman, Michael Aregger, Megha Chandrashekhar, Nicole Hustedt, Sahil Seth, Avery Noonan, Andrea Habsid, Olga Sizova, Lyudmila Nedyalkova, Ryan Climie, Leanne Tworzyanski, Keith Lawson, Maria Augusta Sartori, Sabriyeh Alibeh, David Tieu, Sanna Masud, Patricia Mero, Alexander Weiss, Kevin R. Brown, Matej Usaj, Maximilian Billmann, Mahfuzur Rahman, Michael Constanzo, Chad L. Myers, Brenda J. Andrews, Charles Boone, Daniel Durocher, and Jason Moffat. Evaluation and design of genome-wide CRISPR/SpCas9 knockout screens. *G3: Genes, Genomes, Genetics*, 7(8):2719–2727, 2017.

[53] Matthew G.Vander Heiden, Lewis C. Cantley, and Craig B. Thompson. Understanding the warburg effect: The metabolic requirements of cell proliferation, may 2009.

[54] Albert Herms, Marta Bosch, Nicholas Ariotti, Babu J.N. Reddy, Alba Fajardo, Andrea Fernández-Vidal, Anna Alvarez-Guaita, Manuel Alejandro Fernández-Rojo, Carles Rentero, Francesc Tebar, Carlos Enrich, María Isabel Geli, Robert G. Parton, Steven P. Gross, and Albert Pol. Cell-to-cell heterogeneity in lipid droplets suggests a mechanism to reduce lipotoxicity. *Current Biology*, 23(15):1489–1496, aug 2013.

[55] Brian G. Herndier, Albrecht Werner, Paul Arnstein, Nancy W. Abbey, Francesco Demartis, Robert L. Cohen, Marc A. Shuman, and Jay A. Levy. Characterization of a human Kaposi's sarcoma cell line that induces angiogenic tumors in animals. *AIDS*, 8(5):575–581, 1994.

[56] Joseph A. Hollenbaugh, Joshua Munger, and Baek Kim. Metabolite profiles of human immunodeficiency virus infected CD4+ T cells and macrophages using LC-MS/MS analysis. *Virology*, 415(2):153–159, jul 2011.

[57] Daniel L Holmes, Daniel T Vogt, and Michael Lagunoff. A CRISPR/Cas9 Screen Identifies Mitochondrial Translation as an Essential Process in Latent KSHV Infection of Human Endothelial Cells. *Proceedings of the National Academy of Sciences of the United States of America*, 2020.

[58] D. N. Hu, W. Q. Qiu, B. T. Wu, L. Z. Fang, F. Zhou, Y. P. Gu, Q. H. Zhang, J. H. Yan, Y. Q. Ding, and H. Wong. Genetic aspects of antibiotic induced deafness: Mitochondrial inheritance. *Journal of Medical Genetics*, 28(2):79–83, feb 1991.

[59] Y. Ishino, H. Shinagawa, K. Makino, M. Amemura, and A. Nakatura. Nucleotide sequence of the iap gene, responsible for alkaline phosphatase isoenzyme conversion in Escherichia coli, and identification of the gene product. *Journal of Bacteriology*, 169(12):5429–5433, 1987.

[60] Vaibhav Jain, Karlie Plaisance-Bonstaff, Rajnikumar Sangani, Curtis Lanier, Alexander Dolce, Jianhong Hu, Kevin Brulois, Irina Haecker, Peter Turner, Rolf Renne, and Brian Krueger. A toolbox for Herpesvirus miRNA research: Construction of a complete set of KSHV miRNA Deletion Mutants. *Viruses*, 8(2), feb 2016.

[61] Ruud Jansen, Jan D.A. Van Embden, Wim Gaastra, and Leo M. Schouls. Identification

of genes that are associated with DNA repeats in prokaryotes. *Molecular Microbiology*, 43(6):1565–1575, mar 2002.

[62] Martin Jinek, Krzysztof Chylinski, Ines Fonfara, Michael Hauer, Jennifer A. Doudna, and Emmanuelle Charpentier. A programmable dual-RNA-guided DNA endonuclease in adaptive bacterial immunity. *Science*, 337(6096):816–821, aug 2012.

[63] Martin Jinek, Alexandra East, Aaron Cheng, Steven Lin, Enbo Ma, and Jennifer Doudna. RNA-programmed genome editing in human cells. *eLife*, 2013(2), jan 2013.

[64] Renée F. Johnson, Ini Isabée Witzel, and Neil D. Perkins. p53-dependent regulation of mitochondrial energy production by the RelA subunit of NF-κB. *Cancer Research*, 71(16):5588–5597, aug 2011.

[65] Tiffany Jones, Fengchun Ye, Roble Bedolla, Yufei Huang, Jia Meng, Liwu Qian, Hongyi Pan, Fuchun Zhou, Rosalie Moody, Brent Wagner, Mazen Arar, and Shou Jiang Gao. Direct and efficient cellular transformation of primary rat mesenchymal precursor cells by KSHV. *Journal of Clinical Investigation*, 122(3):1076–1081, mar 2012.

[66] Julia Joung, Silvana Konermann, Jonathan S. Gootenberg, Omar O. Abudayyeh, Randall J. Platt, Mark D. Brigham, Neville E. Sanjana, and Feng Zhang. Genome-scale CRISPR-Cas9 knockout and transcriptional activation screening. *Nature Protocols*, 12(4):828–863, apr 2017.

[67] Sameer Kalghatgi, Catherine S Spina, James C Costello, Marc Liesa, J Ruben Morones-Ramirez, Shimyn Slomovic, Anthony Molina, Orian S Shirihai, and James J Collins. Bactericidal antibiotics induce mitochondrial dysfunction and oxidative damage in Mammalian cells. *Science translational medicine*, 5(192):192ra85, jul 2013.

[68] M Kaposi. Idiopathisches multiples pigmentsarkom der haut. *Arch Dermatol Syph.*, 1872.

[69] Dean H. Kedes, Michael Lagunoff, Rolf Renne, and Don Ganem. Identification of the gene encoding the major latency-associated nuclear antigen of the Kaposi's sarcoma-associated herpesvirus. *Journal of Clinical Investigation*, 100(10):2606–2610, nov 1997.

[70] Michael P. King and Giuseppe Attardi. Human cells lacking mtDNA: Repopulation with exogenous mitochondria by complementation. *Science*, 246(4929):500–503, oct 1989.

[71] David M Knipe and Peter Howley. *Fields Virology*. Wolters Kluwer, Philadelphia, 6 edition, 2013.

[72] Hiroko Koike-Yusa, Yilong Li, E. Pien Tan, Martin Del Castillo Velasco-Herrera, and Kosuke Yusa. Genome-wide recessive genetic screening in mammalian cells with a lentiviral CRISPR-guide RNA library. *Nature Biotechnology*, 32(3):267–273, dec 2014.

[73] Athena Labeau, Etienne Simon-Loriere, Mohamed-Lamine Hafirassou, Lucie Bonnet-Madin, Sarah Tessier, Alessia Zamborlini, Thierry Dupré, Nathalie Seta, Olivier Schwartz, Marie-Laure Chaix, Constance Delaugerre, Ali Amara, and Laurent Meertens. A Genome-Wide CRISPR-Cas9 Screen Identifies the Dolichol-Phosphate Mannose Synthase Complex as a Host Dependency Factor for Dengue Virus Infection. *Journal of Virology*, 94(7), jan 2020.

[74] M. Lagunoff, J. Bechtel, E. Venetsanakos, A.-M. Roy, N. Abbey, B. Herndier, M. McMahon, and D. Ganem. De Novo Infection and Serial Transmission of Kaposi's Sarcoma-Associated Herpesvirus in Cultured Endothelial Cells. *Journal of Virology*, 76(5):2440–2448, mar 2002.

[75] Rebecca Lamb, Bela Ozsvari, Camilla L Lisanti, Herbert B Tanowitz, Anthony Howell, Ubaldo E Martinez-Outschoorn, Federica Sotgia, and Michael P Lisanti. Antibiotics

that target mitochondria effectively eradicate cancer stem cells, across multiple tumor types: treating cancer like an infectious disease. *Oncotarget*, 6(7):4569–84, mar 2015.

[76] Fanny Lanternier, Céleste Lebbé, Noël Schartz, David Farhi, Anne Geneviève Marcelin, Delphine Kérob, Félix Agbalika, Olivier Vérola, Isabelle Gorin, Michel Janier, Marie Françoise Avril, and Nicolas Dupin. Kaposis sarcoma in HIV-negative men having sex with men. *AIDS*, 22(10):1163–1168, jun 2008.

[77] Andrew M. Leidal, David P. Cyr, Richard J. Hill, Patrick W.K. Lee, and Craig McCormick. Subversion of autophagy by Kaposi's sarcoma-associated herpesvirus impairs oncogene-induced senescence. *Cell Host and Microbe*, 11(2):167–180, feb 2012.

[78] Bo Li, Sara M. Clohisey, Bing Shao Chia, Bo Wang, Ang Cui, Thomas Eisenhaure, Lawrence D. Schweitzer, Paul Hoover, Nicholas J. Parkinson, Aharon Nachshon, Nikki Smith, Tim Regan, David Farr, Michael U. Gutmann, Syed Irfan Bukhari, Andrew Law, Maya Sangesland, Irit Gat-Viks, Paul Digard, Shobha Vasudevan, Daniel Lingwood, David H. Dockrell, John G. Doench, J. Kenneth Baillie, and Nir Hacohen. Genome-wide CRISPR screen identifies host dependency factors for influenza A virus infection. *Nature Communications*, 11(1):1–18, dec 2020.

[79] Wei Li, Han Xu, Tengfei Xiao, Le Cong, Michael I Love, Feng Zhang, Rafael A Irizarry, Jun S Liu, Myles Brown, and X Shirley Liu. MAGeCK enables robust identification of essential genes from genome-scale CRISPR/Cas9 knockout screens. *Genome Biology*, 15(12):554, dec 2014.

[80] Yun Li, Julien Muffat, Attya Omer Javed, Heather R Keys, Tenzin Lungjangwa, Irene Bosch, Mehreen Khan, Maria C Virgilio, Lee Gehrke, David M Sabatini, and Rudolf Jaenisch. Genome-wide CRISPR screen for Zika virus resistance in human neural cells. *National Acad Sciences*, 116(19):9527–9532, may 2019.

[81] M. Lichterfeld, N. Qurishi, C. Hoffmann, B. Hochdorfer, N. H. Brockmeyer, K. Arasteh, S. Mauss, and J. K. Rockstroh. Treatment of HIV-1-associated Kaposi's sarcoma with pegylated liposomal doxorubicin and HAART simultaneously induces effective tumor remission and CD4+ T cell recovery. *Infection*, 33(3):140–147, jun 2005.

[82] Marc Liesa and Orian S. Shirihai. Mitochondrial dynamics in the regulation of nutrient utilization and energy expenditure, apr 2013.

[83] Bin Liu, Siwei Chen, Anouk La Rose, Deng Chen, Fangyuan Cao, Martijn Zwinderman, Dominik Kiemel, Manon Aïssi, Frank J Dekker, and Hidde J Haisma. Inhibition of histone deacetylase 1 (HDAC1) and HDAC2 enhances CRISPR/Cas9 genome editing. *Nucleic Acids Research*, 48(2):517–532, 2019.

[84] Tao Ma, Harsh Patel, Savalan Babapoor-Farrokhran, Renty Franklin, Gregg L Semenza, Akrit Sodhi, and Silvia Montaner. KSHV induces aerobic glycolysis and angiogenesis through HIF-1-dependent upregulation of pyruvate kinase 2 in Kaposi's sarcoma. *Angiogenesis*, 18(4):477–88, oct 2015.

[85] Yijie Ma, Michael J. Walsh, Katharina Bernhardt, Camille W. Ashbaugh, Stephen J. Trudeau, Isabelle Y. Ashbaugh, Sizun Jiang, Chang Jiang, Bo Zhao, David E. Root, John G. Doench, and Benjamin E. Gewurz. CRISPR/Cas9 Screens Reveal Epstein-Barr Virus-Transformed B Cell Host Dependency Factors. *Cell Host & Microbe*, 21(5):580–591.e7, may 2017.

[86] Kira S. Makarova, Nick V. Grishin, Svetlana A. Shabalina, Yuri I. Wolf, and Eugene V. Koonin. A putative RNA-interference-based immune system in prokaryotes: Computational analysis of the predicted enzymatic machinery, functional analogies with eukaryotic RNAi, and hypothetical mechanisms of action, mar 2006.

[87] Prashant Mali, Luhan Yang, Kevin M. Esvelt, John Aach, Marc Guell, James E.

DiCarlo, Julie E. Norville, and George M. Church. RNA-guided human genome engineering via Cas9. *Science*, 339(6121):823–826, feb 2013.

[88] Mark Manzano, Ajinkya Patil, Alexander Waldrop, Sandeep S. Dave, Amir Behdad, and Eva Gottwein. Gene essentiality landscape and druggable oncogenic dependencies in herpesviral primary effusion lymphoma. *Nature Communications*, 9(1):3263, dec 2018.

[89] Craig McCormick and Don Ganem. The kaposin B protein of KSHV activates the p38/MK2 pathway and stabilizes cytokine mRNAs. *Science*, 307(5710):739–741, feb 2005.

[90] Duncan J. McGeoch, Simon Cook, Aidan Dolan, Fiona E. Jamieson, and Elizabeth A.R. Telford. Molecular phylogeny and evolutionary timescale for the family of mammalian herpesviruses. *Journal of Molecular Biology*, 247(3):443–458, mar 1995.

[91] Ronald A. Merrill, Kyle H. Flippo, and Stefan Strack. Measuring mitochondrial shape with imageJ. In *Neuromethods*, volume 123, pages 31–48. Humana Press Inc., 2017.

[92] Francisco J.M. Mojica, César Díez-Villaseñor, Jesús García-Martínez, and Elena Soria. Intervening sequences of regularly spaced prokaryotic repeats derive from foreign genetic elements. *Journal of Molecular Evolution*, 60(2):174–182, feb 2005.

[93] Valerie A. Morris, Almira S. Punjabi, Robert C. Wells, Cristina J. Wittkopp, Richard Vart, and Michael Lagunoff. The KSHV viral IL-6 homolog is sufficient to induce blood to lymphatic endothelial cell differentiation. *Virology*, 428(2):112–120, jul 2012.

[94] Joshua Munger, Sunil U. Bajad, Hilary A. Coller, Thomas Shenk, and Joshua D. Rabinowitz. Dynamics of the Cellular Metabolome during Human Cytomegalovirus Infection. *PLoS Pathogens*, 2(12):e132, dec 2006.

[95] Joshua Munger, Bryson D. Bennett, Anuraag Parikh, Xiao Jiang Feng, Jessica McArdle, Herschel A. Rabitz, Thomas Shenk, and Joshua D. Rabinowitz. Systems-level metabolic flux profiling identifies fatty acid synthesis as a target for antiviral therapy. *Nature Biotechnology*, 26(10):1179–1186, oct 2008.

[96] Sumitra Muralidhar, Anne Pumfery, Morad Hassani, M. Reza Sadaie, Norio Azumi, John N. Brady, Peter Medveczky, and Leonard J. Rosenthal. Identification of Kaposin (ORF K12) as a Human Herpesvirus 8 (Kaposi's Sarcoma Associated Herpesvirus) Oncogene. *Journal of Acquired Immune Deficiency Syndromes and Human Retrovirology*, 17(4):A27, apr 1998.

[97] Sumitra Muralidhar, Gary Veytsmann, Bala Chandran, Dharam Ablashi, Jay Doniger, and Leonard J. Rosenthal. Characterization of the human herpesvirus 8 (Kaposi's sarcoma-associated herpesvirus) oncogene, Kaposin (ORF K12). *Journal of Clinical Virology*, 16(3):203–213, may 2000.

[98] Jinjong Myoung and Don Ganem. Generation of a doxycycline-inducible KSHV producer cell line of endothelial origin: Maintenance of tight latency with efficient reactivation upon induction. *Journal of Virological Methods*, 174(1-2):12–21, jun 2011.

[99] Evan Noch and Kamel Khalili. Oncogenic viruses and tumor glucose metabolism: Like kids in a candy store, jan 2012.

[100] Jodi Nunnari and Anu Suomalainen. Mitochondria: In sickness and in health, mar 2012.

[101] Päivi M. Ojala, Marianne Tiainen, Petri Salven, Tanja Veikkola, Esmeralda Castaños-Vélez, Ronit Sarid, Peter Biberfeld, and Tomi P. Mäkelä. Kaposi's sarcoma-associated herpesvirus-encoded v-cyclin triggers apoptosis in cells with high levels of cyclin-dependent kinase 6. *Cancer Research*, 59(19):4984–4989, 1999.

[102] D. O'Mahony, A. H. Gandjbakhche, M. Hassan, A. Vogel, and R. Yarchoan. Imaging techniques for Kaposi's sarcoma, 2008.

[103] Ryan J Park, Tim Wang, Dylan Koundakjian, Judd F Hultquist, Pedro Lamothe-Molina, Blandine Monel, Kathrin Schumann, Haiyan Yu, Kevin M Krupzcak, Wilfredo Garcia-Beltran, Alicja Piechocka-Trocha, Nevan J Krogan, Alexander Marson, David M Sabatini, Eric S Lander, Nir Hacohen, and Bruce D Walker. A genome-wide CRISPR screen identifies a restricted set of HIV host dependency factors. *nature.com*, 49(2):193–203, jan 2016.

[104] Natalya N. Pavlova and Craig B. Thompson. The Emerging Hallmarks of Cancer Metabolism, jan 2016.

[105] Manuele Piccolis, Laura M. Bond, Martin Kampmann, Pamela Pulimeno, Chandramohan Chitraju, Christina B.K. Jayson, Laura P. Vaites, Sebastian Boland, Zon Weng Lai, Katlyn R. Gabriel, Shane D. Elliott, Joao A. Paulo, J. Wade Harper, Jonathan S. Weissman, Tobias C. Walther, and Robert V. Farese. Probing the Global Cellular Responses to Lipotoxicity Caused by Saturated Fatty Acids. *Molecular Cell*, 74(1):32–44.e8, apr 2019.

[106] C. Pourcel, G. Salvignol, and Gilles Vergnaud. CRISPR elements in Yersinia pestis acquire new repeats by preferential uptake of bacteriophage DNA, and provide additional tools for evolutionary studies. *Microbiology*, 151(3):653–663, mar 2005.

[107] Stoyan A. Radkov, Paul Kellam, and Chris Boshoff. The latent nuclear antigen of Kaposi sarcoma-associated herpesvirus targets the retinoblastoma-E2F pathway and with the oncogene Hras transforms primary rat cells. *Nature Medicine*, 6(10):1121–1127, 2000.

[108] Mark A Samols, Jianhong Hu, Rebecca L Skalsky, and Rolf Renne. Cloning and

identification of a microRNA cluster within the latency-associated region of Kaposi's sarcoma-associated herpesvirus. *Journal of virology*, 79(14):9301–5, jul 2005.

[109] Erica L Sanchez, Patrick A Carroll, Angel B Thalhofer, and Michael Lagunoff. Latent KSHV Infected Endothelial Cells Are Glutamine Addicted and Require Glutaminolysis for Survival. *PLoS pathogens*, 11(7):e1005052, jul 2015.

[110] Erica L. Sanchez and Michael Lagunoff. Viral activation of cellular metabolism, may 2015.

[111] Neville E. Sanjana, Ophir Shalem, and Feng Zhang. Improved vectors and genome-wide libraries for CRISPR screening, jul 2014.

[112] Johannes Schindelin, Ignacio Arganda-Carreras, Erwin Frise, Verena Kaynig, Mark Longair, Tobias Pietzsch, Stephan Preibisch, Curtis Rueden, Stephan Saalfeld, Benjamin Schmid, Jean Yves Tinevez, Daniel James White, Volker Hartenstein, Kevin Eliceiri, Pavel Tomancak, and Albert Cardona. Fiji: An open-source platform for biological-image analysis, jul 2012.

[113] Priya S. Shah, Nichole Link, Gwendolyn M. Jang, Phillip P. Sharp, Tongtong Zhu, Danielle L. Swaney, Jeffrey R. Johnson, John Von Dollen, Holly R. Ramage, Laura Satkamp, Billy Newton, Ruth Hüttenhain, Marine J. Petit, Tierney Baum, Amanda Everitt, Orly Laufman, Michel Tassetto, Michael Shales, Erica Stevenson, Gabriel N. Iglesias, Leila Shokat, Shashank Tripathi, Vinod Balasubramaniam, Laurence G. Webb, Sebastian Aguirre, A. Jeremy Willsey, Adolfo Garcia-Sastre, Katherine S. Pollard, Sara Cherry, Andrea V. Gamarnik, Ivan Marazzi, Jack Taunton, Ana Fernandez-Sesma, Hugo J. Bellen, Raul Andino, and Nevan J. Krogan. Comparative Flavivirus-Host Protein Interaction Mapping Reveals Mechanisms of Dengue and Zika Virus Pathogenesis. *Cell*, 175(7):1931–1945.e18, dec 2018.

[114] Ophir Shalem, Neville E. Sanjana, Ella Hartenian, Xi Shi, David A. Scott, Tarjei S. Mikkelsen, Dirk Heckl, Benjamin L. Ebert, David E. Root, John G. Doench, and Feng Zhang. Genome-scale CRISPR-Cas9 knockout screening in human cells. *Science*, 343(6166):84–87, jan 2014.

[115] Inna N. Shokolenko, Glenn L. Wilson, and Mikhail F. Alexeyev. Persistent damage induces mitochondrial DNA degradation. *DNA Repair*, 12(7):488–499, jul 2013.

[116] Rochika Singh, Lakshmi Sripada, and Rajesh Singh. Side effects of antibiotics during bacterial infection: Mitochondria, the main target in host cell. *Mitochondrion*, 16:50–54, may 2014.

[117] Rebecca L. Skalsky, Mark A. Samols, Karlie B. Plaisance, Isaac W. Boss, Alberto Riva, M. Cecilia Lopez, Henry V. Baker, and Rolf Renne. Kaposi's Sarcoma-Associated Herpesvirus Encodes an Ortholog of miR-155. *Journal of Virology*, 81(23):12836–12845, dec 2007.

[118] Gary E. Stein and William A. Craig. Tigecycline: A Critical Analysis. *Clinical Infectious Diseases*, 43(4):518–524, 2006.

[119] Michael Stürzl, Dominika Gaus, Wilhelm G. Dirks, Don Ganem, and Ramona Jochmann. Kaposi's sarcoma-derived cell line SLK is not of endothelial origin, but is a contaminant from a known renal carcinoma cell line. *International Journal of Cancer*, 132(8):1954–1958, apr 2013.

[120] Qinmiao Sun, Sunny Zachariah, and Preet M. Chaudhary. The Human Herpes Virus 8-Encoded Viral FLICE-inhibitory Protein Induces Cellular Transformation via NF-κB Activation. *Journal of Biological Chemistry*, 278(52):52437–52445, dec 2003.

[121] Zoi E. Sychev, Alex Hu, Terri A. DiMaio, Anthony Gitter, Nathan D. Camp, William S. Noble, Alejandro Wolf-Yadlin, and Michael Lagunoff. Integrated systems biology anal-

ysis of KSHV latent infection reveals viral induction and reliance on peroxisome mediated lipid metabolism. *PLOS Pathogens*, 13(3):e1006256, mar 2017.

[122] An S. Tan, James W. Baty, Lan Feng Dong, Ayenachew Bezawork-Geleta, Berwini Endaya, Jacob Goodwin, Martina Bajzikova, Jaromira Kovarova, Martin Peterka, Bing Yan, Elham Alizadeh Pesdar, Margarita Sobol, Anatolyj Filimonenko, Shani Stuart, Magdalena Vondrusova, Katarina Kluckova, Karishma Sachaphibulkij, Jakub Rohlena, Pavel Hozak, Jaroslav Truksa, David Eccles, Larisa M. Haupt, Lyn R. Griffiths, Jiri Neuzil, and Michael V. Berridge. Mitochondrial genome acquisition restores respiratory function and tumorigenic potential of cancer cells without mitochondrial DNA. *Cell Metabolism*, 21(1):81–94, jan 2015.

[123] Varnesh Tiku, Man Wah Tan, and Ivan Dikic. Mitochondrial Functions in Infection and Immunity, apr 2020.

[124] Tsz Leung To, Alejandro M. Cuadros, Hardik Shah, Wendy H.W. Hung, Yang Li, Sharon H. Kim, Daniel H.F. Rubin, Ryan H. Boe, Sneha Rath, John K. Eaton, Federica Piccioni, Amy Goodale, Zohra Kalani, John G. Doench, David E. Root, Stuart L. Schreiber, Scott B. Vafai, and Vamsi K. Mootha. A Compendium of Genetic Modifiers of Mitochondrial Dysfunction Reveals Intra-organelle Buffering. *Cell*, 179(5):1222–1238.e17, nov 2019.

[125] Aleksandra Trifunovic, Anna Wredenberg, Maria Falkenberg, Johannes N. Spelbrink, Anja T. Rovio, Cari E. Bruder, Mohammad Bohlooly-Y, Sebastian Gldlöf, Anders Oldfors, Rolf Wibom, Jan Törnell, Howard T. Jacobs, and Nils Göran Larsson. Premature ageing in mice expressing defective mitochondrial DNA polymerase. *Nature*, 429(6990):417–423, may 2004.

[126] Aviad Tsherniak, Francisca Vazquez, Phil G. Montgomery, Barbara A. Weir, Gregory

Kryukov, Glenn S. Cowley, Stanley Gill, William F. Harrington, Sasha Pantel, John M. Krill-Burger, Robin M. Meyers, Levi Ali, Amy Goodale, Yenarae Lee, Guozhi Jiang, Jessica Hsiao, William F.J. Gerath, Sara Howell, Erin Merkel, Mahmoud Ghandi, Levi A. Garraway, David E. Root, Todd R. Golub, Jesse S. Boehm, and William C. Hahn. Defining a Cancer Dependency Map. *Cell*, 170(3):564–576.e16, jul 2017.

[127] For Yue Tso, Andrew V. Kossenkov, Salum J. Lidenge, Owen Ngalamika, John R. Ngowi, Julius Mwaiselage, Jayamanna Wickramasinghe, Eun Hee Kwon, John T. West, Paul M. Lieberman, and Charles Wood. RNA-Seq of Kaposi's sarcoma reveals alterations in glucose and lipid metabolism. *PLOS Pathogens*, 14(1):e1006844, jan 2018.

[128] Livia Vastag, Emre Koyuncu, Sarah L. Grady, Thomas E. Shenk, and Joshua D. Rabinowitz. Divergent effects of human cytomegalovirus and herpes simplex virus-1 on cellular metabolism. *PLoS Pathogens*, 7(7), jul 2011.

[129] Eleni Venetsanakos, Amer Mirza, Christie Fanton, Serguei R. Romanov, Thea Tlsty, and Martin McMahon. Induction of tubulogenesis in telomerase-immortalized human microvascular endothelial cells by glioblastoma cells. *Experimental Cell Research*, 273(1):21–33, feb 2002.

[130] Valerie A. Villareal, Mary A. Rodgers, Deirdre A. Costello, and Priscilla L. Yang. Targeting host lipid synthesis and metabolism to inhibit dengue and hepatitis C viruses, dec 2015.

[131] Timothy Wai and Thomas Langer. Mitochondrial Dynamics and Metabolic Regulation, feb 2016.

[132] Tim Wang, Jenny J. Wei, David M. Sabatini, and Eric S. Lander. Genetic Screens in Human Cells Using the CRISPR-Cas9 System. *Science*, 343(6166):80–84, jan 2014.

[133] Xiuyan Wang, Ella R. Hinson, and Peter Cresswell. The Interferon-Inducible Protein Viperin Inhibits Influenza Virus Release by Perturbing Lipid Rafts. *Cell Host and Microbe*, 2(2):96–105, aug 2007.

[134] O Warburg, F Wind, and E Negelein. THE METABOLISM OF TUMORS IN THE BODY. *The Journal of general physiology*, 8(6):519–30, mar 1927.

[135] Otto Warburg. On the origin of cancer cells. *Science*, 123(3191):309–314, 1956.

[136] WHO. Executive Summary The Selection and Use of Essential Medicines Selection and Use of Essential Medicines. Technical report.

[137] Simon N. Willis, Lin Chen, Grant Dewson, Andrew Wei, Edwina Naik, Jamie I. Fletcher, Jerry M. Adams, and David C.S. Huang. Proapoptotic Bak is sequestered by Mcl-1 and Bcl-xL, but not Bcl-2, until displaced by BH3-only proteins. *Genes and Development*, 19(11):1294–1305, jun 2005.

[138] Miao Xu, Youyuan Yao, Hui Chen, Shanshan Zhang, Su Mei Cao, Zhe Zhang, Bing Luo, Zhiwei Liu, Zilin Li, Tong Xiang, Guiping He, Qi Sheng Feng, Li Zhen Chen, Xiang Guo, Wei Hua Jia, Ming Yuan Chen, Xiao Zhang, Shang Hang Xie, Roujun Peng, Ellen T. Chang, Vincent Pedergnana, Lin Feng, Jin Xin Bei, Rui Hua Xu, Mu Sheng Zeng, Weimin Ye, Hans Olov Adami, Xihong Lin, Weiwei Zhai, Yi Xin Zeng, and Jianjun Liu. Genome sequencing analysis identifies Epstein–Barr virus subtypes associated with high risk of nasopharyngeal carcinoma. *Nature Genetics*, 51(7):1131–1136, jul 2019.

[139] Xiaoping Yang, Jesse S. Boehm, Xinping Yang, Kourosh Salehi-Ashtiani, Tong Hao, Yun Shen, Rakela Lubonja, Sapana R. Thomas, Ozan Alkan, Tashfeen Bhimdi, Thomas M. Green, Cory M. Johannessen, Serena J. Silver, Cindy Nguyen, Ryan R. Murray, Haley Hieronymus, Dawit Balcha, Changyu Fan, Chenwei Lin, Lila Ghamsari,

Marc Vidal, William C. Hahn, David E. Hill, and David E. Root. A public genome-scale lentiviral expression library of human ORFs. *Nature Methods*, 8(8):659–661, aug 2011.

[140] Jin Ye and Russell A. DeBose-Boyd. Regulation of cholesterol and fatty acid synthesis, jul 2011.

[141] Jin Ye, Chunfu Wang, Rhea Sumpter, Michael S. Brown, Joseph L. Goldstein, and Michael Gale. Disruption of hepatitis C virus RNA replication through inhibition of host protein geranylgeranylation. *Proceedings of the National Academy of Sciences of the United States of America*, 100(26):15865–15870, dec 2003.

[142] Ohad Yogev, Dimitris Lagos, Tariq Enver, and Chris Boshoff. Kaposi's sarcoma herpesvirus microRNAs induce metabolic transformation of infected cells. *PLoS pathogens*, 10(9):e1004400, sep 2014.

[143] Autumn G. York, Kevin J. Williams, Joseph P. Argus, Quan D. Zhou, Gurpreet Brar, Laurent Vergnes, Elizabeth E. Gray, Anjie Zhen, Nicholas C. Wu, Douglas H. Yamada, Cameron R. Cunningham, Elizabeth J. Tarling, Moses Q. Wilks, David Casero, David H. Gray, Amy K. Yu, Eric S. Wang, David G. Brooks, Ren Sun, Scott G. Kitchen, Ting Ting Wu, Karen Reue, Daniel B. Stetson, and Steven J. Bensinger. Limiting Cholesterol Biosynthetic Flux Spontaneously Engages Type i IFN Signaling. *Cell*, 163(7):1716–1729, dec 2015.

[144] A A Yunis. Chloramphenicol: Relation of Structure to Activity and Toxicity. *Annual Review of Pharmacology and Toxicology*, 28(1):83–100, 1988.

[145] Rong Zhang, Jonathan J. Miner, Matthew J. Gorman, Keiko Rausch, Holly Ramage, James P. White, Adam Zuiani, Ping Zhang, Estefania Fernandez, Qiang Zhang, Kimberly A. Dowd, Theodore C. Pierson, Sara Cherry, and Michael S. Diamond. A

CRISPR screen defines a signal peptide processing pathway required by flaviviruses. *Nature*, 535(7610):164–168, jul 2016.

[146] W Zhong, H Wang, B Herndier, and D Ganem. Restricted expression of Kaposi sarcoma-associated herpesvirus (human herpesvirus 8) genes in Kaposi sarcoma. *Proceedings of the National Academy of Sciences of the United States of America*, 93(13):6641–6, jun 1996.

[147] Joseph M. Ziegelbauer, Christopher S. Sullivan, and Don Ganem. Tandem array-based expression screens identify host mRNA targets of virus-encoded microRNAs. *Nature Genetics*, 41(1):130–134, jan 2009.